Ricardo José de Jesus Duarte

Estudo Comparativo das Técnicas de Colmatação de Perda Óssea na A.T.J.

A comparative study of bone defects repair techniques in T.K.A.

Ricardo José de Jesus Duarte

Estudo Comparativo das Técnicas de Colmatação de Perda Óssea na A.T.J.

A comparative study of bone defects repair techniques in T.K.A.

Ricardo José de Jesus Duarte

Estudo Comparativo das Técnicas de Colmatação de Perda Óssea na A.T.J.

Comparative study of the techniques to bridge the bone loss in T.K.A.

Dissertação apresentada à Universidade de Aveiro para cumprimento dos requisitos necessários à obtenção do grau de Mestre em Engenharia Mecânica, realizada sob a orientação científica de António Manuel Godinho Completo, Professor Auxiliar do Departamento de Engenharia Mecânica da Universidade de Aveiro e co-orientada por António Manuel Amaral Monteiro Ramos, Professor Auxiliar Convidado do Departamento de Engenharia Mecânica da Universidade de Aveiro.

Work submitted to Universidade de Aveiro in order to satisfy the necessary requirements for Master's Degree in Mechanical Engineering, performed under the scientific orientation of António Manuel Godinho Completo, Assistant Professor of Departamento de Engenharia Mecânica da Universidade de Aveiro and co-oriented by António Manuel Amaral Monteiro Ramos, Invited Assistant Professor of Departamento de Engenharia Mecânica da Universidade de Aveiro.

o júri / the jury

presidente / president

Professor Doutor Rui Pedro Ramos Cardoso
Professor Auxiliar do Departamento de Engenharia Mecânica da Universidade de Aveiro

vogais / examiners committee

Professor Doutor Fernando Manuel Pereira Fonseca
Professor Auxiliar da Faculdade de Medicina de Coimbra

Professor Doutor António Manuel Godinho Completo
Professor Auxiliar do Departamento de Engenharia Mecânica da Universidade de Aveiro

António Manuel Amaral Monteiro Ramos
Professor Auxiliar Convidado do Departamento de Engenharia Mecânica da Universidade de Aveiro

Aos meus pais e irmã.
Adoro-vos

agradecimentos / acknowledgements

A realização deste trabalho não teria sido possível sem a ajuda de diversas pessoas, como tal, aproveito esta oportunidade para agradecer a todas elas o apoio e disponibilidade demonstradas.

Em primeiro lugar, gostaria de agradecer ao meu orientador, o Professor Doutor António Completo, por todos os ensinamento, apoio, disponibilidade e paciência demonstrados, sendo ele uma peça chave para a conclusão deste trabalho.

Gostaria também de agradecer ao meu co-Orientador Professor Doutor António Ramos, pela ajuda na identificação de alguns erros, permitindo assim a sua correcção atempadamente.

Um agradecimento especial para todo o pessoal do talho BioBom Talhos de Aveiro pelo fornecimento do material usado para alguns dos testes, bem como ao Professor António Bastos e á Professora Gabriela Vincze pela ajuda com o material de medição por vídeo.

Gostaria também de agradecer a todo o pessoal do Laboratório de Biomecânica, em especial á Eng. Joana Silva por toda a ajuda prestada ao longo da execução deste trabalho.

Agradeço à Ana Marques todo o apoio, incentivo, entrega e amizade demonstrados durante a execução deste trabalho, o qual sem a sua ajuda não teria sido possível.

Finalmente, gostaria de agradecer aos meus pais e irmã, por terem sempre uma palavra de incentivo e conforto nas alturas mais complicadas permitindo assim ultrapassar as dificuldades e encarar com um maior optimismo situações futuras.

A todos vós o meu mais sincero obrigado!

Palavras-chave

Biomecânica, articulação do joelho, cunhas metálicas, enxertos ósseos, haste metálica, medição experimental de extensões, método dos elementos finitos, revisão da artroplastia total do joelho

Resumo

Nesta tese foi objectivo estudar os aspectos biomecânicos das diferentes técnicas de colmatação de perda óssea na tibia proximal aquando da revisão da artroplastia total do joelho. Procurou-se especificamente avaliar como cada uma das diferentes técnicas altera a transferência de carga ao osso de suporte, aferindo assim potenciais riscos de reabsorção óssea ou mesmo falha por fadiga do osso de suporte. Foi também avaliada de uma forma comparativa a estabilidade de cada construção de colmatação do defeito relativamente à solução sem defeito ósseo. Procurou-se também nesta tese avaliar o efeito da utilização da haste intramedular quando associada às diferentes técnicas. Para o efeito numa primeira fase procurou-se realizar uma analise detalhada à articulação do joelho na sua vertente anatómica e biomecânica com especial enfoque na artroplastia e no processo de revisão desta. Foi seleccionada a prótese do joelho P.F.C. Sigma como elemento para a realização do estudo comparativo, os elementos protésicos metálicos utilizados nas diferentes construções da substituição óssea foram também do mesmo modelo; hemi-cunha, cunha total e bloco. Em complemento foram também comparadas mais duas técnicas de colmatação óssea; uma com recurso apenas ao cimento ósseo e outra com a utilização de um enxerto de osso bovino. Na fase seguinte desenvolveram-se modelos experimentais com recurso à tibia em material compósito, onde os defeitos ósseos foram gerados e as diferentes técnicas de colmatação aplicadas através da realização de cirurgias "in-vitro". A fim de aferir as alterações de transferência de carga e estabilidade foram colocados extensometros na região anexa ao defeito permitindo a avaliação das deformações principais na superfície dos modelos, assim como recorreu-se a utilização de técnicas de vídeo para avaliação da estabilidade do prato tibial nas diferentes técnicas. Estes modelos foram submetidos a um severo caso de carga no condilo medial onde se situa o defeito, tendo-se procedido à avaliação e comparação dos resultados das deformações no osso e estabilidade do prato. Numa fase posterior procedeu-se ao desenvolvimento de modelos numéricos de elementos finitos que procuram replicar os modelos avaliados experimentalmente. Este modelos foram submetidos a dois casos de carga, um idêntico ao aplicado nos modelos experimentais que permitiu a validação destes modelos numéricos e um outro caso de carga representativo de uma condição de carga mais fisiológica durante o ciclo de marcha. Este modelos numéricos permitiram a avaliação de parâmetros biomecânicos não passíveis de avaliação com recurso aos modelos experimentais anteriores. Foram assim analisadas as deformações impostas aos osso cortical e esponjoso na vizinhança do defeito e na interface com este. Estes mesmos modelos foram comparados com os resultados obtidos nos modelos experimentais de forma a avaliar a sua correlação.

Os resultados experimentais e numéricos obtidos permitiram evidenciar boa correlação entre estes demonstrando que os modelos numéricos são capazes de replicar com fidelidade o comportamento dos modelos experimentais. Os resultados obtidos em ambos os tipos de modelos evidenciam alterações de transferência de carga e estabilidade entre os diferentes tipos de técnicas. Os modelos com cunha total e bloco aumentaram em média as deformações no lado medial (lado do defeito) do osso cortical adjacente ao implante quando comparados com o modelo de colmatação só com cimento ósseo e hemi-cunha. No entanto, os valores de máximos de incremento de deformação no osso cortical no lado medial ocorram para a construção com enxerto ósseo bovino. Estes incrementos observados no osso cortical para as construções de maior dimensão é oposto ao comportamento observado no osso esponjoso na interface com o implante, pois neste caso estas construções originam uma redução das deformações relativamente à solução sem defeito. Assim, temos que as soluções mais invasivas potenciam o risco de dano por fadiga óssea do osso cortical e simultaneamente potencializam o risco de reabsorção óssea no osso esponjoso adjacente. Em termos de estabilidade apenas a construção com bloco se revelou significativamente mais estável que as restantes técnicas. O efeito adicional de estabilidade das hastes apenas se fez sentir nas construções menos invasivas com recurso ao cimento ósseo e hemi-cunha.

keywords

Biomechanics, bone grafts, experimental strain measurements, finite element method, knee joint, metal wedges, metal stem, revision of total knee arthroplasty

abstract

This thesis objective was to study the biomechanical aspects of the different repair techniques of bone loss in the proximal tibia, in the revision of total knee arthroplasty. We sought to specifically evaluate how each of the different techniques changes the load transfer to the supporting bone, thus gauging the potential for bone resorption or fatigue failure of the supporting bone. Was also assessed, in a comparative way, the stability of each repair construction of the bone defects, relatively to the solutions without bone defects. We also sought, in this work, to evaluate the effect of the use of intramedullary stems when associated to different techniques. For this purpose, as a first step, we tried to perform a detailed analysis of the knee joint in its anatomical and biomechanical aspects, with special focus on arthroplasty and its revision process. We selected the knee prosthesis P.F.C. Sigma as an element for the realization of the comparative study. The prosthetic metal elements used in the different bone replacement constructions were also the same model, hemi-wedge, wedge and block total. As a complement two more bone repair techniques were also compared: using only bone cement in contrast with the use of a bovine bone graft. In the following phase experimental models were developed using the tibia in composite material, where the bone defects were created and the different techniques applied during "in vitro" surgeries. In order to assess the changes of load transfer and stability in the region annexed to the bone defect were placed gauges, allowing the evaluation of the models main surface deformations, as well as the use of video techniques for assessing the stability of the tibial plateau in the different techniques. These models were subjected to a severe case of load on the medial condyle where the defect is located, proceeding to evaluation and comparison of results of deformation and stability of the bone plate. At a later stage we proceeded to the development of finite element numerical models that seek to replicate the models evaluated experimentally. The models were subjected to two load cases, one case identical to the one applied in experimental models that allowed the validation of numerical models and another load case representing a physiological load condition during the walking cycle. The numerical models have allowed the assessment of biomechanical parameters, not eligible for evaluation before, using experimental models. Thereby the strains imposed on cortical and cancellous bone in the vicinity of the defect and in the interface with this have been analysed. These same models were compared with results obtained in experimental models in order to assess their correlation.

The experimental and numerical results obtained allow us to show a good correlation between these numerical models demonstrating that they are able to faithfully replicate the behaviour of experimental models. The results obtained in both types of models show changes in load transfer and stability between the different types of techniques. The models with full wedge and block, on average, increased the strains on the medial side (the one with defect) of the cortical bone adjacent to the implant when compared with the bone and cement graft model and metallic hemi-wedge. However is during the construction with bovine bone graft that takes place the maximum increment of strain in cortical bone, on the medial side. These increases observed in the cortical bone for larger buildings is opposite to the behavior observed in the cancellous bone at the implant interface, in which case these constructions originate a reduction of deformation on the solution without defect. So the more invasive solutions potentiate the risk of fatigue damage in cortical bone and simultaneously increase the risk of bone resorption in the adjacent cancellous bone. In terms of stability only the metallic block implant proved to be significantly more stable than the other techniques. The additional stability provided by stems was felt only in less invasive constructions with the use of bone cement and hemi-wedge.
The experimental and numerical results obtained allow us to show a good correlation between these numerical models demonstrating that they are able to faithfully replicate the behaviour of experimental models. The results obtained in both types of models show changes in load transfer and stability between the different types of techniques. The models with full wedge and block, on average, increased the strains on the medial side (the one with defect) of the cortical bone adjacent to the implant when compared with the bone and cement graft model and metallic hemi-wedge. However is during the construction with bovine bone graft that takes place the maximum increment of strain in cortical bone, on the medial side. These increases observed in the cortical bone for larger buildings is opposite to the behavior observed in the cancellous bone at the implant interface, in which case these constructions originate a reduction of deformation on the solution without defect. So the more invasive solutions potentiate the risk of fatigue damage in cortical bone and simultaneously increase the risk of bone resorption in the adjacent cancellous bone. In terms of stability only the metallic block implant proved to be significantly more stable than the other techniques. The additional stability provided by stems was felt only in less invasive constructions with the use of bone cement and hemi-wedge.

Contents

List of Figures

List of Tables

Chapter 1

Introduction

One of the most challenging problems to orthopaedics and the most debatable topic nowadays is the fact that surgeons don't know what methods and techniques available to correct the bone defects on the knee joint.

The bone tissue is one of the strongest and most rigid tissues of the human body, as an unique tissue to support pressures. Next to the cartilage and like cartilaginous tissue, the bone belongs to the connective group tissues hold up, being the major constituent of the skeleton, acting as a sustain for soft tissues and protecting the vital organs.

The knee joint is composed by three bones: femur, tibia and knee-cap or patella which is linked to the muscles that make the extension of the knee acting as a pulley.

Sometimes, and because the knee, is one of the most requested joints of the human body and the most loaded part during the walk, receiving rotation, extension and compression movements, through the years it can show some wear or injuries, causing to the person discomfort or even some pain during the walk.

Therefore, to provide quality of life to the patients, they are submitted to a surgical intervention named Total Knee Arthroplasty.

The main goal of this intervention is the substitution of the cartilage for a prosthesis, providing pain relief and giving back the lost amplitude of movements to patient.

After the first surgery and through the years, the patients faces some problems which leads to a revision of total knee arthroplasty.

One of the main reasons to perform the revision of total knee arthroplasty, is the bone loss around the primary implants, questioning its stability and making compulsory a surgical intervention.

The bone loss is linked to osteolysis and stress-shielding effects (Wolff's Law).

According to this, when the patient needs a revision of his arthroplasty, the surgeons are commonly confronted with the need to repair the bone losses with the materials that ensure the possibility to put a new implant that provides the desired stability. To accomplish properly this task, the surgeons can use many techniques such as cement, bone graft, metallic wedges or metallic blocks and stems.

Usually, each one of these techniques is directly linked to the dimension of the bone defect. However, the surgeons don't have a specific answer about the best solution for each case.

According to this, the main objectives on this thesis is to assign to the orthopaedic surgeons which method/technique is more appropriate to each kind of defects during the revision of total knee arthroplasty.

The first step was to generate a bibliographic research about the most common defects in the total knee arthroplasty and its classification in dimensional and local terms.

At this point was crucial to know the different techniques that surgeons can appeal to ensure the stability of all the components in the revision of the total knee arthroplasty.

In this thesis we analysed the main tibia defects as well as the main components of the knee prosthesis according to the collected data in the previous point.

An experimental models were developed, which allowed to assess the principal strains and stability on the different studied techniques. At the same time, a numerical models, using finite element methods (F.E.M.),was developed in order to assess the complementary biomechanical parameters that are impossible to evaluate with experimental models. These numerical models were then compared to the same load conditions.

Finally, were compared and analysed the principal strains on the numerical and experimental models, in order to identify the advantages and disadvantages of the several techniques.

Chapter 2

Revision of Total Knee Arthroplasty

2.1 The Knee Joint

The knee joint is essentially composed of four adjacent bones: femur, tibia, patella and fibula. As it's function is to provide movement in a rigid network, that is the human skeleton, the biomechanical system involved is very complex.

This is the largest joint in the human body and structurally the more complex one. As a synovial bicondilar folding joint between the femur condyles and tibia condyles, this articulation can be divided in three main articulations, tibiofemoral articulation (two joints) and patellofemoral articulation, [1] therefore this articulation is an important anatomical system in the human skeleton. This joint is constantly dealing with the high developed forces and moments in order to transfer static and dynamic forces to the leg, allowing simultaneously the skeleton mobility but also its stability.

A joint should have both stability and mobility but usually one of them is sacrificed over the other. The knee joint, however combines the both conditions, allowing the free movement in one plane, combining at the same time the stability and the mobility of the joint, particularly when extent.

The stability and mobility provided by this joint are due, in large part, to the interaction of ligaments, muscles, complex movements of planar slip and rotational movements in the articular surfaces. When the knee joint is totally flexed the free rotation of this joint can be seen.

This joint, beyond the great stability particularly when extended, has at the same time a large range of movements due to the type of the fitting joint surfaces that are relatively small. With this type of connection, the knee joint is prone to developing various deseases.

The great stability presented by this joint may appear incoherent at first sight because it is basically the joint of the two biggest bones on its vertically opposite ends, but it's not. The safety of the knee is then provided by many compensatory mechanisms, such as, an expansion of the weight bearing areas of the femur and the tibia, collateral and intracapsullar ligaments, a capsule and the aponeurosis ("aways" or muscular "ends" of flat board, histologically similar to tendons [11]) and tendons reinforcement effects. [12]

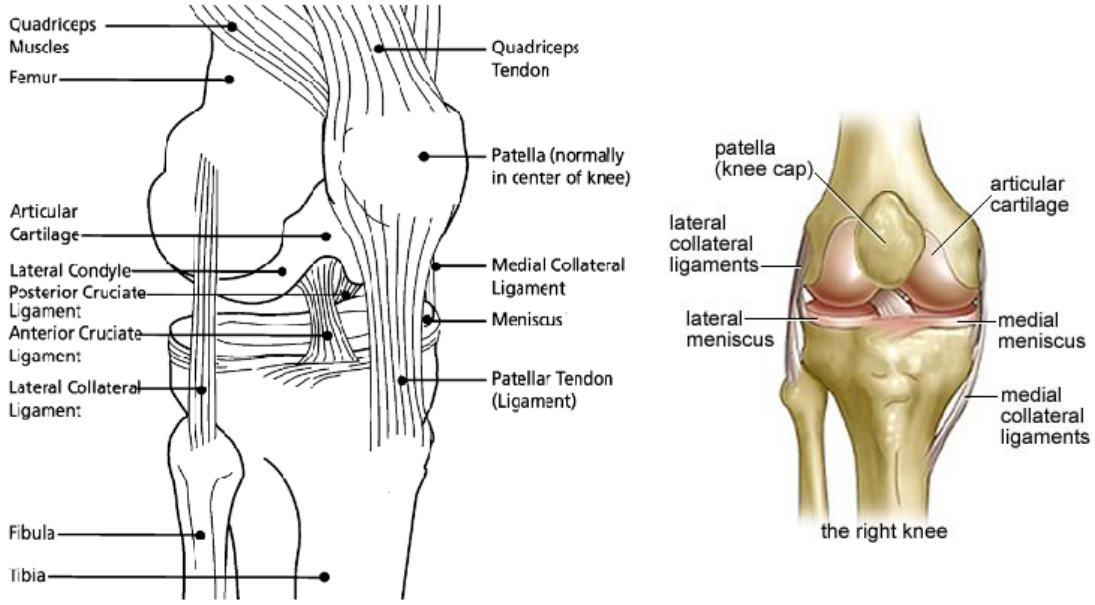

Figure 2.1: Knee joint scheme
[http://www.aclsolutions.com]

2.2 Articular surfaces of the knee joint

It is then necessary to understand how each constituents of the knee joint interact in order to provide motion and stability. According to this, the three main bones of the knee joint will be summary described.

2.2.1 Femur

Femur, is the longest and the most voluminous bone of the human body. It is located in the hip, transmitting the weight of the body from the hip bone to the tibia bone, when the person is standing. [5, 13]

Just as all human body bones, it's size varies in proportion to the person's height. The length of the femur is usually around $\frac{1}{4}$ of a person's height. This bone consists of a body (diaphysis) and two ends, superior and inferior end. The upper end of the femur bone consists of the femoral head, which is joined to the bone shaft by a narrow piece of the bone known as the neck of the femur, two laps and trochanters (greater tronchanter, lesser tronchanter).

The articular surfaces of femoral condyle are the two areas that bear, on the tibia and patellar surface joining, the condyles in front.[12]

The medial condyle area may be divided into two parts: the posterior one, parallel to the lateral condyle and with the same extension; and an anterior extension that goes obliquely and laterally. [12]

The patellar surface is divided by a furrow on the medial side and by a larger and prominent surface on the lateral side. [12]

The femoral condyles form two convex relief on both planes. The femoral condyles are longer anteroposteriorly than transversely, while the medial condyle is narrower and more prominent than the lateral one. The femoral axis diverge in its posterior position, however, the intercondylar incisure continues the line of the furrow patellar surface.

In the transverse plane, the femoral convex condyles corresponds more or less to the tibial concavity condyles, in matters that they fit together to form the femorotibial articulation. In the sagittal plane, the curvature radius of the condyle isn't uniform, varying in spiral. The condyle spirals of the femur are not simple spires since it has a series of rotation centres that are themselves into a spire. [12] In other words, the condyle curvature represents a spiral of a spiral. However,the condyles did not show the same curvature because their curvature radius are different, and so the internal form of the femoral condyles will reflect its geometry as well as the applied efforts. However, this curvature radius decreases in anterior and posterior flanks. [12]

In each condyle can be identified the furrow that separates the condyle areas and patellar surface. [12]

The femur is smaller in women than in men due to the lower pelvis and the major obliquity of the femur's shaft, therefore allowing more mobility of the femur at the hip's articulation. However this leads to increased stress on the neck of the femur.

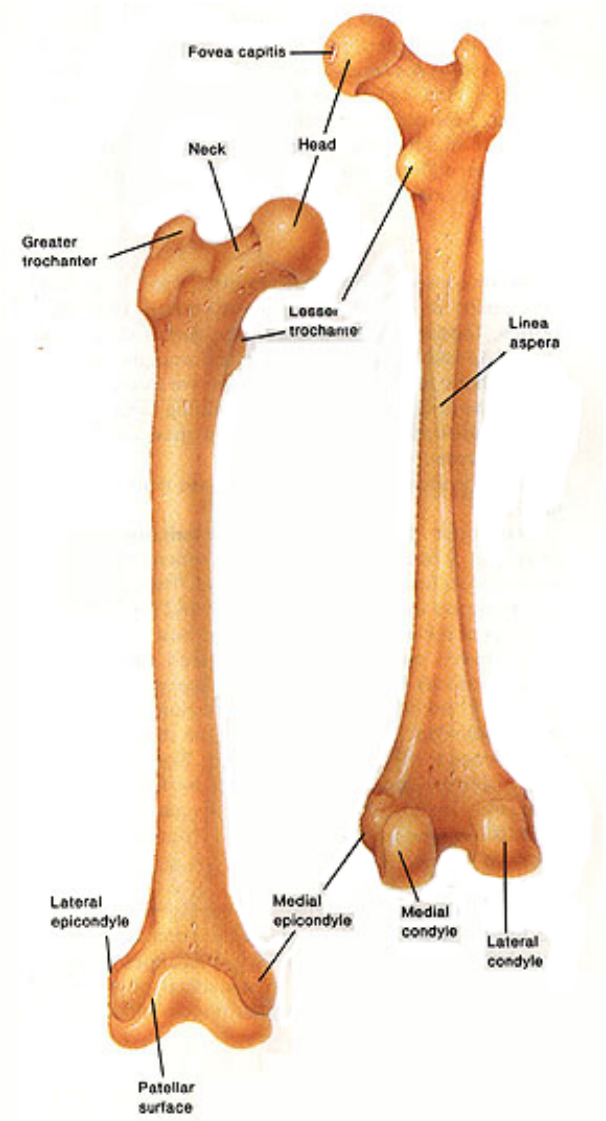

Figure 2.2: Femur's scheme
[http://www.edoctoronline.com/]

2.2.2 Tibia

Tibia, the second biggest bone in the human body, is located in the anteromedial part of the leg, almost parallel to the fibula. The top surface of the tibia presents a flat form, forming the tibial plateau, composed by the medial and lateral condyles and by an intercondylar eminence between the tibial and femural condyles. These joint surfaces of the tibia are covered areas, covered for cartilage in the upper region of each condyle. [5, 12]

The lateral condyle of the tibia internally has a face for the fibula's head.

The body of the tibia presents a triangular shape, having medial, lateral and posterior faces which is divided in four faces: medial; lateral; posterior and anterior face or peak composed by a broad and oblique tuberosity that provides distal fixation to the patellar ligament.

The most prominent area of the tibial bone is the anterior one, which is thinner at the junction of its middle and distal thirds.

It should also be noted that the distal end of the tibia is smaller than the proximal, having faces for the articulation with the fibula and talus. [5]

The Basic parts of the tibia and femur surfaces essentially allows motion in one plane (flexion and extension). The axial rotation involves torsion of the femur against the tibia or the opposite, where the intercondylar eminence of the femur acts as a pivot. The pivot consists of the intercondylar tubercles forming the lateral edge of medial condyle and lateral condyle of the medial.

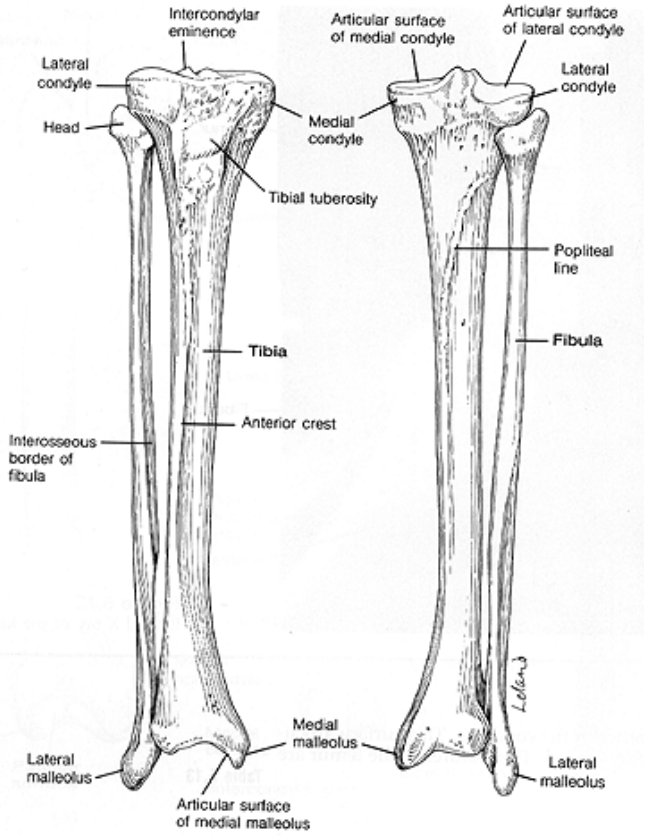

Figure 2.3: Tibia's scheme
[http://homepage.mac.com]

2.2.3 Patella

The patella, or knee-cap as it's usually called, is the largest sesamoid bone, which name derived from its similarity to sesame seeds.

This bone often varies from more than one place, lasting on two or three parts over the life.

As mentioned previously, the bones of the femur and tibia articulate themselves in order to create the knee joint, as well as the anterior condyles of the femur with the patella. The quadriceps femoris muscle is a very important muscle in various phases of the quotidian, like walking running and so on.

This muscle tendons join the distal thigh in order to form a single tendon, which is fixed at the base of the patella. The base of the patella is set by the patellar ligament to the tibial tuberosity.

The patella has an important function when the knee is flexed or extended, specially during the kneeling, once it provides the ability to resist and protect, the quadriceps tendon from the compression exerted on it.

The knee–cap provides additional leverage for the quadriceps femoris muscle, putting the tendon to the back, approximating it to the tibia. [12]

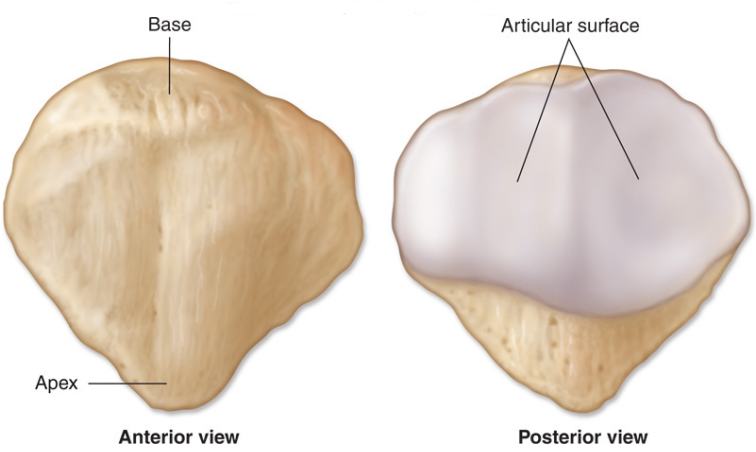

Figure 2.4: Patella or Knee–cap scheme
[http://aftabphysio.blogspot.com]

2.3 Knee Joint Biomechanics

To improve the artificial joints is necessary to understand correctly the biomechanics of this articulation.

The load reduction in this articulation during the daily activities and the implants design that supports these loads contributed to approximate the performances of this joint articulation to the natural one.

Although the knee apparently performs a movement similar to a hinge, this joint actually works with much more complex movements. The knee joint can be subjected to many types of movements such as, flexion and extension, medial to lateral, anterior to posterior and axial rotation. Because of this, its easy to understand that abnormal or even normal motion causes wear on these structures.

Beyond all the bone structures that makes up this joint, the knee joint is also composed by menisci and ligaments, surrounded by muscle.

The knee joint has six degrees of freedom, with flexion and extension, translation, rotation, varus or adduction (moving closer to the midline) or valgus or abduction (movement of the segment away from the midline). [14, 15, 16]

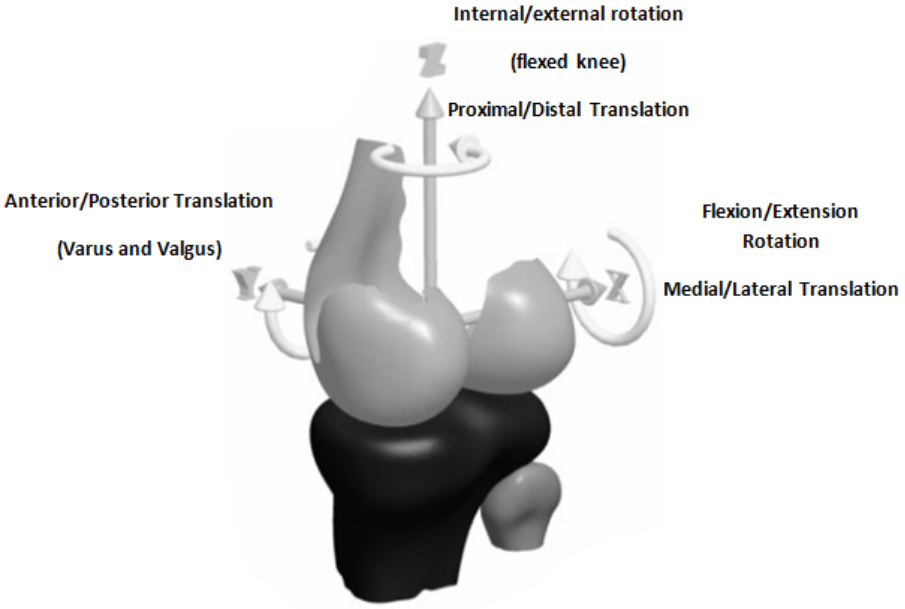

Figure 2.5: Schematic representation of the knee motion
[www.gustavokaempf.com.br]

Nordin et al [1] have measured motion in this joint during the walk. Full or nearly full extension was noted at the beginning of the stance phase (0% of cycle), at heel strike, and at the end of the stance phase before toe-off (around 60% of cycle) as showed in the figure 2.6 by blue oval. Maximum flexion was observed during the middle of the swing phase pointed in figure 7.2 by pink oval. These measurements are velocity dependent and must be interpreted with caution.

Taking the walking cycle into account, it is possible to describe the movement from full flexion to full extension in three phases. In the fully flexed condition the posterior parts of the femoral condyles rest on the corresponding portions of the meniscotibial surfaces, and in this position slight

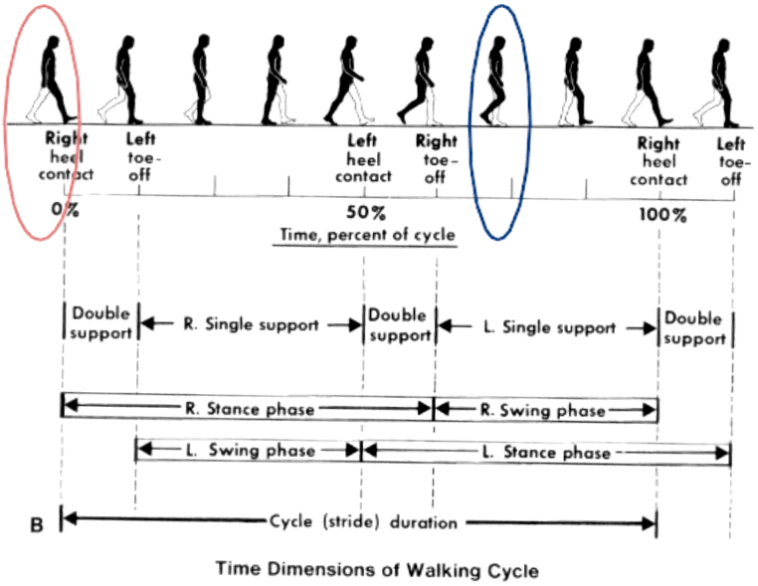

Figure 2.6: Distance and time dimensions of walking cycle [1]

amount of simple rolling movement is allowed. During the passage of the limb from the flexed to the extended position, a gliding movement is superposed on the rolling, so that the axis, which at the beginning is represented by a line through the inner and outer condyles of the femur, gradually shifts forward. In this part of the movement, the posterior two–thirds of the tibial articular surfaces of the two femoral condyles are involved, and as these have similar curvatures and are parallel one to another, they move forward equally.

The lateral condyle of the femur is brought almost to rest by the tightening of the anterior cruciate ligament; it moves, however, slightly forward and medialward, pushing before it the anterior part of the lateral meniscus.

The tibial surface on the medial condyle is prolonged further forward than that on the lateral, and this prolongation is directed lateralward.

When, therefore, the movement forward of the condyles is checked by the anterior cruciate ligament, continued muscular action causes the medial condyle, dragging with it the meniscus, to travel backward and medialward, thus producing an internal rotation of the thigh on the leg. When the full extension position is reached the lateral part of the groove on the lateral condyle is pressed against the anterior part of the corresponding meniscus, while the medial part of the groove rests on the articular margin in front of the lateral process of the tibial intercondyloid eminence. Into the groove on the medial condyle is fitted the anterior part of the medial meniscus, while the anterior cruciate ligament and the articular margin in front of the medial process of the tibial intercondyloid eminence are received into the forepart of the intercondyloid fossa of the femur. This third phase, by which all these parts are brought into accurate apposition, is known as the screwing home, or locking movement of the joint.

The human knee joint is a complex articulation, because it is actually composed by a double articulation, the tibiofemoral and patellofemoral articulation where large forces and moments are involved [1]

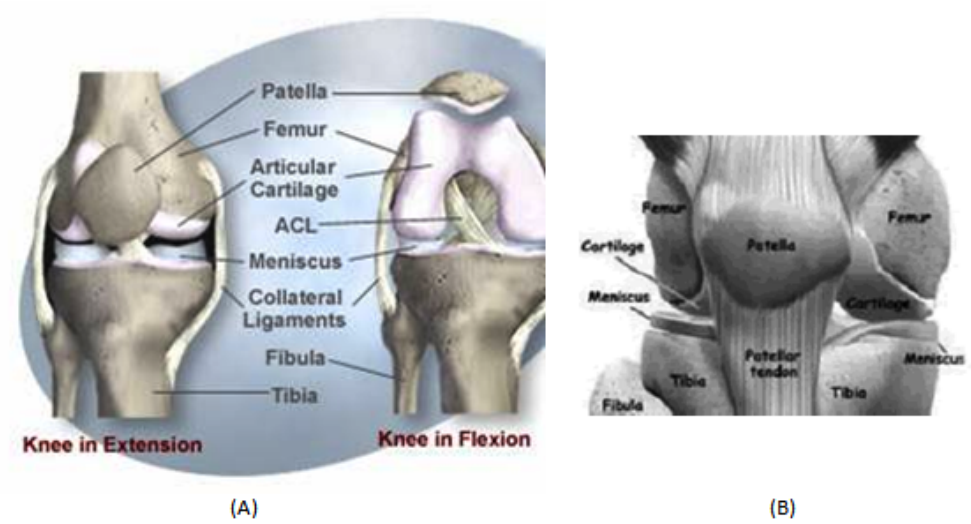

Figure 2.7: Knee joint components
[http://sotstenio.blogspot.com(A); www.veloxfitness.com.br (B)]

2.4 Anatomic Planes

The motion of the knee takes place simultaneously in three planes, sagittal, frontal and transverse plane.

The movement analysis in any joint requires the kinematic data. Kinematics is the part of mechanics that deals with the body movements without taking into account the loads and the weight. The analysis of forces and moments acting on the joint, involves both kinetic and kinematic data.

The kinematics defines the range of motion and describes the motion surface in an articulation on the previously described three planes. The reference point for measurements is defined as the body's natural position.

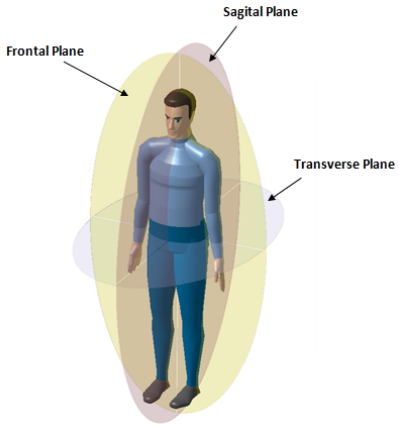

Figure 2.8: Anatomic biomechanical planes

The movement in the frontal plane is affected by the flexion degree of the knee joint, because when the knee is at full extension the movement in the frontal plane is denied. [12]

The angle that makes the difference between an easy or difficult movement in the frontal plane is at 30º. To angles till 30º, a passive valgus and varus increases while to angles higher than 30º, the motion in frontal plane decreases because of the limiting function of the soft tissues. [17] The sagittal plane is where the larger movements happens, because when it goes from full extension to full flexion the angle varies between 0º and 140º. [1, 12]

According to this, Laubenthal et al (1972) studied that the values of the range of motion of the knee joint in sagittal plane vary according the kind of activities. For example, climbing stairs varies between 0^0 and 67^0, tying a shoe from 0^0 to 106^0 or lifting an object from 0^0 to 117^0. [12] The movements of the knee joint in the transverse plane are influenced by the position of the sagittal plane. Because of the tibial and the femoral condyle, when the knee is at full extension the joint rotation is fully restricted since the medial femoral condyle length is greater than the lateral condyle.

The range of rotation increases as the knee is flexed, reaching a maximum at 90^0 of flexion; with the knee in this position, external rotation ranges from 0^0 to approximately 45^0 and internal rotation ranges from 0^0 to approximately 30^0. Beyond 90^0 of flexion, the range of internal and external rotation decreases, primarily because the soft tissues restrict rotation. [1, 12]

The movement in the sagittal plane is highest relatively to the frontal and to the transverse plane and because of that, this plane could be considered to be the main movement plane of the knee. Consequently, and in order to simplify the analysis, and its variables, the biomechanical variables can be restricted to one simple plane and to the forces exerted by a group of muscles, allowing this way an easy understanding of the movements and previous prediction of the main forces and moments in the joint. [5]

Advanced dynamic analysis of the biomechanics of the knee joint include all the soft tissues on the articulation, such as ligaments, meniscus and cartilage, as well as the previous complex structures.

2.5 Ligaments

The knee joint, in order to stabilize and control the movements, is composed by four main ligaments, two collateral and two cruciate ligaments, as well as three secondary ligaments, patellar, oblique popliteal and arcuate popliteal ligament. The ligaments work better when the load is in the fibber direction. [12, 18, 19]

Subdivided into two classes, according to their location: the medial collateral ligament (MCL) once that is on the medial side. and the Lateral Collateral Ligament (LCL) once it is on the lateral side.

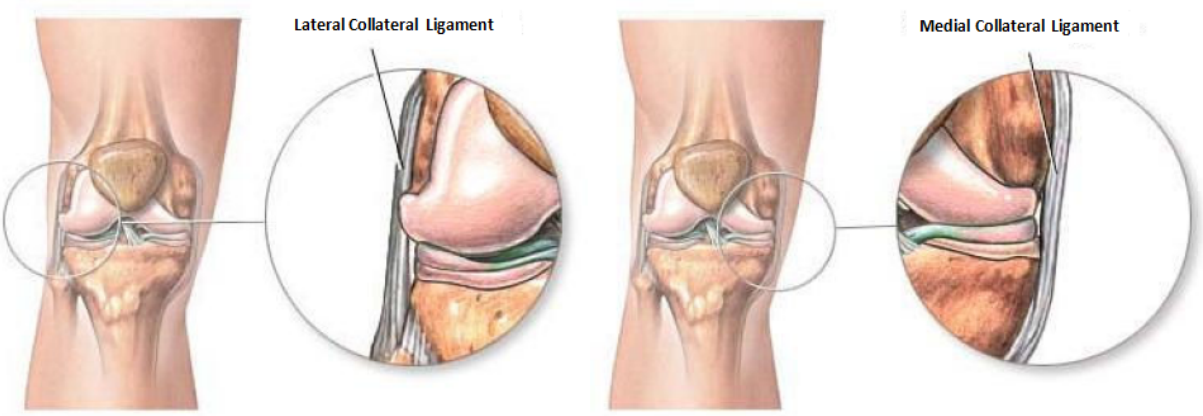

Figure 2.9: Anterior view of the knee with the representation of the collateral ligaments [2, 3]

The Medial Collateral ligament (MCL) joins the medial condyles of the femur and tibia, helping the resistance to the valgus stress, tibia rotation, lateral rotation and anterior displacement of the tibia. Its deep surface covers the inferior medial genicular vessels and nerve and the anterior portion of the tendon of the semimembranosus, with which it is connected by a few fibbers; it is intimately adherent to the medial meniscus. [3, 14, 20]

The Lateral Collateral ligament (LCL) is located at the lateral site of the knee, connecting the lateral condyles of the femur and tibia, improving the resistance forces in varus, rotation of the tibia and rotation of the tibia with posterior displacement. [20]

The cruciate ligaments are located inside the intercondillar space of the joint and they have a very important role in the knee kinematics, having a high structural organization. This ligaments are rolled up on themselves and on each other in all planes except the horizontal. This ligaments are subdivided into anterior cruciate ligament (ACL) and in posterior cruciate ligament (PCL), limiting the rotation and causing the sliding of the condyles on the inflected tibia.[19]

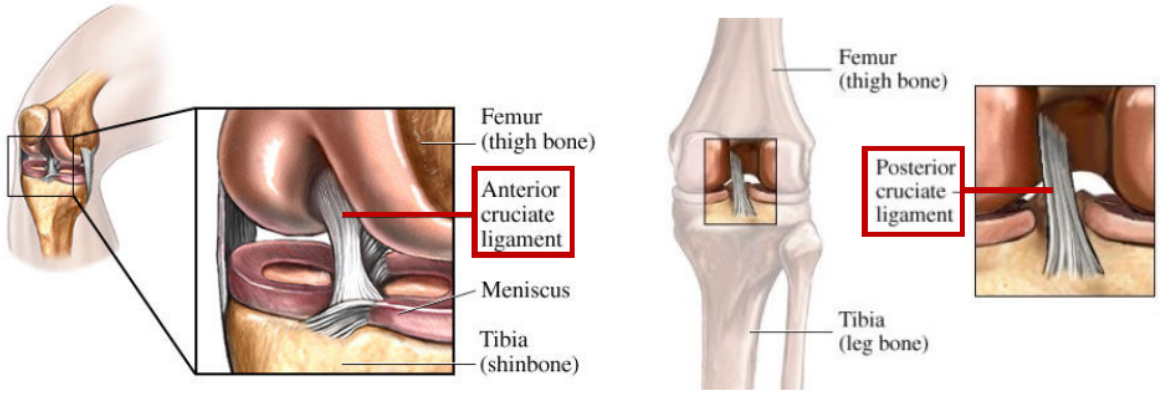

Figure 2.10: Anterior and posterior view of the knee with the representation of the cruciate ligaments [3, 4]

The anterior cruciate ligament provides the primary constrain to the anterior movement of the tibia under the femur. It resists to medial rotation of the knee, and in complete extension there is the maximum stress. This ligament is the weakest ligament of the cruciate ligaments once its blood supply is reduced. The anterior cruciate ligament has its origin in the anterior intercondylar area of the tibia, soon after the medial menisci fixation. [14]

The posterior cruciate ligament, is the strongest cruciate ligament, having its origins in the posterior intercondylar area of the tibia, passing over and in front of the medial side of the anterior cruciate ligament to settle on the anterior side of the lateral face of the medial femoral condyle. This ligament creates primary restriction to the posterior movement of the tibia under the femur; it resists to knee rotation and also helps to prevent hyper extension of the knee joint. This ligament is also the main factor for stabilization of the femur when the knee is flexed. [14]

Pattelar ligament is composed by the tendon of the femoral quadriceps muscle and extends from the patellar apex to the tibial tuberosity. The medial and lateral portions of the tendon of the quadriceps pass down on either side of the patella, to be inserted into the upper extremity of the tibia on either side of the tuberosity. The patellar ligament is the anterior ligament of the knee joint. It merges with the patellar medial and lateral retinaculum, since the retinaculum are responsable for the lateral support of the articular capsule of the knee. [5]

The oblique popliteal ligament is an expansion of the muscle tendon semimebranaceo which reinforces the knee joint in the posterior face. The origin of this ligament is on the posterior medial condyle of the tibia and passes upper laterally to settle in the center of the posterior surface of the fibrous capsule. [5]

The arcuate popliteal ligament is a ligamentar reinforcement of the posterior fibrous capsule which is positioned in an arc. It begins in the posterior face of the fibula's head, passing superomedially to the tendon of the popliteo muscle and spreading itself under the posterior face of the knee joint. This ligament performs the reinforcement of the fibrous capsule on the posterior part of the knee. [5, 12, 19]

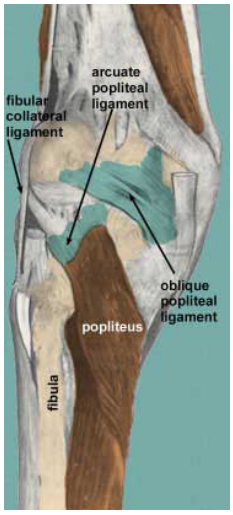

Figure 2.11: Popliteal ligament of the knee joint
[http://wapedia.mobi]

A tendon is a glistening white cord of connective tissue that attaches muscle to bone. It is similar in structure to a ligament, which connects bone to bone. Tendons play a critical role in the movement of the human body by transmitting the force created by muscles to move bones. In this way, they allow muscles to control movement from a distance.

Like ropes, tendons are tough, fibrous and flexible. They are not, however, particularly elastic. If they were, much of the muscular force tendons are intended to carry would dissipate before it had a chance to even reach bones.

Tendons are formed from the same components that make up other kinds of connective tissue, such as cartilage, ligaments and bones. These components are collagen fibers, ground substance, and cells, which in the tendon are called fibrocytes. At the point where a tendon touches bone, the tendon fibers gradually pass into the substance of the bone and meld with it. The tendon microstructure can be observed in Figure 2.12. [3, 20]

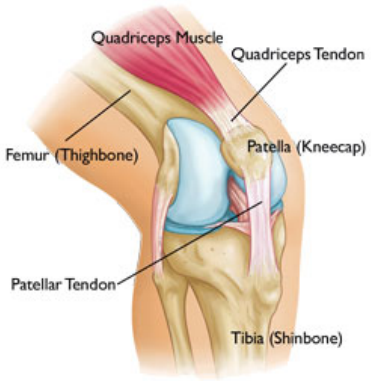

Figure 2.12: Quadriceps Tendon
[http://orthoinfo.aaos.org]

2.6 Minisci

One of the fibrocartilages is the meniscus of the knee. Minisci from the greek word meniskos, that means growing, are present mainly in the joint femorotibial cartilage, between the tibia and femur condyles.

Minisci can be subdivided in medial and lateral minisci, and are composed by resistents fibrocartilages. [21]

Both, the medial menisci than the lateral, are located above the tibia, with a similar shape of a half moon. As a cartilage, menisci have a few blood vessels, hindering its regeneration in case of injury.

The upper surfaces of the menisci are concave, and are in contact with the condyles of the femur; their lower surfaces are flat and rest upon the head of the tibia; both surfaces are smooth, and invested by synovial membrane.

Each meniscus covers approximately the peripheral two-thirds of the corresponding articular surface of the tibia.The menisci plays an important role in the articulation of the knee, since it directly assists in joint stabilization, deepening the joint surfaces of tibia and femur. The menisci also helps to absorb the impact, giving a part of the sustention load because of the weight in full extension and a part of flexion load. The menisci promote joint lubrication and also limit the movement between the tibia and femur. [22]

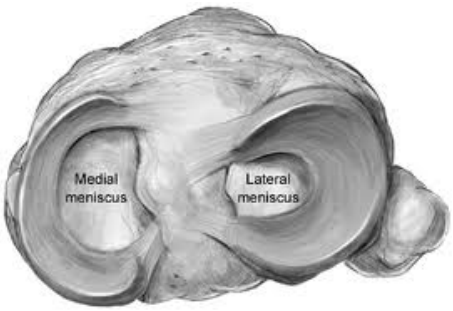

Figure 2.13: Minisci
[http://www.msd.com.mx]

2.7 Articular Capsule

The articular capsule is another important structure to support the knee. The articular capsule that surrounds the articulation is thin and scare in some areas such as lateral condyle in order to allow the tendon of the popliteus muscle fixate on the tibia.

The strong fibrous capsule is fixed to the upper femur, near the banks of the articular condyles and also in the intercondylar notch. Inferiorly, the fibrous capsule attaches to the tibia at the articular margin, except where the popliteo tendon muscle crosses bone.

The establishment of tibia is more complete than in the femur. The only problem is in the region of the tibial tuberosity, wich gives attachment to the patellar ligament. It is convenient to think that the articular capsule is a cylindrical sleeve that passes between the femur and tibia with a crash at the anterior face that houses the patella. [5, 12, 23]

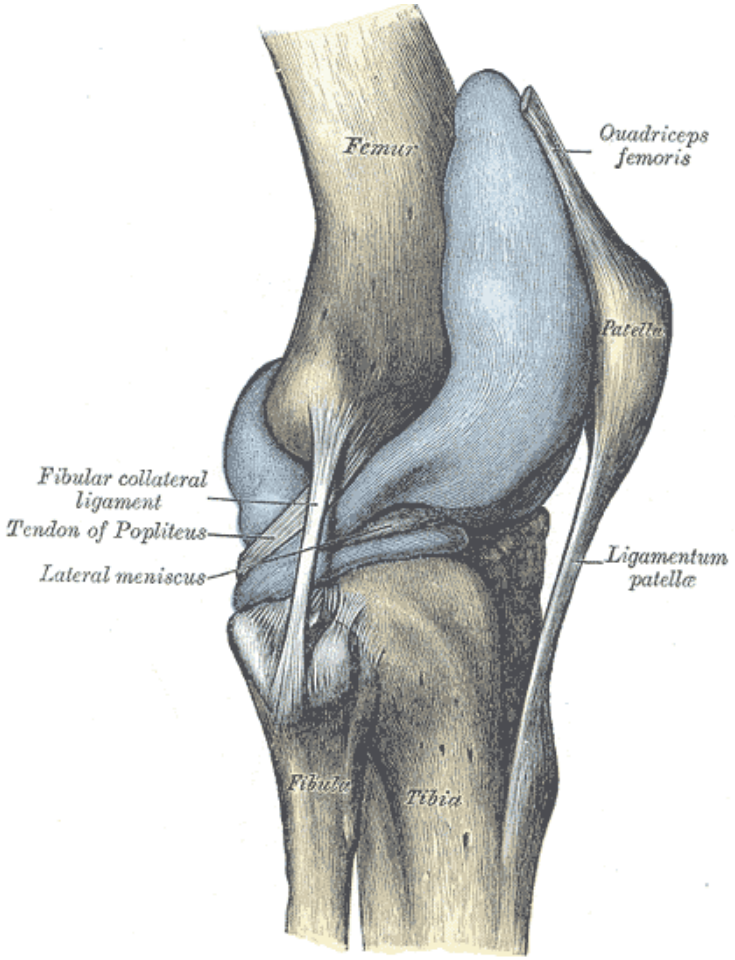

Figure 2.14: Articular capsule
[http://www.wikipedia.com]

2.8 Varus and Valgus malalignment

The knee joint combines the two bigger bones of the human body and because of the forces that are concentrated on it, in some cases or illness/injury in others, the correct alignment of these bones isn't achieved.

In normal circumstances, where the knee is correctly aligned, its load-bearing axis is on the line that runs down the middle of the leg through the hip, knee and ankle. However, there are cases where this axis is shifted from the center a few degrees, creating an articulation malalignement.

The joint with angular deformities often has a tense complex capsuloligamentar in the compartment where the arthrosis is installed and slack in the other side. If the surgery does not correct this deviation, the overload leads to a progressive slack, instability and the short sustainability of the knee joint. [10]

During the revision of total knee arthroplasty, sometimes is found this malalignement is found between the femur and the tibia. To this type of malalignment is given the name of varus or valgus deformity (varus or valgus knee). This term refers to the direction pointed by the distal segment of the knee joint points. [5]

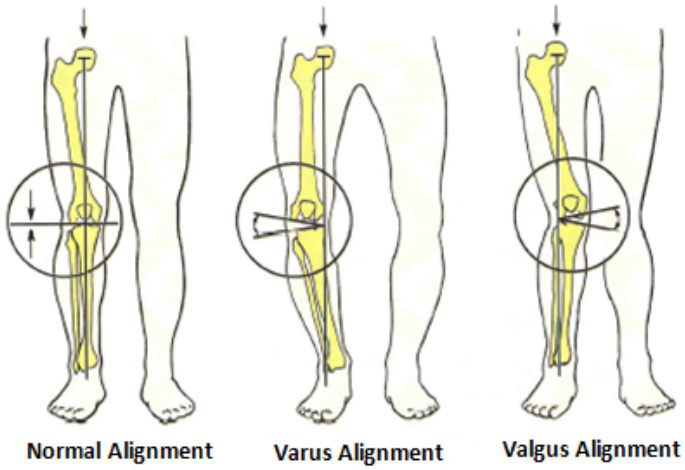

Figure 2.15: Varus and Valgus malalignment [5]

This kind of malalignment between tibia and the femur can cause arthrosis, i.e. the cartilage destruction in the knee joint, causing pain and sickening sense on the patients.

The characterization of these two types of malalignment is mainly based on the side that the angle occurs, as previously mentioned. A lateral angle leg is called as valgus knee (genu valgum), which results in an extra tensile stress being placed on the medial side of the knee and the lateral side of the ankle. Although the valgus can be at least partly compensated for by strengthening the quadriceps muscles which stabilize the knee, and strengthening the muscles which support the lateral side of the foot. [24]

On the other hand, when the angle is from the inside of the knee joint, that malalignment is called as varus knee. In other words, the varus knee deformity is basically the opposite of valgus knee deformity. The varus deformation will cause greater stress on the medial compartment of the knee. [25]

However, this kind of deformities and malalignment can be corrected as states Russel E. Windsor, at "Current Concepts in Joint Replacement 2010 Winter Meeting" in Orlando, Fla. [26]

Since the varus deformity is characterized by joint space narrowing with medial joint erosion, potentially occurring in a normal medial collateral ligament (MCL), Windsor et al.[26] states that if this deformities occur in small angles (between 10 to 15 degrees), should be corrected using a rectangular space of both flexion and extension. However, if the angle deformity is bigger than 15 degrees, it could require a release to equalize the flexion gap.

Regarding to valgus deformity, Windsor [26] says that this is characterized by a contracted or tight lateral ligament (LCL), iliotibial band, popliteus muscle and ligament complex. In this cases the goal, according to Windsor, is to achieve a deformity between 0 and 5 degrees.

A passively correctable valgus deformity could be handled by restoring the epicondylar axis without lateral release. Formal releases are usually necessary, and Windsor reported there is a controversy regarding which release should be performed first. [26]

For moderate valgus of 15° to 45°, Windsor starts with the iliotibial bands either step-cut or distal off of Gerdy's tubercle, then the posterolateral corner of the arcuate ligament, then the LCL. He added that with bigger releases, the popliteus should be preserved to avoid a "significant gaping" in the lateral side inflection. [26]

Merely as a note, although at the first sight we could think that this kind of deformities only occur in older people who may have already performed a first surgical intervention in the knee joint that is not true. Sometimes, children one or two years after starting to walk have this kind of malalignment on their knees. The persistence of these abnormal angles of the knee in late childhood usually means that there are deformities that may require an intervention. If this intervention does not happen, the articular cartilage will be rapidly eroded. [5]

2.9 Total Knee Arthroplasty

The Parisian, Jules P'eau (1830-1898), defined an arthroplasty as "the creation of an artificial joint for the purpose of restore motion".

As stated above the knee articulation is a joint that depends mainly on two bones, the femur and tibia. Each end is covered by a cartilage that allows movement. When that cartilage is damaged or degraded the bones contact each other directly, causing an inflammatory response and pain to the patient [27].

To solve this problem arose the knee arthroplasty, in order to restore a normal life to the patients, allowing them to walk without pain. At this chapter we will introduce the first total knee arthroplasty. This is a surgical procedure where parts of the knee joint are replaced by artificial parts, [28] usually metallic and plastic parts, whose main objectives are the elimination of painfully symptoms, the correction of deformations and stabilization of the knee.

It was back in the nineteenth century that took place the first attempts to perform a knee arthroplasty, using techniques such as interposition or resections. In 1826 Barton attempted one of the first simple resection in a joint but he was unsuccessful because later on he came to suffer from ankylosis (joint stiffness). Only a few years later, in 1861, took place the first successful knee arthroplasty, using soft tissue interposition, performed by Ferguson at the Medical Times.

At this time, the material used for reconstructing the joints was soft tissue. The problem with using this kind of material is that it's prone to suffer from infections and anchylosis, so there was a need to search for new materials, such as plastics and metals. With this need, in 1938, came a new age in the knee arthroplasty. In 1951 Borje Walldius invented the first prototype of a hinged prosthesis in acrylic resin, in Sweden. [5]

So that being said, one can conclude that this intervention, which has been practised for over 50 years and initially was not so successful, due to the complexity of the knee joint [29] , nowadays, thanks to the advancements in the knowledge of knee mechanics and technology, [29]is one of the most successfully performed operations, with 95% to 98% good to excellent results reported at 10 to 15 years.

Although there are a lot of factors which can cause problems in the knee joint, the most common ones are usually related to the absence or deterioration of the articular cartilage. Among the various diseases we can quote the most common ones: osteoarthritis, which can be caused by an old trauma, overexertion or by changes in the knee shape, causing the surfaces of the knee joint to become rough and irregular; and rheumatoid arthritis which is a chronic inflammatory disease. [5, 30, 31]

Mestriner et al. [32] show, by a study made with twenty six T.K.A. in arthritic knees, quite satisfactory results for the treatment of osteoarthritis.

In another study performed by the same authors, with the objective of establishing possible differences in the behaviour of TKA in twenty six knees with rheumatoid arthritis and twenty six knees with osteoarthritis, concluded that there were significant differences between the two groups, reaching the conclusion that the results were excellent, 92% for rheumatoid arthritis and 80% for osteoarthritis. [32]

This type of surgery has had a very significant increase in the last years, mostly due to the ageing of the population and also due to good functional results provided by the progressive development of both implants and instrumentation used. [31]

Although the results of the first knee replacement surgery are very satisfactory, there are several factors that influence the durability of the knee prosthesis and the success of total knee arthroplasty

and sometimes complications occur, such as joint stiffness, instability and infection. The infection is the most feared complication and it's usually caused by bacteria. [33]

The factors that influences the durability of prostheses are inherent to the surgical techniques adopted, the design of materials to correct the defects and also to the material used to make the implants. Despite all this there are two more complications one has to consider concerning this type of procedure: osteolysis and stress-shielding.

Osteolysis generally refers to a problem common to artificial joint replacement such as total hip replacements, total knee replacements and total shoulder replacements. This problem is the end result of a biologic process that begins when the number of wear particles generated in the joint space overwhelms the capsule's capacity to clear them. The residual particles stimulate a macrophage-induced inflammatory response that can lead to bone loss and subsequent implant loosening. Although cement particles were once exclusively blamed for osteolysis, it has become clear that any particle debris can result in bone resorption. [34]

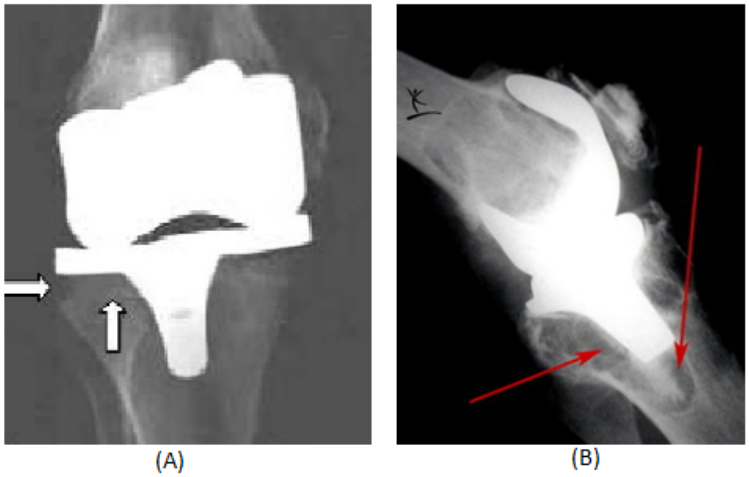

Figure 2.16: Osteolysis in the knee arthroplasty
[www.medscape.com]

By the other hand, stress-shielding refers to the reduction in bone density as a result of the removal of normal stress from the bone, by an implant. This was explained by Julius Wolff, a German physiologist, whom in 1892 proposed an explanation to this problem name as Wolf's Law. This law states that bone density changes in response to changes in the functional forces on the bone.

Wolff proposed that changes in the form and function of bones are followed by changes in the internal structure and shape of the bone, in accordance with mathematical laws. Thus, in mature bone, where the general form is established, the bone elements place or displace themselves, and increase or decrease their mass, in response to the mechanical demands imposed on them. This theory is supported by the observation that bones atrophy when they're not mechanically stressed and hypertrophy when they are stressed. [35]

2.10 Bone defects on the proximal tibia

On this chapter the most common defects will be addressed. The identification of bone defects in the tibia during the revision of knee arthroplasty is important in order to provide a proper evaluation, thus providing a more appropriate intervention. Preoperative radiographs should be used to classify bone defects into categories of comparable difficulty.

When carrying out the preparation for revision of total knee arthroplasty, surgeons should anticipate the worst possible scenario, being the experience of the surgeon a very important factor, and taking into account all the difficulties that this surgery entails.

There have been various attempts over the years to establish a classification of bone defects, both for first arthroplasty and for the revision arthroplasty.

Dorr et al. [36] in 1989 established a classification, Dorr's classification, considered to be the most straightforward one, in which defects are defined as either central or peripheral and cases are separated as primary or revision procedures, not being made any attempt to define the size and location of the defect.

Years later, Insall et al. [37] used a similar terminology in primary cases of central and peripheral bone defects. This classification was based on three stages of how the defect should be handled: in the first stage treatment involves the simple use of cement; the second stage is related with the use of cement or augmentation plus a stemmed component; and the third stage involves the use of block augmentation and stem extension.

Although several attempts have been made, no bone defect classification has been accepted by orthopedic surgeons until the classification developed by the Anderson Orthopedic Research Institute (Aori) emerged, which goal is to make an easy system to understand and apply. [38]

This new classification system is based on five main criteria:

– use of the same terminology for both femoral and tibial defects due to the similarities in the both metaphyseal segments;

– the commonly used definitions in most classifications of bone defects, as central or peripheral, cortical or cancellous, contained or uncontained were eliminated because of the absence of cortical bone in the metaphyseal segments of the distal femur and proximal tibia;

– clear and precise definitions were established to minimize ambiguity when bone defects are categorized;

– was established a minimum number of defects to permit clinical investigators to accumulate enough cases to allow meaningful statistical comparisons;

– finally, this classification was created to allow retrospective categorization of cases through intraoperative information and post-operative radiographs. [5, 6]

In the evaluation system Aori defects are classified only when a component has been removed, based on preoperative radiographs for anticipated bone deficiency and then the classification is either confirmed or changed intra-operatively. Sometimes, due to lack of clarity of preoperative methods, there is the need to classify the bone defects through the post-revision radiographs.

Therefore, and based on previously described, the defects can be classified into three distinct classes:

2.10.1 Type 1 defect – intact metaphyseal bone

Is a bone defects that don't compromise the stability of the component.

In this type of defects there is a correctly aligned tibial component significant implant subsidence or tibial osteolysis. In T1 defects the metaphyseal area is intact, and though minor defects might be expected, they are not enough to put the stability of the joint at risk. Usually, in order to control and correct these defects, it is used either a standard component with a combined polyethylene and metal thickness of less than 20 mm, or cement grafts. [5, 6]

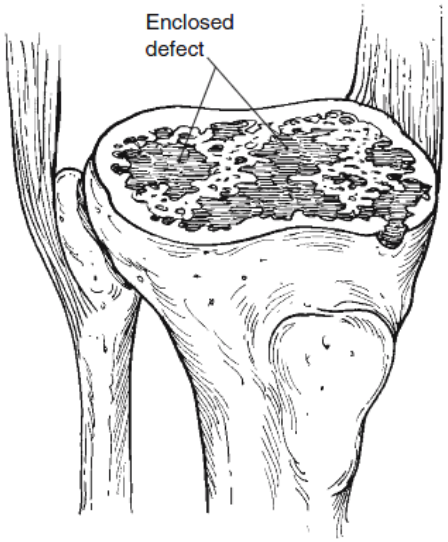

Figure 2.17: Bone Defect Type 1. [6]

2.10.2 Type 2 defect – damaged metaphyseal bone

Is the bone defects that don't compromise the stability of the component.

The type 2 defect is often caused by component loosening and secondary subsidence of the tibia, commonly into a varus orientation. This type of defect requires the filling with bone graft, cement or metal wedges. A circumferential radiolucency develops between the cement and bone as the component subsides. The distance between the top of the fibula and the component is diminished. The lateral radiograph is useful in measuring this distance. Osteolysis may present as cavitary defects beneath the component. This kind of defect can still be subdivided into two classes, 2a and 2b: in the type 2a only one of the condyles is affected and in 2b both condyles are affected. [5, 6]

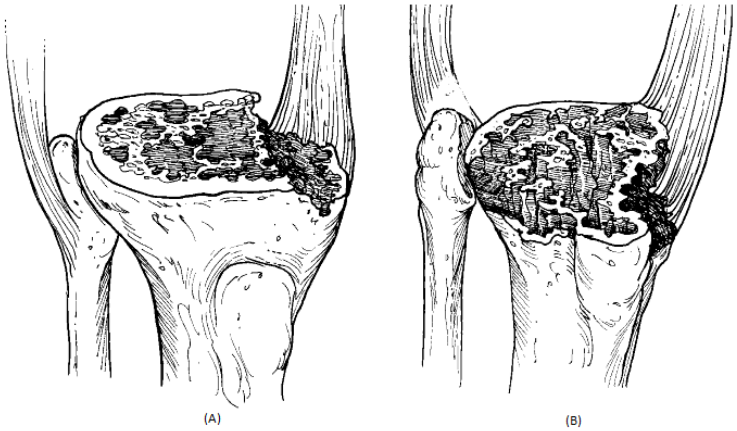

Figure 2.18: Bone Defect Type 2a (A). Bone Defects Type 2b (B). [6]

Type 2a defects is when the bone defects occur either in a femoral condyle or in a tibial plateau.

The type 2a defect is usually the result of tibial component loosening and subsiding into varus. The tibia rarely subsides into a valgus orientation, even in knees with valgus alignment. On preoperative radiographs, a widening radiolucency is frequently seen beneath the tibial component. Bone in the opposite tibial plateau is present at a relatively normal joint line level. Type 2a defects can also occur with aseptic loosening of a unicondylar tibial component.

It is important to avoid converting a type 2a defect into a type 2b defect by resecting the tibial plateau at a more distal level. When a type 2b defect is created iatrogenically, a thicker tibial component is required. [5, 6]

Type 2b defects is when the bone defects occur on both femoral condyle or in the plateau.

In its turn, as stated previously, defects of type 2b involve both plateaus, since in this type of defect a metaphyseal segment of tibia is damaged. The damage may extend to the level of the fibular head, but should not include extensive destruction of bone below this level. The surgical management of a type 2b defect usually includes the use of a long-stemmed tibial component and reconstruction of the tibial plateaus by bone graft, augments, or an extra thick tibial component. In this defect is convenient to use wedgeshaped components when one notes a significant bone loss in both plateaus, although that bone loss may be larger in one of the sides. A stem can also be used, especially if a structural bone graft has been used. The use of cement, on the other hand, isn't very common in this type of defects. [5, 6]

2.10.3 Type 3 defect – deficient metaphyseal bone

Bone loss that compromises a major portion of either condyle or plateau. These defects are occasionally associated with collateral or patellar ligament detachment and usually require bone grafts or custom implants.

This kind of defect occurs when there is an insufficient metaphyseal segment. It is also known that an underlying bone fracture may contribute to the development of type 3 defects. The type 3 tibial defect extensively damages cancellous bone of the proximal tibia. The fibular head may be retained, leaving it higher than the proximal tibia defects. When this type of defect occurs it is necessary a major structural allograft to repair the proximal tibial segment for joint line restoration and component fixation.

As this defect presents a great loss of the proximal tibia, it is necessary to recourse to a structure allograft or a custom tibial component, being necessary to fill with cement in order to achieve rotational stability. During the correction of type 3 there may be required a varus-valgus constrained implant, as well as a reattachment of collateral ligaments and a reconstruction of the extensor mechanism. [5, 6]

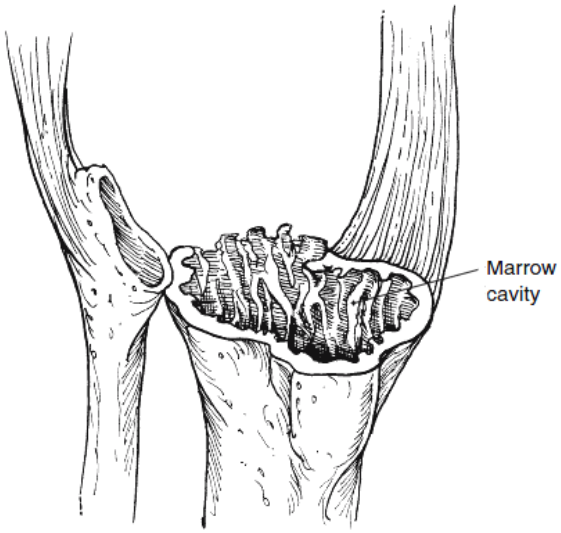

Figure 2.19: Bone Defect Type 3. [6]

Due to the diversity of defects it is also obvious that the methods of solving them are also different. As such, and as previously mentioned, bone defects can be treated by filling the defect with cement, with modular wedges and augmentation, with bone grafts and the use of intramedullary stems in both the tibia and femur, since its classification is identical, although component loosening in tibial implants are more frequent then in femoral, since the tibial prosthesis subsides into varus creating a bone defect in the medial tibial plateau. [39, 40]

These defects definitions will be described in the follow summary table:

So, generally a type 1 defect is indicated when cancellous bone is present at a normal joint line level, permitting the use of standard non stemmed implants. The type 2 defects indicate a damaged cancellous bone that requires augmentation, small structural grafts or thick cement fill to

Defect type	Identifying features	Treatment
T1	no component subsidence or osteolysis; no cancellous defects in the peripheral rim; cancellous bone that will support an implant; defects can be filled by small amounts of particulate bone graft or cement; a normal joint line is present	no augments (>4 mm), structural grafts, or cement fill (>1 cm);
	tibia—component above the fibular head and a full metaphyseal segment	no stemmed components necessary
T2	cancellous bone inadequate to support the implant; cancellous defects may require bone grafts; the component used requires augmentation to restore the joint line; osteolysis may be more extensive than radiographs indicate	joint line restored with an augmented component (>4 mm), particulate autograft or allograft, or cement fill (>1 cm);
	tibia—component is at or below the tip of the fibular head and the tibial flare is reduced	stemmed components should be used
T3	marked component migration; knee instability; deficient metaphyseal segment	structural graft, augment or cement, or a hinged component used to reconstruct the condyle or plateau;
		stemmed components required

Figure 2.20: Bone defects summary [6]

restore joint line level and knee stability. The type 3 defect should be reserved primarily for those severe cases in which the damaged metaphyseal segment of bone must be repaired with a salvage hinged implant or with major bone grafts to support the component. [6]

It is noteworthy that in any classification scheme there may be cases where classification is difficult because they are in the borderline, and when that happens the postoperative radiographs and the surgical treatment mode should be evaluated, never forgetting that the target in the treatment of the defects described is to create a good support surface for the tibial plateau.

Although in the case of revision arthroplasty the grafts are from other donors, which may in the long term develop complications either because of lack of union of the halogens to the bone (other donor),or due to the graft migration because of the resorption of the graft or because of infections. [5, 37, 39]

Like any other joint replacement implant, the total knee arthroplasty implant doesn't last forever and it may fail after ten to fifteen years or even sooner. [41] Therefore there is a need for maintenance of the prosthesis. As such, in cases of total knee arthroplasty, the treatment used is a revision of the total knee arthroplasty which, in very general terms, can be defined as an operation to replace in part or to replace the entire previous prosthesis (prosthesis, cement, surrounding tissue and dead bone) that wears out, loosens or develops a problem, before inserting a new prosthesis.

The symptoms indicating the need for an arthroplasty revision are pain and limited mobility. Another way to detect the need for review is through an X-Ray examination, which is recommended to be made lifelong following the total knee arthroplasty. This failure, and the need of a new surgical intervention, may result from many causes such as: plastic wear (in this case only the plastic insert is changed); instability (the knee is not stable and may giving way or not feel safe when the patient walks); loosening (loosening of either femoral, tibial or patella component which can be detected on regular follow-up X-Ray examinations); infections (usually presents as pain but may present as swelling or an acute fever); fracture; recurrent dislocation; ongoing unrelieved pain; osteolysis. [41]

As stated above, revision surgery is much more complex and technically more difficult than the primary total knee arthroplasty due to the difficulty removing the old prosthesis and also due to the reduced amount of bone to place the "new knee" into. [41]

In other words, bone loss is closely related to the revision of total knee arthroplasty, as it is necessary to make a new incision in an area previously traumatized during the first surgery. We also need to consider bone loss by osteolysis and the phenomenon of bone resorption as a consequence of stress-shielding effect, caused by the implant placed in the first surgery. All this leads to increased risk of inflammation and difficulty removing the prosthesis components. [5]

(a) (b) (c)

Figure 2.21: Revision of total knee arthroplasty
[http://juninhobarboza.blogspot.com/ (a); www.zimmer.com (b)]

2.11 Materials to repair the bone loss

Sometimes extra bone is required since the revision arthroplasty requires, in many cases, the removal of large bone volume. This problem, of bone loss, can be solved in several ways: bone grafts from the bone bank, artificial bone substitutes or even the patient's bone [42]; modular wedges that add to tibial and femoral components; intramedullary stem; and bone cement extracts in cases of minor bone loss, to fill the empty spaces. [5]

Figure 2.22: Materials used to repair the defects in R.T.K.A.
[www.rmedinc.com]

This whole procedure is very invasive to the bone, thereby increasing the time of surgery and also the risks associated with post-operative. The purpose of the replacement bone is to ensure stability of the new components used in the revision.

Typically, the components developed for the primary arthroplasty don't give the necessary guarantees of stability since, its areas of support are usually substitute materials of primary bone loss. [5]

Thus, in cases of revision of total knee arthroplasty it's essential to use components developed specifically for each case, to ensure joint stability.

2.11.1 Metal Wedges

Metal wedges are used in order to give stability to the joint. In revision total knee arthroplasty, durable long-term fixation of the tibial components is dependent on component stability within host bone [43]

Although this is rarely an issue in primary procedures, in the revision setting component fixation poses a significant challenge due to the loss of metaphyseal bone stock and to the presence of bone defects.

Therefore, and because this assessment is very important, the management of bone defects of the tibia in R.T.K.A. is controversial [44, 45] since there is a wide variety of defects and there's lack of evidence from clinical studies on experimental basis to the surgical decisions.[45]

The defects can be rebuilt/repaired through the use of several techniques such as filling with cement, modular metal augments, structural allografts and compact morsellised bone graft. [46]

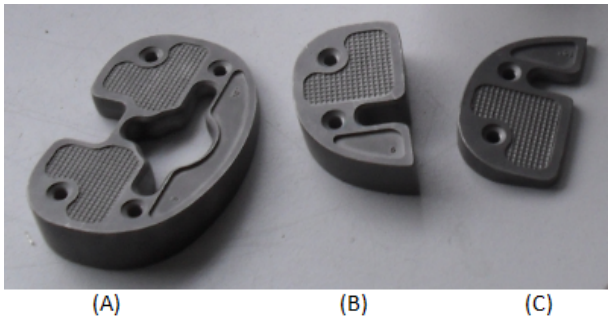

Figure 2.23: Metallic Total Wedge (A); Metallic Block (B); Metallic Hemi–Wedge (C)

Modular augments used beneath the tibial tray are usually wedges shaped, which fit above an oblique bone resection, or blocks. Hemi–wedges can be used to fill small peripheral defects, whereas full wedges augments can be used to correct axial alignment beneath the tibial tray or to substitute for more extensive proximal cortical bone loss [47]

Block augments, often also called as step wedges, are employed when bone loss at cortical rim includes segmented medial (or lateral) bone and supporting anterior or posterior cortical bone at the level of the tray-bone resection.[47]

Studies published by Fehring et al [48], indicate that tensile strain within the cement-bone interface was less with block augments, when compared with other wedges. Although the maximal strain differential between step wedges and other wedges was only slight, one should use the augments that best fill the defects.

However, as the first clinical reports using metal wedges for tibial bone deficiencies were in 1989 by Brand et al. [49] there aren't long term results in what refers to modular augments in the revision of total knee arthroplasty.

In that same study, Brand et al.reported that twenty two knees with modular metal wedges were used, in which three of the twenty two knees treated were cases of revision of arthroplasty. In each case a small cemented stem was used. It was reported that in the past thirty seven months, in six of the operated knees the follow up revealed radiolucent lines beneath the tibial wedges, however no tibial tray was judged to be loose. [47, 49]

Modular augmentation represents an attractive option in re constructive surgery, allowing a surgeon to produce a custom implant, to re establish correct component levels with respect to the joint line, maintaining or re establishing limb alignment, and to adjust soft tissue balance.

Tibial augmentation with modular metal wedges or block is usually applied to defects of 5 to 20 mm in depth, particularly when these defects fail to support more than 25 % of the tibial base plate.

The depth of modular augmentation has to take into account that most commercially available augmentations don't taper as the host bone metaphysic does, and that larger tibial augments may likewise expose a sharp prosthetic edge at the base of the augment and may cause pain. It's important to note that the depth of a modular augmentation is additionally limited by the extensor mechanism. Resection levels greater than 20 mm below the native joint line place the tibial tubercle and extensor mechanism in jeopardy, especially on the lateral side. [47]

Extensive proximal tibial bone loss over both surfaces of the proximal tibia may be handled with thicker polyethylene inserts. However, as the polyethylene inserts thickness increases, the stress at the insert locking mechanism also increases, potentially leading to increased micro motion. This negative biomechanical consequence can be offset by elevating the tibial base plate and reducing the thickness of the polyethylene insert required. Full tibial base plate augments or bilateral matched medial and lateral augments can be used to raise the tibial tray closer to the native joint line. [47]

However, clinical results in which metal augments are used are excellent in what concerns to their use related to potential bone loss, and related to fretting and dissociation of the modular components. [50]

This bone loss occurs because the use of modular metal augment does not involve restoration of bone stock, and may actually require further resection of bone to accommodate the component. [45]

2.11.2 Stem

With the aim to create an increased consistency of TKA revision, many systems and components have been developed. One system often used is modular stem, because it provides additional fixation and ensures a better alignment between the components of the tibia and femur. These stems are used especially when there is a lower quality of bone or the existence of bone defects in the metaphysic area. Its use is also recurrent when metallic wedges or bone excerpts are also used [5]

Figure 2.24: Some stems used on knee arthroplasty
[www.biotech-medical.com; www.djosurgical.com]

There are several types of stems, which differ depending upon the diameter, length, and it's type of attachment to the bone. In cemented stems the stem fixation is ensured by the layer of cement between stem and bone, whereas in the press-fit stems the fixation is established through the intramedullary canal, being in direct contact with the bone. If the stem is short the contact is made in the metaphysic, on the other hand if the stem is long the contact takes place in the diaphysis. [5]

There is a main difference between cemented stems and press-fit stems. Although cemented stems offer a bigger contact surface between the stem and the bone, due to the cement, it's much more difficult to remove them during a revision of total knee arthroplasty, leading to the destruction of the adjacent bone. On the other hand the press-fit stem, is very easy to remove and doesn't damage the adjacent bone but it is more likely to cause pain in its end. This type of stem leads to great effort in its end due to its length, causing bone hypertrophy and even bone fractures. [31, 51, 52]

It is worth noting that a study by Jazrawi et al., in a cadaveric tibia, described that long press-fit stems provide the same stability as a totally cemented short stem, without noticing an increased stress-shielding effect in the proximal area of the tibia. [18]

In another study, developed by Akbrektsson et al, was demonstrated that non cemented long stems allow good stability and less sinking [53]

These stems are usually made of titanium alloys due to studies conducted by Barrack et al, demonstrating that 18.8 % of patients who had stems of Cr-Co alloys have been complaining of pain while this number dropped to 8.1% when titanium stems were used. [31, 54]

2.11.3 Grafts

Although modular metal augments are useful for large bone defects, they aren't justified for small defects, since it would need a larger and unnecessary removal of bone. As such, in order to remedy small bone defects (AORI T1), the choice should be to use bone grafts. [39]

The use of bone grafting is an important tool to manage the irregularly sized and shaped bone defects observed in revision total knees. Impaction bone grafting was originally described in the treatment of bone loss after total hip arthroplasty . [55, 56]

That technique has been modified to use with revision knees. The bone grafting fixation requires the use of screws or pins or, on the other hand, the graft can be fashioned into a wedge to fit the tibia defect, although one must consider that the intrusion of cement into the host graft interface must be avoided because it impairs bone union.

Grafts that fill contained defects provide more reliable support for tibial component than the grafts that fill uncontained defects. The goal is to obtain firm seating of the tibial tray on a rim of viable bone along with rigid press fixation of the medullary stem. Bulk and morselized allogenic bone are more commonly used in revision arthroplasty, and are fixed using the same techniques described for autologous grafts. The long-term outcomes for allogenic grafts are not yet available;

A study directed by Paul et al [57] to evaluate the use of bone grafts concludes that the impaction bone grafting appears to be a valuable tool in the management of patients with severe bone loss noted during R.T.K. surgery.

This same study also shows that bone grafts are useful for filling irregular defects or flaws of all sizes, and also has great potential to reconstitute bone and to remodel host bone with large defects [57]

It is also referred in this study that impaction bone graft in revision of total knee arthroplasty for patients with substantial bone defects is very positive for the early and midterm outcome. The reconstructed bone in these irregularly sized and shaped defects appears to be mechanically stable although there may be some complications such as[57]:

- non union at the allograft-host bone junction;
- loosening with formation of radiolucent lines or migration of prosthesis;
- infection (may occur in about 12% of patients)

Windsor et al reported that tibial bone grafting is an excellent option because of the reduced costs, when compared with prosthetic adding wedges. [58]

The use of cement grafts is an option that's only usable for small defects. The cementing of bone defects is readily available, and its use is less technically demanding than the other procedures. The cement augmentation will work for small circumscribed areas within intact peripheral rim, when using methylmethacrylate cement. However it will not support peripheral rim defects. The use of cement should be limited to defects smaller than 10 mm. However it can be used along with screws, to reinforce the cement, for flaws greater than 10 mm.

So, one can conclude that there are several possible techniques to implement in a revision of total knee arthroplasty, and as Bourne and Crawford et al. concluded, approximately 70 % of the total knee revisions are satisfactory for three and a half years, yet not reaching the clinical results and the success rate of primary arthroplasty. [59]

We can also conclude that the revision of total knee arthroplasty is essentially similar to the first intervention but the revision however, has to deal with the probable loss of bone incurred during the removal of the original knee replacement, named as defects. [41]

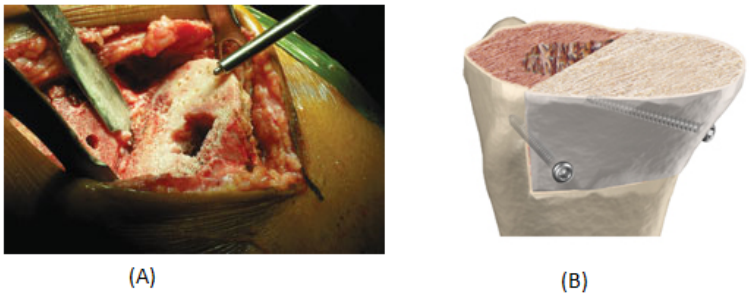

Figure 2.25: Cement Graft(A); Bone graft (B)
[http://www.innomed.net; http://www.wephysio.co.uk]

2.12 Revision Total Knee Arthroplasty Surgery

The revision of total knee arthroplasty surgery focuses on several stages such as extraction of the implants from the primary surgery, joint space assessments, alignment of tibia system and the prosthesis assembly and final tibia preparation.

Before this, it's obvious that a pre-operative analysis and surgical considerations should be taken into account (bone defects analysis and repair techniques and materials).

The first step in order to start the surgical procedure is to choose where the incision will be made. Usually, the surgeons prefer to perform the incision in the exact same place where the first cut was made.

This incision extends from the proximal margin of the rectus femoris to the distal margin of the tibia tubercle, following the medial border of the patella.

The next step is to remove the previous implants. In this step, the surgeons try to keep as much bone as possible, using for that a large number of tools and materials such as, osteotomes (used to cut and prepare bone, invented by Bernhard Heine in1830) [60], oscillating saws (used to cut the bone), Gigli saw (flexible wire saw for bone cutting, used specially in amputation surgeries where the bone has to be smoothly cut). Although in the majority of surgeries just an osteotom is used.

Figure 2.26: R.T.K.A. used materials, removal procedure (A); Mini-Lexer Osteotomes (B); Oscilating Saw (C); Gigli Saw (D)

[[7] (A); www.innomed.net (B); http://topfreebiz.com (C); www.shopmedvet.com (D)]

Before the extraction of the components from the first surgery, these materials are slackened in order to facilitate easier the removal of the first surgery components, preventing fractures and bone waste.

After this, it is essential to ensure the true joint line evaluation and the joint space assessments where the joint space is determined and ensured. The flexion / extension gap ratio and the symmetry of both flexion and extension gaps are evaluated with spacer blocks in order to decide if prosthetic augmentation is needed or not.

After this, the tibial alignment system is defined, which could be extramedullary or intramedullary.

The differences between these two types is because the first alignments are performed outside the tibia and the intramedullary ones inside the tibia. These methods are used in order to guarantee the three types of alignments: rotational alignment, varus/ valgus alignment and flexion/extension alignment.

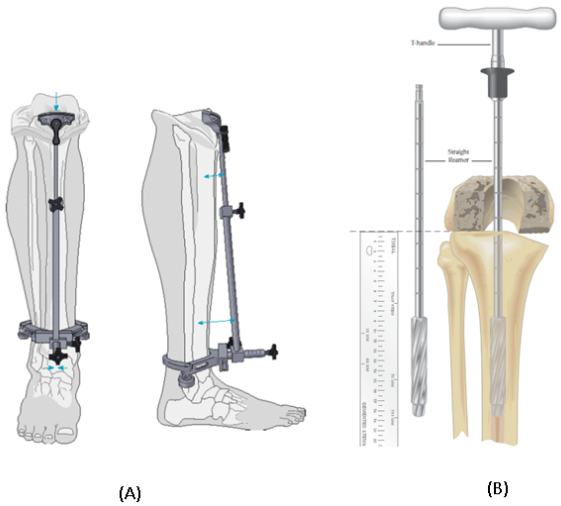

Figure 2.27: Joint space [7]

In order to provide a biggest articular stability, sometimes a stem is used by orthopaedic surgeons.

According to this, in the surgical procedure, the cancellous bone is drilled, avoiding to damage the cortical bone.

During the surgical procedure it's essential to ensure the good support of the materials such as tibial tray, metallic wedges and augmentations, so, the most proximal surface of the tibia is prepared.

Due to the first surgical intervention, in the revision surgery, and in order to save bone, a cut not superior than 1–2mm should be performed in the most prominent condyle is performed.

Afterwards, the step wedge cutting block or hemi wedge cutting block is placed in order to proceed to the sectioning of the tibia, to place the different options.

Finally, the components are prepared to be placed on the tibia, however, after its positioning, the surface where the materials will be placed needs to be cleaned, in order to avoid posterior problems, like infections.

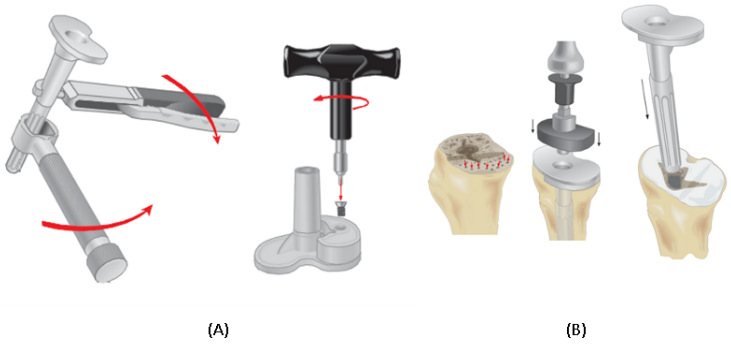

Figure 2.28: Assembly of the implant components(A); Set procedure of the tibial components(B)[7]

Chapter 3

Experimental tests with different bone defect repair techniques

3.1 Introduction

At this chapter, we intended to experimentally analyse and evaluate the influence of the different wedges and grafts, as well as the use of a metallic stem.

This procedures has as main goal ensure how each one of this repair techniques, provide an additional knee stability in the revision of total knee arthroplasty.

The knee stability provided by each implant is important to assess because, this factor excessively influence the durability of the arthroplasty.

The experimental analysis in *in vitro* studies is usually performed whether on cadaveric or artificial bone, including composite bones.

At this chapter were made experimental tests with composite bones where the strains were measured on the models surfaces on each model configuration.

At the experimental tests, a medial load was applied on the medial condyle of the polyethylene component. The principal strains were measured on the cortical tibia surface in order to assess the maximal and minimal principal strains near the prosthesis.

In order to evaluate the stability provided by each prosthesis technique, displacement between the tibial tray and the tibia bone was also measured.

These results were used to analyse the structural changes on the tibia surface after the revision of the total knee arthroplasty, specially the stress–shielding effect and osteolysis.

3.2 Materials and Methods

The tibia used in the experimental tests is a composite bone of the left leg, which is commercially available from Sawbones Pacific Research Labs, Vashon Island, WA, U.S.A. with a reference 3302.

This composite model is made by short fibber glass reinforced with epoxy resin on its external structure and polyurethane foam on its internal which, according to Condit et al [61], is an adequate material to reproduce the real models.

In our study we used three kind of implants, metallic (metallic wedges), bone (bone grafts) and cement (cement graft) implants.

The tibial tray used on or model was from P.F.C. Sigma Knee System, DePuy International, Inc. Johnson and Johnson Warsaw/Indiana, size 5 - Ti-6Al-4V, 83mm M/L and 55mm A/P, with a 10mm polyethylene component above.

The metallic wedges and block are made by a chromium–cobalt alloy (Cr–Co) and was provided by DePuy International, Inc. Johnson and Johnson Warsaw/Indiana. Was used three types of metallic implants, metallic hemi–wedge and metallic total wedge with a inclination of 10º, and metallic block.

The bone graft used on our experimental model was a bovine bone, provided by BioBom Talhos, Aveiro–Portugal. The bovine bone was cut and prepared with the same dimension than the metallic block in order to be applied on the composite model.

The cement used either as cement graft or just as fixation cement was provided by DePuy International, Ltd. Johnson and Johnson Blackpool, England. Its a bone cement (CMW1) self–curing radiopaque, composed by polymethyl methacrylate, specially recommended for securing a metal prosthesis to living bone in arthroplasty procedures.

At last, a press-fit stem used on the experimental model was provided by DePuy International, Inc. Johnson and Johnson Warsaw/Indiana with $\phi 16mmx115mmonTi-6Al-4v$.

This materials are summarized on the table 3.1.

Table 3.1: Resume table of the components used (n/a - not applicable)

Component	Materials	Dimensions	Supplier
Composit bone	Fiber glass and epoxy resin with polyurethane foam	Reference 3302	Sawbones
Tibial Tray	Ti-6Al-4V	83mm M/L 55mm A/P Size 5	DePuy
Polyethylene Component	Polyethylene	Stabilized 10mm component	n/a
Metallic Total Wedge	Cr-Co	Size 5 - 10º	DePuy
Metallic Hemi–Wedge	Cr-Co	Size 5 - 10º	DePuy
Metallic Block	Cr-Co	16mm x 34mm x 55mm	DePuy
Metal Stem	Ti-6Al-4V	$\phi 16mmx115mm$	DePuy
Bone graft	Bovine Bone	16mm x 34mm x 55mm	BioBom Talho
Cement	PMMA	n/a	DePuy

Some of the experimental test materials are presented in the next figure.

Figure 3.1: Materials used on the Experimental Tests

In our experimental tests were used six experimental models in order to simulate the type 2 defects on the tibia. The sequence of use of the implants was: cemented tibial tray without any implant; metallic hemi–wedge; cement graft model; metallic total wedge; metallic block and finally the bone graft model. All these models were testes, first with stem but also without stem.

In order to set the tibial implants on the tibia, a surgery procedure was needed on our composite models.

The surgical procedure was performed following the methodology of a normal surgical procedure on a patient. At first, a cut was made from 2 mm on the most proximal tibia with a conventional saw, creating a flat and stable surface to place the tibial tray.

Then, a ϕ 16mm hole in the intercondylar region of the tibia was made in order to place the both tibial tray and metallic stem.

Finally, the different sections were made in order to place the different implants used in this study.

The first cut performed was at 5mm with a 10º angle on the medial side of the tibia in order to place the metallic hemi–wedge.

When a cement graft was placed, any cut was needed because, we used the previous cut of the metallic hemi–wedge and full fill it with cement, placing above this cement layer the tibial tray.

After this, a new cut was needed in order to set the metallic total wedge. According to this a cut on the medial side of 15mm from the reference and a 10º degrees was made.

Finally, in order to place the both metallic block and bone graft, a rectangular cut on the medial side of 16mm from the reference was made. Because of this, a small part of the lateral side of the tibia was cemented in order to fill the area removed during the placing of the metallic total wedge.

Before placing the bone graft, a bovine bone was prepared and cut with the same dimensions of the metallic block.

The referred sections were made by the described specific order, because this way way a better utilization of the materials was made.

That order was also important to preserve the maximum number of strain gauges as long as possible, since one of them had to be removed, because of the metallic total wedge dimensions, which turned out to be incompatible with the strain gauge set position.

Between each implant, a thin layer of cement was set in order to guarantee that the implant is completely secure to the bone.

We had a special attention on the cement application because the temperature has a special interference in the cement, since to higher temperatures there is a lower solidification time. According to this, the registered temperature on the experimental room was between 22ºC and 24ºC.

The sequence used is represented from the left to right on the figure 3.2.

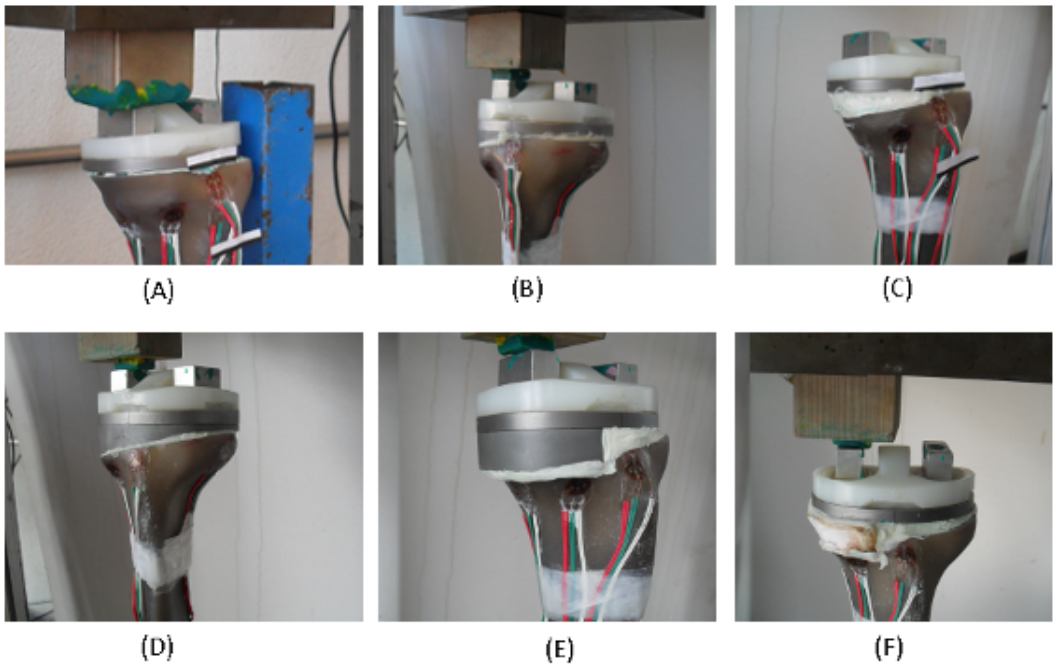

Figure 3.2: Implants used on the experimental tests: Cemented tibial tray (A); Metallic hemi–wedge (B); Cement graft (C); Metallic total wedge (D); Metallic block (E); Bone graft (F)

In order to evaluate the use of several implants and the stabilization promoted by each prosthesis, a several measurements was made in the experimental test models.

On this study we tried to evaluate essentially two types of measurements. The measurements of the principal strain on the cortical surface of the tibia and also the measurement of the displacement between the tibial tray and the tibia surface.

In other words, to analyse how each model behaved in terms of principal strain, a group of six strain gauges were placed on the composite model of the tibia.

The strain gauge is a transducer capable of measuring deformations on the bodies.

The principle of operation of the strain gauges is, when the model is shrunken the length of the filament is also shrunken which decreases its length in diameter, causing a decrease in the filament's electrical resistance. Therefore by measuring the electric intensity of the conductive filament, we can obtain a continuous and precise reading of the strain, according to the load increment.

The tri-axial strain gauges contains three filaments aligned 45º between it selves, which allows to obtain enough information to completely describe the Cauchy's deformation tensor on the models surfaces. This procedure is vital to validate the numerical models. According to this, we have chosen tri-axial strain gauges (KFG-3-120-D17-11L3M2S, Kyowa Electronic Instruments Co, Ltd, Tokyo, Japan) as measurement system.

The positions of the strain gauges were selected with the purpose of measuring the strains on the anterior, posterior, medial and lateral sides of the tibia models. Was also taken into account the increase of the dimensions of the prosthesis in order to keep the strain gauge positions as much as possible.

In this context, initially 6 strain gauges were placed on the experimental model.

After a certain point of the experimental work, one of the strain gauges was sacrificed due to the metallic total wedge interference, since its geometry was incompatible to this strain gauge position. According to this, after the metallic total wedge just 5 strain gauges was used.

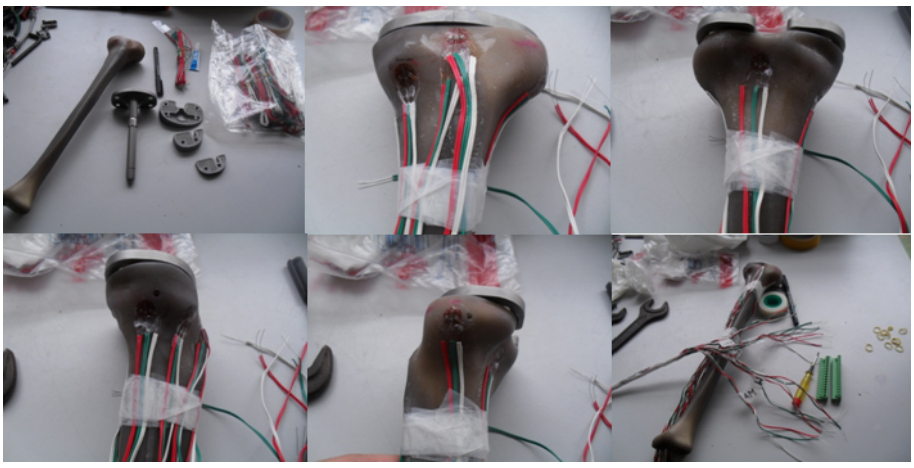

Figure 3.3: Strain gauge setting

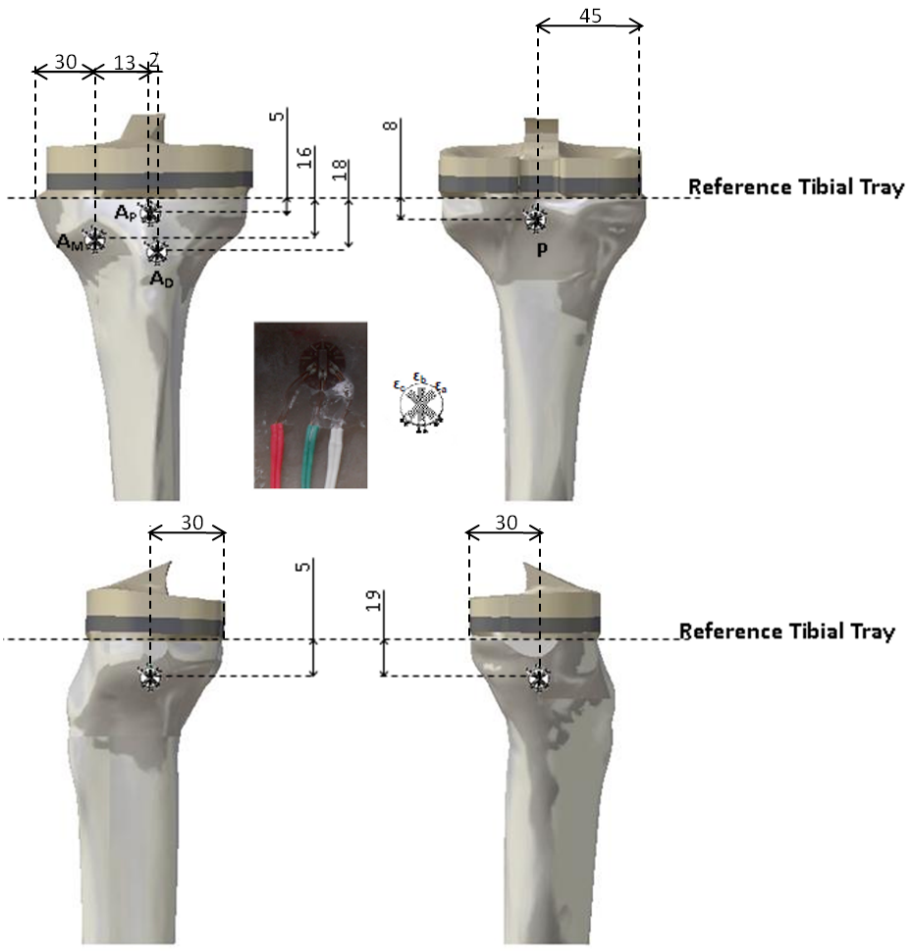

Figure 3.4: Strain gauge position

The implementation of the strain gauges at the surface of the models requires a prior surface preparation. According to that, the tibial surface was grinded with a dry grind P400 and cleaned with alcohol. After that, a little portion of glue was applied on the back of the gauges and then the gauge was placed on the tibia by pressing it against the surface of the tibia at the desired location (the pressure made was about one minute to complete the drying). [62]

Note that we have aligned the middle filament of the the strain gauge with the tibia vertical axis. After that, each strain gauge was identified according to its position on the model, as well as the filament that follows from them, in order to easily identify it.

Before the connection between strain gauges and the acquisition data software, the internal resistance of the strain gauges was checked, verifying that its internal resistance is 120 Ω as recommended by the supplier. After this, the connection between equipments was made. This procedure was very cautious, verifying that there are no wire changes or connection errors because error would compromise the results.

All strain gauges were connected to the National Instruments PXI 1050 acquisition data system, which in its turn was connected to a computer where the results were stored and processed by a Lab View Signal Express application.

Note that the strain gauges were kept test by test, in order to compare as best as possible, the different models and the influence of the different implants on the principal strain distribution on the tibia surface.

Table 3.2: Position and connection table

Strain Gauge Reference	Discrition	Distance to Tibial Tray (mm)	Plugin	Pin
AP	Anterior Proximal	5	2	1–3
AD	Anterior Distal	18	2	4–6
AM	Anterior Medial	17	3	0–2
M	Medial	19	4	0–2
P	Posterior	10	3	3–5
L	Lateral	7	4	3–4–6

The main variables assessed in this part of our study were the maximal and minimal principal strain by using strain gauges).

On the tibia surface, the principal strains were calculated using each 45º strain filament($\varepsilon_a, \varepsilon_b and \varepsilon_c$) of each strain gauge.

The values obtained in each filament was registered and using the mathematical expressions (3.1) and (3.2) the maximum and minimum principal strain were calculated.

$$\varepsilon_1 = 0,5(\varepsilon_a + \varepsilon_c) + 0,5\sqrt{(\varepsilon_a - \varepsilon_c)^2 + (2\varepsilon_b - \varepsilon_c - \varepsilon_a)^2} \tag{3.1}$$

$$\varepsilon_2 = 0,5(\varepsilon_a - \varepsilon_c) + 0,5\sqrt{(\varepsilon_a - \varepsilon_c)^2 + (2\varepsilon_b - \varepsilon_c - \varepsilon_a)^2} \tag{3.2}$$

Since the measurement of the principal strain on the tibia surface is guaranteed, we proceeded to compare the sinking of the tibial tray on the tibia using for that videoextensometer.

With conventional extensometers it is important to attach them to a known gauge length as they produce a calibrated displacement signal wich must then be converted into a strain signal. This process can result in some errors, because it is not possible to verify the exact gauge length once the extensometer is fitted to the specimen. The videoextensometer operates directly as a "strain meter" by continuously measuring the distance between the marked targets and calculating strain based upon the initial measured length. With this technique, strain (ε) is directly calculated. [63]

In this measurement technique it's used a high resolution monochrome camera, capable of capturing to high speed image and processing it in order to enable a point by point continuous measurement.

The camera is rigidly fixed to the machine frame, if possible or on a tripod mounted and focused on the specimen to which contrasting marks (targets) have been attached. It is imperative that the distance between camera and specimen remains constant during the test, because any movement alters the image size and the change is interpreted by the software as a change in specimen measurements. [63]

Using the buffer data it is possible to produce grey scale (contrast) diagrams for every horizontal scan line and for every vertical pixel column. Due to the vast amount of data produced by each picture scan, it is imperative that this is efficiently processed, in order to achieve an adequate dynamic response thus allowing the videoextensometer to be used with conventional static testing machines.

The Videoextensometer software uses the frame buffer data to automatically detect and follow the targets during testing. The targets produce rapid grey scale contrast transitions along a scan line and this data is differentiated to produce distinct peaks, which are chosen as the measuring points. Reference marks are shown on the monitor, indicating the selected targets, and the operator is provided with the opportunity to manually select alternatives in the eventuality that software makes an incorrect interpretation.

The target datum point values are selected where the contrast line crosses the mean value of the maximum and minimum target grey scale levels. This value is dynamically adapted throughout the testing process and compensates if the contrast points fade due to the specimen stretching.

Beyond the evident advantages of the equipment installation, the accuracy level is 0,3 microns, according to the supplier. Since that we are working with a very low range of values, this accuracy level seemed to be indicated to our study.

The installation of this equipment requires some caution in terms of illumination levels, since the software recognizes the displacements by measuring the contrasts of the strip targets. Obviously, this contrast is much more evident if the workplace has a good illumination level. So this factor is very important while using a videoextensometer. [64]

Before starting any displacement measurement on each model, a calibration of the equipment was made, using a calibrated ruler provided with the equipment, that sets the initial distance between targets to the software.

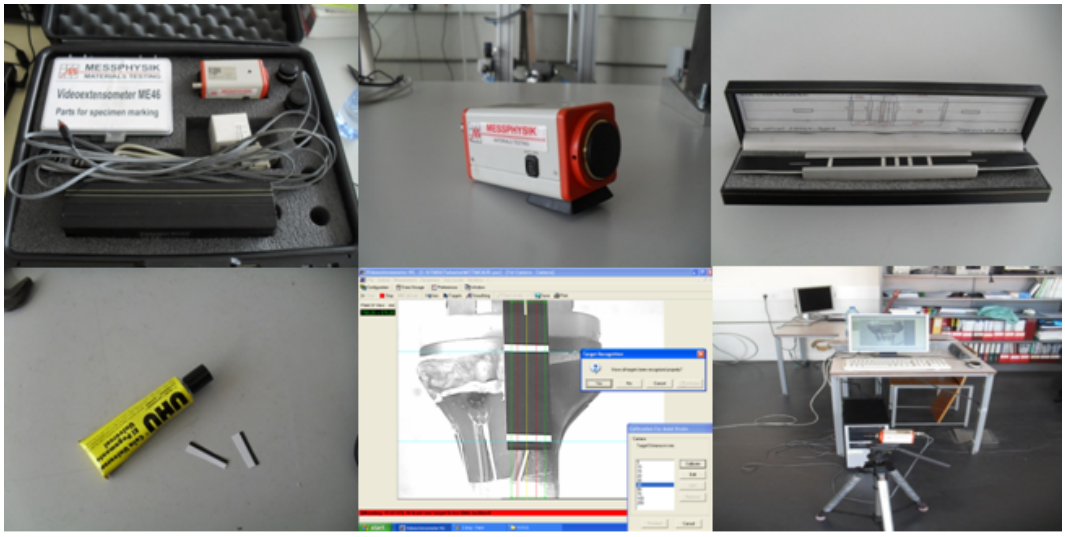

Figure 3.5: Videoextensometer materials

We also placed the videoextensometer (Videoextensometer ME46, Messphysik, Materials Testing) at 1,5 m of distance from the model in order to measure the displacement between tibial tray and tibia. At this point, was necessary to give special attention to setting the target as well as the equipment calibration between tests in order to ensure that the luminosity differences that occurs in the lab, according to the day time don't influence the results.

The videoextensometer was connected to a computer with the Videoextensometer NG Version 5.25.0 software in order to provide the acquisition data from the experimental tests.

After the models assembled, they were submitted to a severe load case on the medial condyle.

In everyday activity, the tibia bone is exposed to many different loads, as flextion, rotation and compression. The compression is the most important one in the knee joint. So, for this study, a person with 85 kg, with a fully extended knee was considered.

According to the bibliographic research, the load on the knee joint is three times the weight of the person. So according to this and as well as in the numerical models, a 1600N load was applied on the medial condyle of each model. [65, 66]

To apply the desired load was necessary to use an adapter on the side of the applied load which was made with a piece of wood and a metal sphere. On the condyle surface of the tibia another adapter was set. A polyethylene component with a support on each concave surface of the condyles was fixated with epoxy adhesive and prepared to get the metal sphere from the other adapter.

Was also needed to create some constrains on our model. According to this, in the load machine, conception of the Laboratório de Biomecânica do Departamento de Engenharia Mecânica da Universidade de Aveiro, was implemented a mechanical clamping system in its lower base in order to fixate the model, leaving the superior part of the model free to be loaded. We considered that the tibia would be recessed at it most distal face, using for that a mechanical clamping system that allows the complete fixation and recess of the composite tibia, preventing any deviation.

The main goal of this load case was to severe the location of the bone defect, since all the defects were located on the medial side.

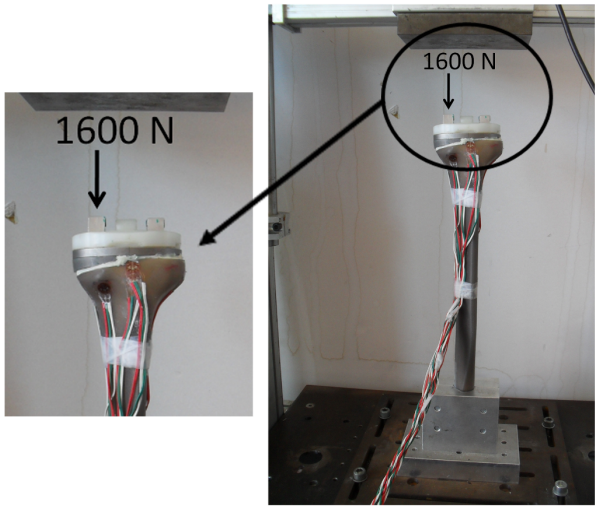

Figure 3.6: Load and constrain components

On our study, just the medial side of the polyethylene condyle was loaded, although the both sides of the tibia, at the beginning were planed to be loaded. The tests were limited only on the medial side, because we faced with a fixation problem on the load distribution bar.

According to this, each one of the models received a medial load on the polyethylene component, applied vertically, therefore allowing strain registration and further comparison.

Each experiment was performed according to the sequence shown in the table 3.8, based on the description given by Finlay et al [8]. Note that each one of the load sequences was repeated five times to each model in a total of 60 essays.

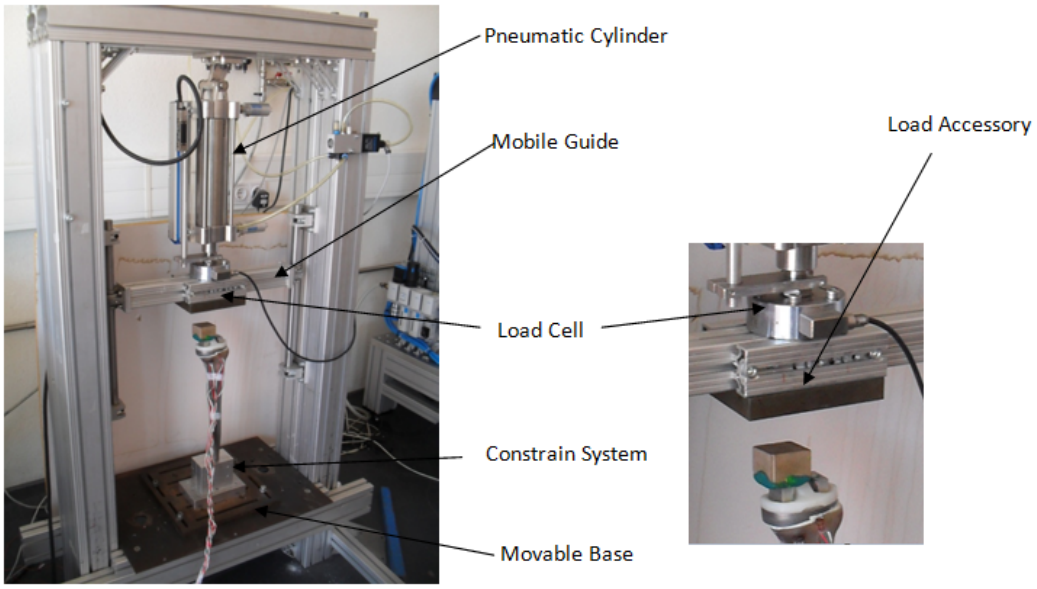

Figure 3.7: Test machine

Table 3.3: Procedure sequence table [8]

Step	Definition	Period (s)
A	Conditioning to the test load	60
B	Strain gauge calibration	30
C	Videoextensometer start	10
D	Preloads	60
E	Stabilization of the load on the model	60
F	Videoextensometer stop	10
G	Strain gauge value save	15
H	Discharging	60
I	Break between measurements	60
	Total Time	6 min

The duration of step E is related with the viscoelastic behavior of the composite models, which is recommended by Cristofolini et al. [67]

All of this components were mounted according to the figure 3.8 in order to save space on the lab and allowing free movements between controlling computers from the load machine, strain gauge acquisition data and videoextesometer acquisition data.

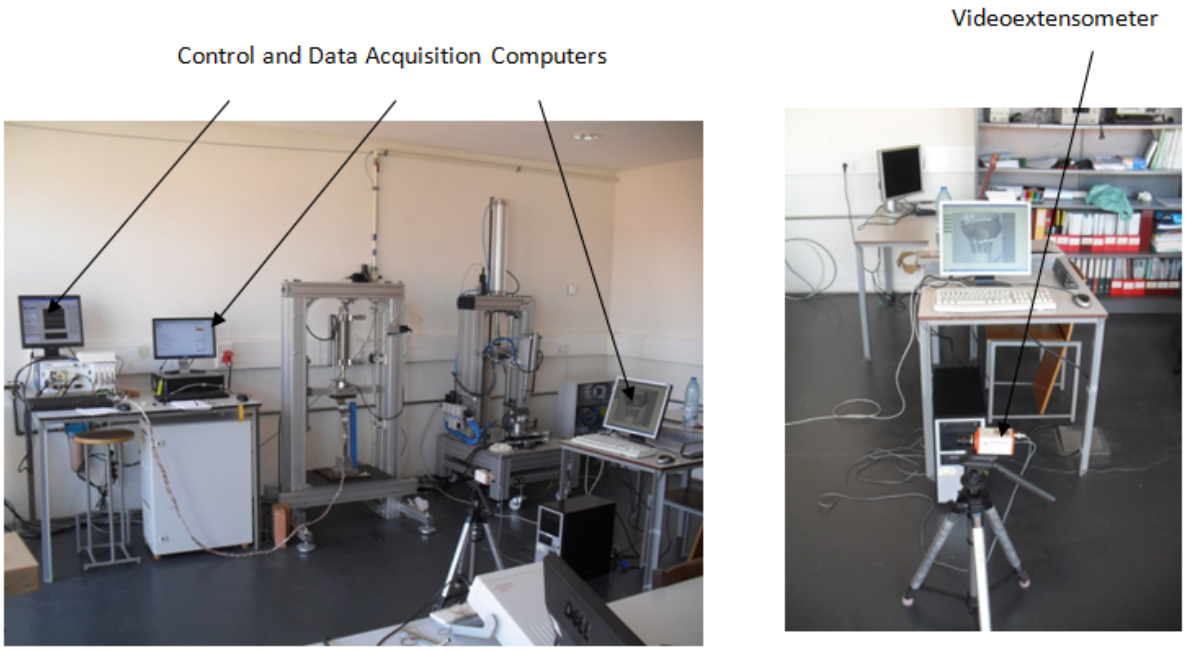

Figure 3.8: Experimental test apparatus

On the experimental results were analysed the mean and the standard deviation for both ε_1 and ε_2 on the different models, as well as, the displacement of the tibial tray using a video measuring system.

3.3 Results

After the experimental tests, the collected data was treated in order to calculate the principal strains and standard deviations obtained with the strain gauges on each test.

The results from videoextensometer were also treated in order to evaluate the displacement between tibia and tibial tray.

This procedure provided essential information about what happened on our twelve experimental models.

The information collected with the strain gauges will allow us to know what happens around the tibia surface, on the previous set positions.

Table 3.4: Resume experimental table

		Models Without Stem											
		Cemented Tibial Tray		Hemi Wedge		Cement graft		Total Wedge		Block		Bone Graft	
		Mean	σ	Mean	σ	Mean	σ	Mean	σ	Mean	σ	Mean	σ
AP	e2	-36	7,34	-179	17,31	-119	8,57	-	-	-	-	-	-
	e1	263	6,48	793	64,82	570	46,43	-	-	-	-	-	-
AD	e2	-56	4,49	-47	1,58	-61	2,67	-51	3,51	-86	2,75	-48	4,65
	e1	530	13,02	500	6,82	570	2,47	438	10,79	384	4,49	296	15,61
AM	e2	-197	57,43	-88	4,22	-145	1,69	-104	4,86	-252	4,98	-3	4,31
	e1	110	12,21	129	3,98	89	1,74	193	7,54	176	5,67	117	6,84
P	e2	-313	5,75	-532	5,25	-899	4,91	-410	1,38	-34	17,78	-48	4,96
	e1	110	73,45	132	137,67	252	260,1	236	81,53	33	6,07	84	13,75
M	e2	-551	10,12	-848	15,67	-811	0,97	-873	22,72	-872	33,17	-1204	42,51
	e1	-46	2,17	-11	1,03	-34	1,18	2	2,44	187	7,32	334	7,34
L	e2	12	1,73	-11	4,79	-34	7,06	6	2,08	-28	3,26	36	16,15
	e1	21	3,18	31	5,48	56	7,73	81	2,76	38	5,16	121	4,93
		Models With Stem											
AP	e2	-93	24,04	-446	34,04	-173	31,21	-	-	-	-	-	-
	e1	282	93,51	570	77,43	478	184,49	-	-	-	-	-	-
AD	e2	-77	2,42	-60	5,65	-50	4,74	-39	5,55	-70	11,73	-54	5,97
	e1	399	84,01	285	4,29	405	9,5	452	46,39	399	14,86	125	4,17
AM	e2	-95	11,19	-88	5,06	-115	4,86	-120	4,2	-173	19,03	5	3
	e1	113	15,27	125	5,58	113	2,43	257	3,09	222	20,33	172	6,98
P	e2	-332	15,45	-431	8,65	-625	11,17	-394	22,77	-19	9,63	-62	12,36
	e1	116	99,97	90	117,83	185	192,24	197	118,61	15	7,69	95	25,02
M	e2	-431	3,14	-640	9,23	-497	3,33	-781	31,64	-787	39,33	-1166	103,71
	e1	-29	10,58	6	1,61	-13	3,26	-37	17,88	146	13,16	305	4,08
L	e2	27	10,24	-23	24,88	0	13,9	15	46,51	6	14,81	53	6,48
	e1	66	20,87	64	23,37	60	5,31	105	5,09	57	5,35	106	4,77
												* Mean =	(1x10-6 m/m)

The mean value of standard deviations, regarding non stemmed models, is about 17μstrain.

The cemented tibial tray model shows that the values of standard deviation are higher on the M position for the ε_1.

Using a metallic hemi–wedge or a cement graft we've obtained higher values of standard deviation of ε_1 on the P position. When compared to the standard deviation mean of all models, these models show a difference of approximately 85%. The metallic total wedge also has higher values of standard deviation on the P position, but in this case the difference is approximately 80%.

On the metallic block model, as well as on the bone graft model, there is nothing to mention regarding the P position. However the major differences, relatively to the standard deviation mean, occur on the M position for ε_2.

As shown in table 3.4, concerning the other positions in the models without stem, almost all standard deviation values are lower than 18 μstrain, revealing an insignificant dispersion between tests.

On the models with stem, the value of the standard deviation mean suffers an increase, when compared to the models without stem. On these models, this value is about 27%.

On the metallic hemi–wedge model and on the cement graft model we've observed the highest values of ε_1 on the P position, as seen before on the same non stemmed models. On these models,

the difference to the standard deviation mean is about 85%. The metallic total wedge model also shows higher values of ε_1 on the same position, with a 75% difference to the standard deviation mean.

In what concerns the metallic block model, the highest standard deviation values are seen on ε_2 of the M position, showing a 30% difference to the standard deviation mean. However we have observed, on the same position of the bone graft model, an increase of the standard deviation value, showing a difference of approximately 73% to the standard deviation mean.

All the other stemmed model positions register standard deviation values inferior to 40 μstrain.

Through the observation of table 3.4, when we compare the overall values of standard deviation between stemmed and non stemmed models, we can state that they are higher in stemmed models. However, when we compare the same values between specific positions in both stemmed and non stemmed models, we won't find a significant difference.

A graphical description was made in order to compare and analyse a few aspects:

- first, the influence of the several types of implants in what refers to principal strain distribution around the tibia surface, on the set positions;
- second, the difference between using or not a metal stem.

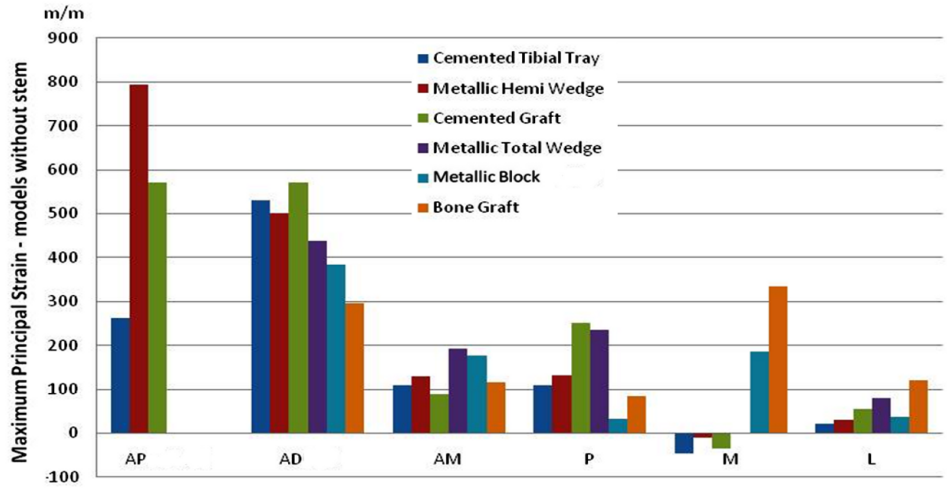

(a)

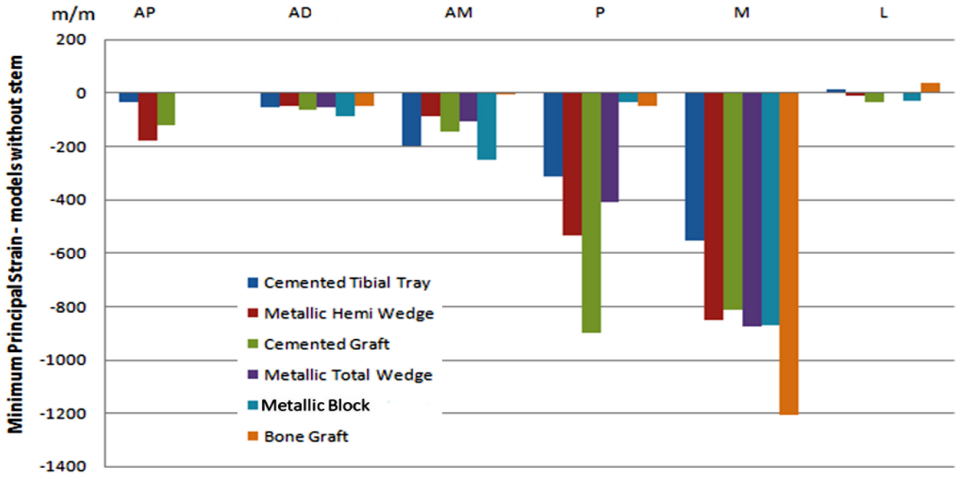

(b)

Figure 3.9: Maximum Principal Strain – ε_1 (a); Minimum Principal Strain – ε_2(b) of the models without stem

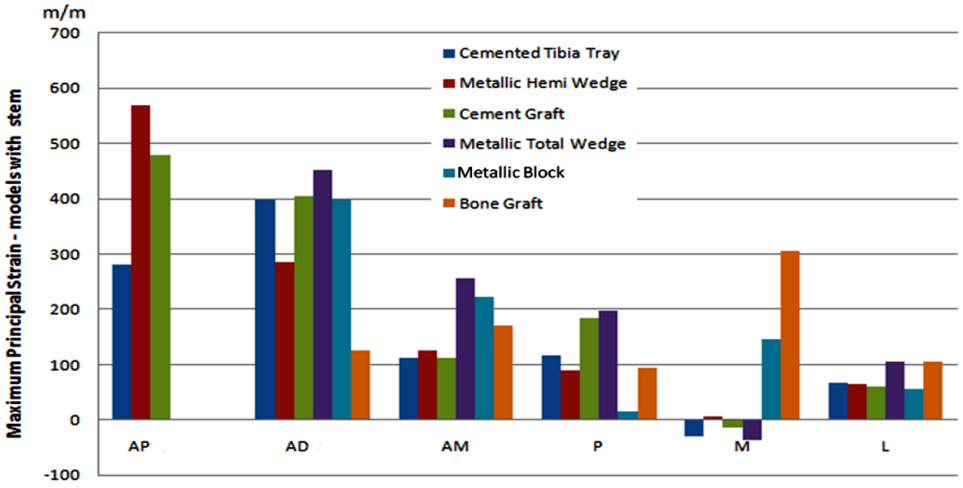

(a)

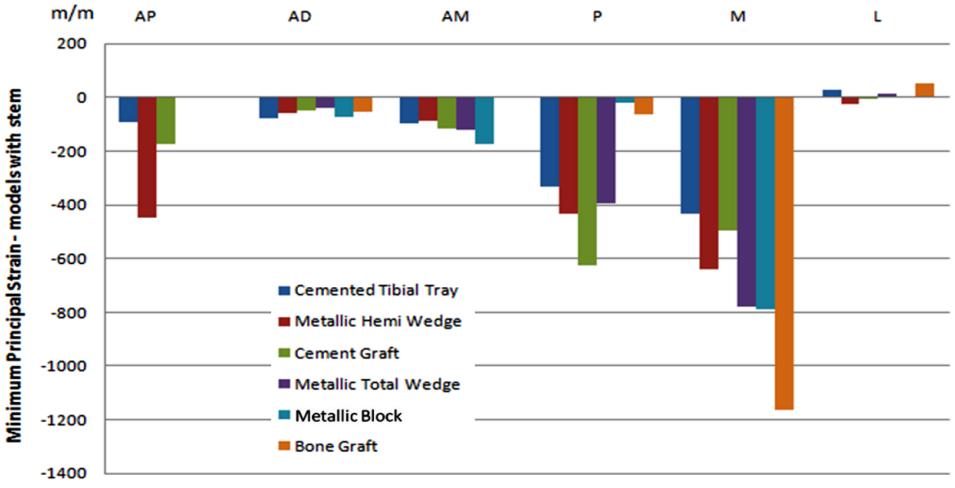

(b)

Figure 3.10: Maximum Principal Strain – ε_1 (a); Minimum Principal Strain – ε_2(b) of the models with stem

As we can see in the graphical results for the models without stem, the higher values on the A_P position occur on the models with a metallic hemi-wedge, either in maximum and minimum principal strains. The model with lower values of ε_1 and ε_2 is the model where a cemented tibial tray was used. The model that shows a bigger difference, when compared to the cemented tibial tray model, is the one where a metallic hemi–wedge was used, showing a difference of 530 μ strain for ε_1 and 143 μ strain for ε_2.

On the A_D position, the highest maximum principal strain value is achieved on the cement graft model and the lowest ε_1 value on the bone graft model. In the same position, the models with the closest ε_1 to the cemented tibial tray model are the cement graft and the metallic hemi–wedge, although one is higher and the other is lower, respectively. In this position, the minimum principal strains do not show any significant differences between models. The bone graft model is the one that presents the greatest difference to the cemented tibial tray model, showing a decrease of 234 μ strain for ε_1.

On the A_M position the situation is completely different, since the range of values is smaller than on the previous strain gauge positions. On this position the model that shows a higher value of ε_1 is the model with a metallic total wedge, although this value is very similar to the one obtained from the metal block model The model that shows lower values on this position of ε_1 is the model where a cement graft was used. On this position, the biggest difference to the cemented tibial tray happens on the model with a total wedge. The difference between these two models is about 83μ strain. Regarding the minimum principal strain (ε_2), the metallic block model shows the highest value. The difference from this model to the cemented tibial tray model is very small, about 55μstrain. Despite that, the cement graft model, whose $_2$ is lower than the cemented tibial tray value, shows a difference of only 52μstrain, which makes it the closest one. On the other hand the biggest difference occurs with the model where a hemi–wedge was used, showing a difference of 109μ strain.

On the P position the values of ε_1 are higher on the cement graft model, but the values of metallic total wedge are very near to this one. The lower value is registered on the model with metallic block. On the cement graft model the ε_1 value increases 142μstrain, compared to the cemented tibial tray model, which is the biggest difference. The graphical representation of the ε_2 on the same position shows that the cement graft model is the one with the highest value, registering an increase of 586 μstrain when compared to the cemented tibial tray model. On this position, the difference between the model with higher value and the other models is very significant. The metallic block model is the model with the smallest ε_2 value. The decrease registered between this model and the model with cemented tibial tray is about 279 μ strain.

On the M position, the maximum principal strain value is higher on the model with bone graft, with a difference of 380 μ strain from the cemented tibial tray model. Regarding the minimum principal strain, on the same position, we have that the bone graft model is also the one with the highest value, and that the cemented tibial tray also is the model with the lowest value, having a difference of 653μstrain between them. Next we have all the other models, showing very similar values between them, with a difference of 270μstrain to the cemented tibial tray.

Finally, on the L position, the ε_1 has its highest value on the model with bone graft and the lowest on the cemented tibial tray model, with a difference of 100 μ strains. Regarding the ε_2, the model that shows the highest value is the cement graft model, despite all the results are very similar.

Now we proceed with the comparison of ε_1 and ε_2 values between both non stemmed and stemmed models, on the different strain gauge positions.

On the A_P position the biggest difference was found on the metallic hemi–wedge models.

The ε_1 values show a decrease of 30% (about 223 μstrain) from the non stemmed model to the stemmed model. However, the ε_2 values register an increase of 60% (approximately 267μstrain) from the non stemmed model to the stemmed one.

On the A_D position the biggest difference on ε_1 was also found on the metallic hemi–wedge models, registering a decrease of 215 μstrain, which represents a reduction of 43%, from non stemmed to stemmed models. Regarding the minimum principal strains, we may observe a decrease of about 20% in all the models.

The ε_1 on the A_M position registered the main difference between non stemmed and stemmed models on the metallic total wedge models, which shows an increase of about 63 μ strain, which represents a raise of 24%. On the same position, but concerning the ε_2, we can see that the main difference occurs on the cemented tibial tray models, where a decrease of 79 μstrain, or a 31 % reduction, is registered when we use a stem. We should note that there are no differences on the hemi–wedge models.

On the P position, the ε_1 shows a reduction of 67 μstrain on the cement graft model with stem, representing a 27% decrease, when compared with a non stemmed model. Something similar occurs with the ε_2 on the cement graft models, although the difference in this case is about 274 μ strain, representing a decrease of 30%, which is the biggest difference between non stemmed and stemmed models.

The maximum principal strains on the M position show that the biggest difference occurs on the metallic total wedge models, showing a difference of 41 μstrain, which represents a decrease of 22%. The minimum principal strain values on the same position show that the main difference occurs on the cement graft models, registering a decrease of 314 μstrain, representing a reduction of 38% from the non stemmed model to the stemmed one.

Finally, the maximum principal strain values on the L position show that the biggest difference happens on the cemented tibial tray model, an increase of 45μstrain that represents a rise of 68%. On this position, the bone graft models are the ones who register a bigger difference of the ε_2 values, increasing 32% (about 17μ strain).

As mentioned before, the displacement between tibia and tibial tray was also measured, in order to evaluate the displacement/sinking of the tibial tray on the tibia. This measurement was made in each test.

Due to the applied forces on the medial condyle of the polyethylene component, the tibial tray suffered a soft sinking in the tibia, causing a poor positioning of this component in the knee and, consequently a poor stability. In order to assess this phenomenon an experimental measurement was made.

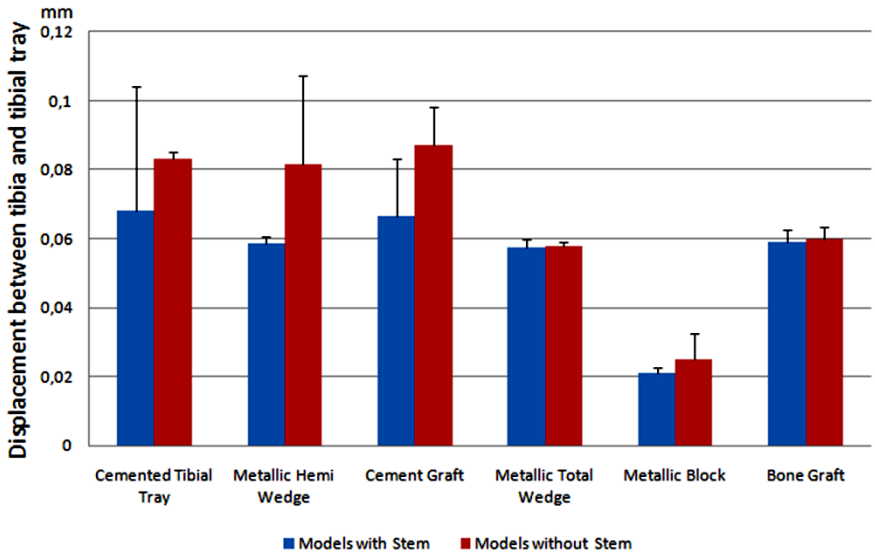

Figure 3.11: Displacement comparison between models with and without stem

Table 3.5: Displacement table

Model	Displacemente (mm)	between Stem and without Stem
Cement Tibial Tray with Stem	0,0682	0,0148
Cement Tibial Tray without Stem	0,083	
Metallic Hemi–Wedge with Stem	0,0386	0,0428
Metallic Hemi–Wedge without Stem	0,0814	
Cement Graft with Stem	0,0664	0,0206
Cement Graft without Stem	0,087	
Metallic Total Wedge with Stem	0,0576	0,0004
Metallic Total Wedge without Stem	0,058	
Metallic Block with Stem	0,0212	0,0040
Metallic Block without Stem	0,0252	
Bone Graft with Stem	0,0592	0,0008
Bone Graft Tray without Stem	0,06	

The table 3.5 shows the displacement values between tibia and tibial tray on the different models, with and without stem, in order to complete the graphical information.

In the cemented tibial tray, metallic hemi–wedge and cement graft models there is an important difference between stemmed and non stemmed models. In opposite to that, in the metallic total wedge and bone graft models that difference is very small. The metallic block, although showing small displacements between tibial tray and tibia, are also the models that show the major difference to the cemented tibial tray with and without stem. The cement graft models are the ones that present higher similarities to the cemented tibial tray model.

3.4 Discussion

Usually in this kind of in vitro experimental tests, in order to evaluate the stability of the arthroplasty, a measurement of the displacements between tibial tray and tibia is made. According to this, in the previous studies a LVDT (Linear Variable Differential Transformer) technique is used. This technique requires a fixation system on the models, in order to place the LVDT measurement equipment. This said, and because in our study we would have to measure the displacements between the tibial tray and the tibia surface, we would need to create a fixation system between both bodies to allow the LVDT connection. This fixation system requires two holes in the tibial tray in order to fixate the movable supports of the measuring system. [5] According to this, and because that technique would need a greater preparatory work, other possibilities were considered, such as the videoextensometer. Although the videoextensometer wasn't used in any previous biomechanical study, it came as a good alternative since it would only be necessary to set the measurement targets in each component. With this method we can save both time and materials. This method seemed to be a good alternative to the "traditional" methods. [63, 64] According to all of this, and since it has a desired range of measurement accuracy as well, we chose this method.

On this part of our study an experimental comparison using a composite tibia and different types of implants was made, as well as the use of a metal stem or not in each implant.

Nowadays, with the development of the composite materials, the substitution of the cadaveric bones by composite bones was exponential, since its behaviour is very similar to the real bones and also because it's easier to obtain and treat.

It's also important to refer that the use of such models in composite materials allows a distribution of the strains caused by beading loads, compression and torsion, identical to the real bone. According to Heiner et al [68]the results repeatability between tests on the same model shows that the range of results is between 0,5% and 7,8%. This results are superior in the cadaveric models which has a 4,5% of repeatability [61, 67], despite this, a composite bone was used on this study.

The standard deviation values are good on all the positions, showing a small dispersion of values between tests. However, in the P position we've observed high standard deviation values, leading to a greater dispersion on this position. This may be explained by the poor positioning of the P strain gauge. According to this we ensure that the repeatability of our tests is good.

In what concerns the models without stem, and according to the obtained results we may conclude that the implants that cause less changes to the bone, when compared to the cemented tibial tray model, are the cement graft and the metallic hemi–wedge. This goes in favour with the

work of A.D.Toms et al [45], which states that the use of cement to repair the defects seemed to be a good choice. On the other hand, the model that more changes causes to the bone is the bone graft model, because its values are distant to the cemented tibial tray model values.

Regarding the models with stem, we may conclude that the ones that less changes cause to the bone are the cement graft model and the metallic hemi–wedge model. As well as seen in the models without stem, the bone graft model is the one that shows a major difference from a cemented tibial tray model. However, when we go from non stemmed models to stemmed ones we observe a general reduction of all principal strain values.

According to the variation of principal strain values some problems may occur. When it suffers a big increment, there is a possibility of hypertrophy or fatigue failure. On the other hand, when we observe a substantial decrease of principal strain values, the bone density also decreases, causing bone resorption, according to Wolf's Law.

Although the metallic hemi–wedge model has a strong probability of hypertrophy or fatigue failure on the A_P position, on the other positions, the principal strains present similar values to cemented tibial tray model, which shows that this model is the least harmful to the bone.

According to the obtained results when the displacement between tibia and tibial tray was measured, we may conclude that the implant that more stability ensures when a medial load is applied, is the model with the metallic block, because its values of displacement are lower than the other models.

We may also see that the use of metal stem does not make sense on the models with bone graft and metallic total wedge because when we compare the displacement obtained on the these models, with and without stem, the values of displacement are very similar. However, there is a significant increase of stability on the cemented tibial tray, metallic hemi–wedge and cement graft, therefore justifying the reinforcement of stability with a metal stem.

We think that the metal stem is not compulsory on the model with metallic block, despite the increase of stability that occurs with it. We concluded this because the displacement observed on tibial tray is not much when a stem is used. According to this, and because the stem installation on the tibia requires extra time, materials and bone damage we think that it shouldn't be used.

So, although the use of a metal stem increases stability and the reduction of the principal strain values, we think that this instrument is only justified on the models with metallic hemi–wedge and cement graft because it is on these models that it has greater influence.

Regarding the obtained results we may say that, in general, the values were as expected, according to Brooks et al [69] studies.

Chapter 4

Computational models with different bone defect repair techniques

4.1 Introduction

As complement the experimental models, several numeric models were developed. Using finite element methods (F.E.M.)techniques which allowed an evaluation of other important biomechanical parameters, that are impossible to be studied on the experimental models because of physical limitations. Two of this parameters are the principal strains on the cancellous bone under the implants as well, as on the cortical surface adjacent to the implants. Using the numeric models was also possible to assess a physiological load case which was impossible with the experimental models. In this chapter was used geometric modelling and structural calculations through the F.E.M. techniques.

4.2 Materials and Methods

The geometric modelling of the revision tibia and its components is a complicated task, since the bones have a high degree of complexity in its geometry and dimensions.

The modelling of the constituent components of total knee arthroplasty was based on CAD modelling (computer aided design) software, Dassault System CATIA V5 R19. Tibia, polyethylene component and tibial tray geometric models used were the same used by Completo et al [5] obtained by 3D scanning techniques. The model of the tibia was based on the commercial bones of Sawbone, Pacific Research Labs, Vashon Island, WA. [70].

Note that cortical structure of a real bone has a maximum thickness of 3 mm which changes along the tibia surface. Because of this thickness changes, the two bone structures are difficult to precisely perform on the composite and consequently on the geometric bone. Because of this problem, a constant thickness of 2,5 mm was assigned to the geometric model. [71, 72]

The material properties atrtributed to the bone constituints, cortical and cancellous bone, were the recommended ones by the supplier of the composite bone used on the experimental tests.

This two bone structures were assembled in order to create a geometric model of the human bone. [5, 73]

The material properties of the tibial tray and the polyethylene component was the same that of the real components.

These three components, tibia, tibial tray and polyethylene component were the same geometric models used by Completo et al [5].

The modelled repair technique components, such as: metallic total wedge, metallic hemi–wedge and metallic block was directly modelled in CATIA V5R19 with the same proprieties of the materials that they are made. The bone graft was also directly designed on CATIA V5R19 with the same properties of the bone and the cement with the same properties described by Murphy et al [9].

The stem used on our study was also modelled in CATIA V5R19 with the same properties of the real stems.

As mentioned before, the final geometric model of the tibia was obtained by assembling both parts, cortical and cancellous bone.

The structures assembled were performed following some constrains criteria, in order to make that the both sides of the bone could be entirely in touch. This assembly was performed by the Assembly Design sub-module from the Mechanical Design module.

The figure 4.1 shows some images of the bone constituents.

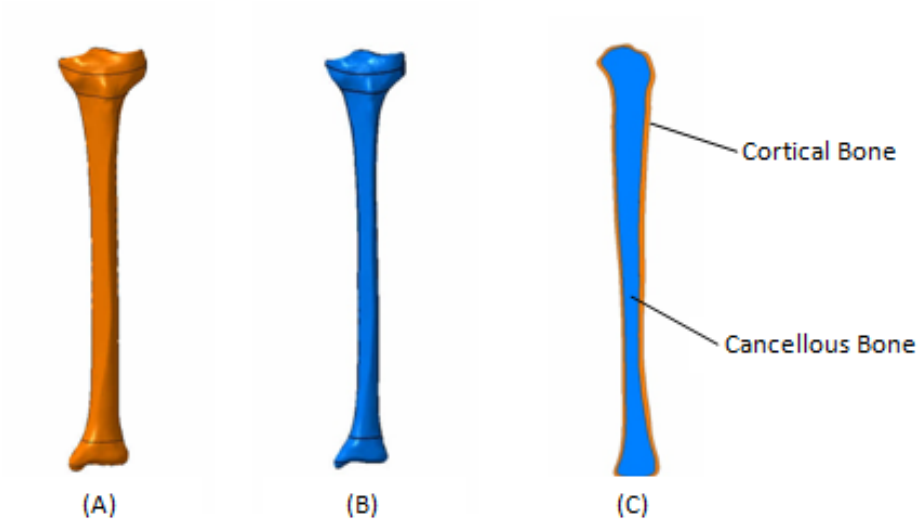

Figure 4.1: Bone structures. Cortical Bone (A); Cancellous Bone (B), Bone section (C)

The geometric models obtained for the different implanted tibia models were based on the surgical procedure, using for that the P.F.C.Sigma, P.F.C. Sigma Knee System, DePuy (Johnson and Johnson Company) documentation.

Based on the available information, several sections were made on the intact tibia models in order to place the desired implants.

These implants were aligned with the anatomical axis and with the articular motion plane, trying, at the same time, to cover the biggest surface on the proximal tibia.

The different cuts and implant models was combined using the sequence on the figure 4.2..

The wedges used were obtained beyond the previous measurement and design of the real wedges, attempting to be as much realistic as possible.

All the components were reproduced on CATIA V5 R19, using the Part Design sub-module from the module Mechanical Design.

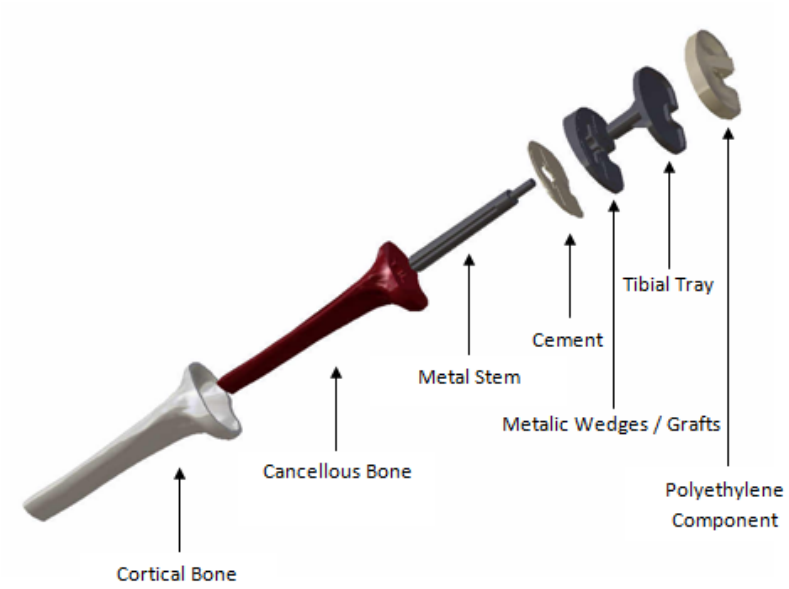

Figure 4.2: Assembling sequence of the numerical models

Note that the metal stem was used in only half of the models, while in the other half just a tibial tray was used. When the stem was not used at the end of the tibial tray, a polyethylene cover was set in its place, in order to minimize the effect of the contact between the cancellous bone and the titanium of the tibial tray.

In this study was used a metal non cemented stem with ϕ16 mm x 115 mm , combined with the tibial tray. According to this, the models could be divided in two large groups of six models each (with and without stem).

On the figure 4.3 the difference between models with and without stem are revealed and it's easy to understand the differences between the two types of models.

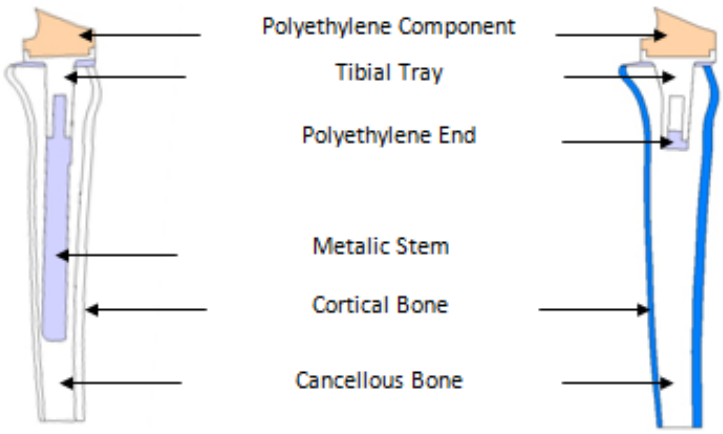

Figure 4.3: Sectioning to represent the model with stem and without stem

Three different types of metal wedges were used, as well as bone grafts and cement to repair the defects on the revision of total knee arthroplasty.

In the figures 4.5, the different sections performed in the tibial bone can be seen as well as the metal and grafts implants.

All these models were obtained through the assembly of each part such as the tibia bone and the many implant components using the Assembly Design of the Mechanical Design module.

The section that took place in each model were performed in the sub-module Part-Design of the Mechanical Design module, using for that tools like Sketch (were the section to cut was drawn) and Pocket (cut tool).

At last, the area in the cancellous bone where the tibial tray takes place was modelled using the Remove tool of the sub-module Part Design. To do so, the tibial tray was selected as the component to be removed from the cancellous bone. This procedure was equally adopted with the cement, metallic stem and metallic wedge.

Since the load will be applied on both condyles, medial and lateral, in order to make easier this task a previous preparation of the surfaces was made. So, a very small thick surface was created in each condyle, using the Skecth tool of the Design Part sub–module to draw the surface and the Pad tool to extrude that.

(a)

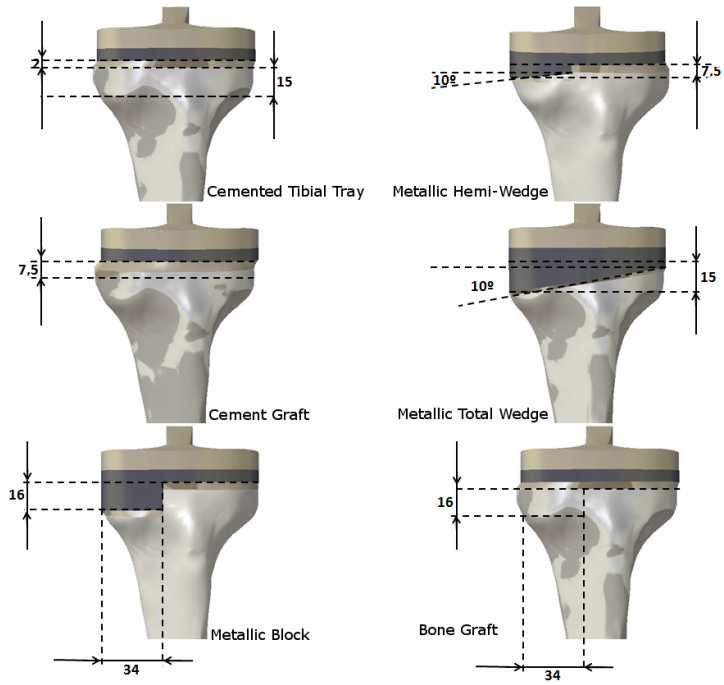

(b)

Figure 4.4: Schematic representation of the sections on the tibia (a); Schematic representation of the dimensions of the prosthesis (b).

The finite element method (F.E.M.) is a numeric computational technique originally developed to obtain the stress-strain state in complex problems.

Nowadays this method is widely used in engineering when we intend to simulate the behavior of real systems.

The finite element models over the years has proven to be capable to providing good results according to the mechanical properties. This method has also proved to be capable of dealing with the requirements of biomechanics problems.

An appropriately developed finite element model is a powerful tool to predict the effects of the different parameters involved and to provide information difficult to obtain from experiments.

It's important to note that, the reliability of these models strongly depends on an appropriate geometrical reconstruction and on accurate mathematical descriptions of the behavior of the biological parts involved and their interactions with the surrounding environment. [3, 74]

A computational analysis may predict possible stress/strain distribution for different geometries or positions, providing a basis for evaluation of surgical procedures, and aid in medical education. [75]

In this study we used a tibia bone, tibial tray and a polyethylene component, metallic wedges and block, bone and cement grafts, and at last a metallic stem. This part of our study has as main goal to investigate the many biomechanical issues around of the tibia model and tibial plateau surface. The use of numerical models was essential once this is very difficult to study with experimental tests on composite materials.

It is known that the quality of the results is directly linked with the type and size of the finite elements. The convergence mesh analysis is important because when this procedure is not taken into account, the final results could show some errors, influencing the conclusions of the numeric analysis. This errors could be avoided when a right mesh size is chosen.

So, in order to chose the proper finite element mesh size, the first step was to perform a convergence study on the cemented tibial tray. According to this, was analysed the maximum displacement and Von Misses stress on the model.

This study permitted to chose the proper mesh size used on the comparative models.

We may say that a mesh convergence is achieved when the maximum displacement of each element do not changes significantly with the increase of the number of elements.

In order to evaluate the mesh convergence, one single model was used, the cemented tibial tray model without stem where a total of 17 meshes with different dimensions were generated(8 mm, 7 mm, 6 mm, 5,5 mm, 5 mm, 4,5 mm, 4 mm, 3,5 mm, 3 mm, 2,8 mm, 2,6 mm, 2,5 mm, 2,4 mm, 2,3 mm, 2,2 mm, 2,1 mm e 2 mm).

We chose to use the tetrahedra elements because, according to Ramos et al [76], the use of tetrahedral linear elements allows closer results to the theoretical ones, although the hexahedral quadractic elements are more stable and less influenced to the degree of refinement of the mesh.

According to this, a comparison between the number of elements and the maximum displacement on each element was made for each mesh size in order to evaluate which mesh should be used.

After the proper mesh was obtained on the "test model", the mesh was also generated on the other models which will allow a posterior principal strain analysis.

In order to generate the numerical models, a geometric models generated previously was used.

On our models was generated tetrahedral finite elements, based on tibia three-dimensional geometry . Each threedimensional finite element mesh was created on the different model surfaces with triangular elements of 3 nodes.

The tibial surface considered extends from the beginning of tibia's anterior crest till its condyle surfaces. We're chosen just this section because the remainder section was not important to our study, since the surface analysed was the proximal surface of the tibia and also, because if all tibia was considered, the computation time would be largely increased.

The cortical bone meshes were created internally and externally in order to create a closed volume. In the other hand, on the cancellous bone, an exterior mesh was created, corresponding to its anatomical limit, resulting also in a completely closed mesh surface.

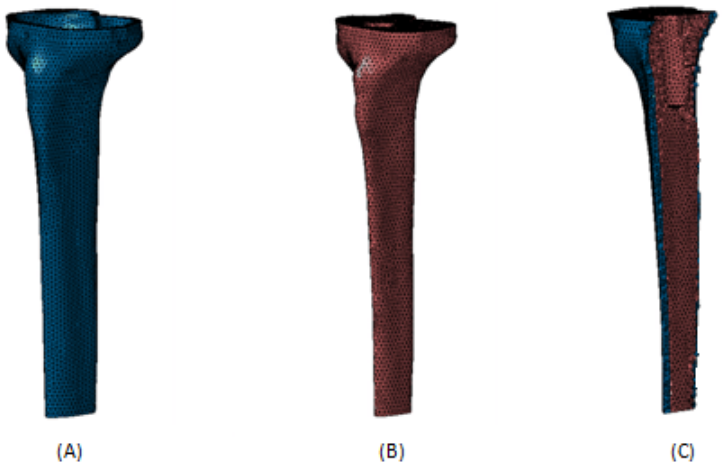

Figure 4.5: Mesh surfaces on the different bone structures. Cortical bone (A); Cancellous bone (B) and both structures (C)

In the cortical bone/cancellous bone interface, we assured that all the elements in this interface were shared between the two bodies, creating this way a rigid border between them. We also created several lines along the tibia periphery in order to ensure that the created mesh passes along the same location on the different models, providing this way the chance to a subsequent analysis between models.

According to this, seven guide lines in seven different planes were created in the tibial surfaces, at 2 mm, 4 mm, 7 mm, 17 mm, 27 mm, 40 mm and 60 mm distanced from the reference on the tibial planteau. Note that despite this seven planes are available, just three of them were used on our analyses(2 mm, 7 mm and 17 mm), because they have revealed to be the most important in this study case, since the 2 mm guide line is the closest line to the beginning of the implant and the 7 mm is on the middle line of the implant. The guide line at 17 mm was considered in order to evaluate what happens on the bone surface after the implant. The planes are represented on the figure 4.6.

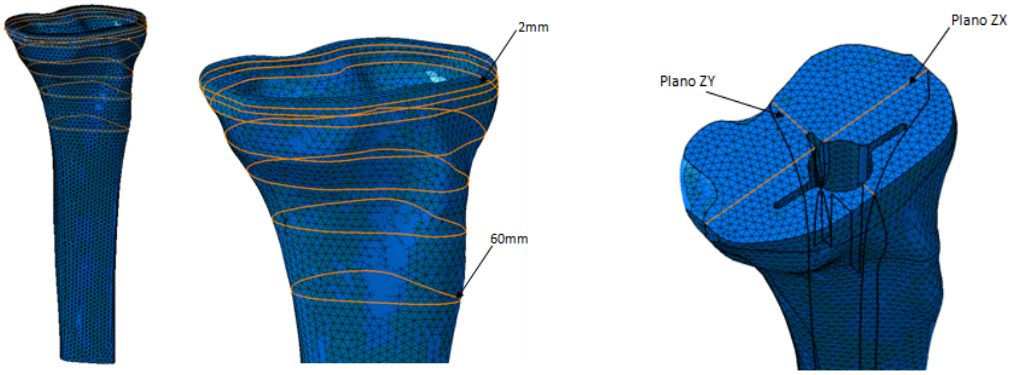

(a) (b)

Figure 4.6: Mesh guide lines: cortical bone guide lines(a);cancellous bone guide line (b).

As well as on the cortical bone, the cancellous bone was also adjusted in order to provide important elements of study. On the reference cut of the tibial plateau, two planes were drawn, one in the sagittal plane and other in the frontal plane, as we can observe on the figure 4.6.

To accomplish this task, the sub-module Wireframe and Surface Design from the Mechanical Design module was used.

After this, a three–dimensional mesh was automatically generated, using for that Tetrahedron Filler tool.

To perform the element propagation, was used the standard quality optimization option although it requires more computation resources.

After this, there were several issues related to the element geometry which were verified, such as: "jacobian" ;"skew"; "warpage"; "aspect ratio" as well as the mesh quality, "quality report", where no abnormal parameters were reported.

It was verified, during the three–dimensional mesh generation, that the mesh quality clearly depends on the surface mesh quality previously generated.

This mesh generation criteria was the same for all the numerical models of all components used on the numerical experiments.

A total of twenty four numerical models were created, divided in four groups, stemmed and non stemmed models, with just medial load and medial/lateral load.

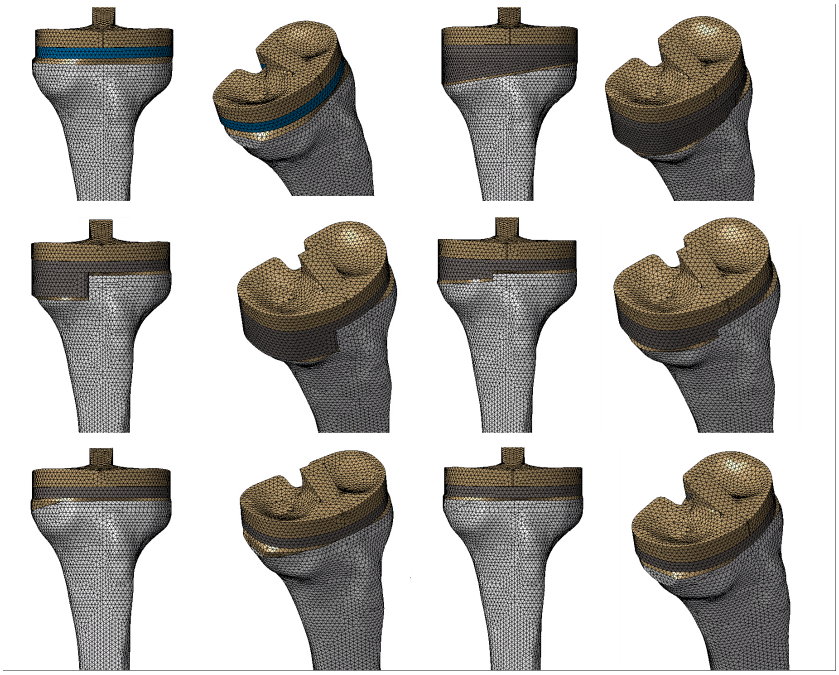

Figure 4.7: Numerical models used

In order to create a similar environment to real bone in our numeric models, a several considerations were made.

In this study we considered that the numeric model was completely clamped on its distal surface, right on the anterior crest. In other words, every displacement or rotation was prevented.

Figure 4.8: Constrain and applied loads on the models

According to the research previously made, everyday the knee joint, in general, and tibia in particular, are exposed to many forces and loads, although the compressive load are the ones that more influences cause on the tibial bone.

For this study, we considered a 85 kg person with a full extension knee. The loads were applied on the condylar surfaces of the tibia.

According to Morrison, the loads in the knee joint are approximately three times bigger than the weight of the person. [65]

The applied load on the condyles of the tibial plateau is non equally divided. According to Harrington, the loads are divided in 60 to 70% of the load on the medial condyle and 40 to 30% on the lateral one. [66]

This asymmetrical distribution allows to increase the flexion effect on the tibia.

According to this, a person with 85 kg has an applied load of 2,5 kN asymmetrical distributed between each condyle, 65% on the medial side and 35% on the lateral. This results in a 1600 N on the medial condyle and 870 N on the lateral one.

So, the applied load was also divided in two classes. The numerical models in which only medial load was applied, the medial condyle received 1600 N, while on the models with medial and lateral loads each condyle receives 1600 N on the medial condyle and 870 N on the lateral condyle.

The loads were applied on the central surface of each condyle of the polyethylene component as we can see in the figure 4.10. The load spots were kept on each numerical tests.

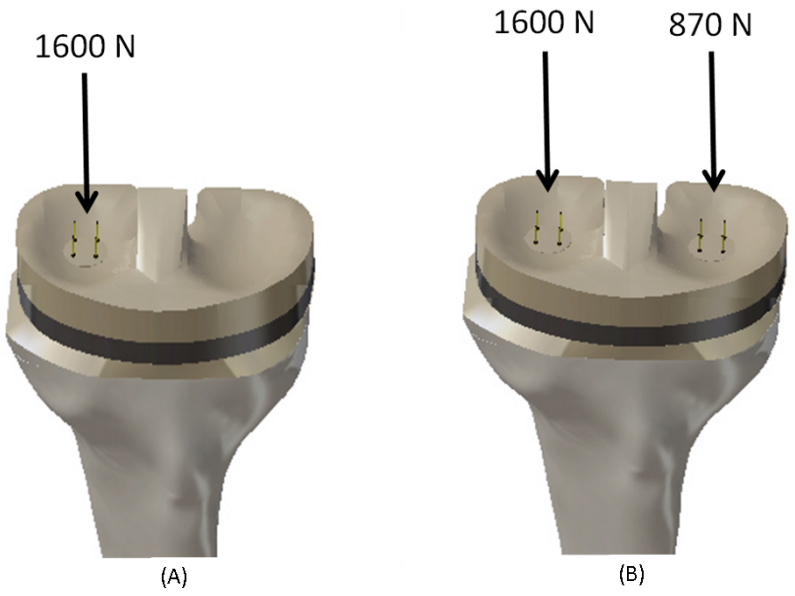

Figure 4.9: Load cases: Medial load (A); Medial and Lateral load (B).

It was also necessary to apply materials to our models in order to indicate how the different components would behave according to the applied load.

The material characteristics of each component used are described in the table 4.1. All the models were considered homogeneous, isotropic and linear elastic.

The contact conditions on each component of each model were considered as a fastened surfaces, except on the bone graft model. On this case, the contact conditions between the screw

Table 4.1: Material properties [9] [10]

Component	Material	Young Modulus (GPa)	Poisson's Ratio
Cortical Bone	Fiberglass - Epoxy Resin	16	0,3
Cancellous Bone	Polyurethane foam	0,104	0,3
Polyethylene Component	Polyethylene	0,5	0,3
Tibial Tray	Titanium	110	0,3
Cement	Polymethyl Methacrylate	2,28	0,3
Bone Grafts	Bovine Bone	16	0,3
Wedges	Co-Cr	210	0,3
Stem	Titanium	110	0,3

used to fixate the graft on the tibia, and the both surfaces of the graft and the cancellous bone, was considered as a friction surfaces (contact connection).

The maximum and minimum principal strain values in the cortical bone and cancellous bone of each different model were obtained and analysed along the schematic guide lines shown before.

All the analysis were performed on a computer COMPAL FL90 with a Intel® Core 2 Duo CPU a 2,40 GHz processor with 4,00 GB of installed memory (RAM), using the CATIA V5R19 Dassault System software

In order to validate the numerical models was used the experimental models described on the last chapter as well as the numerical ones.

The validations was made, measuring on the numeric models the same positions used on experimental models. According to this was possible to analyse the difference between numeric and experimental models.

4.3 Results

At this point of our study we will present the convergence mesh and the numerical analyses results.

In the table 4.2 we can see the number of elements, nodes, maximum displacement and maximum Von Mises stress. According to this values, a graphical representation was made, relating the number of elements with the maximum displacement, in order to obtain an adequate convergence of mesh.

4.3.1 Mesh convergence results

Table 4.2: Validation mesh table

Element dimension	maximum displacement	Maximum Von Mises Stress	nodes	elements
8	2,94259	4,43E+07	7976	30404
7	2,94514	4,48E+07	8319	31776
6	2,98682	4,84E+07	8663	33176
5,5	2,94457	4,23E+07	9036	34592
5	2,98462	4,35E+07	9631	37068
4,5	3,01603	4,32E+07	10467	40404
4	3,00132	4,32E+07	11966	46705
3,5	3,01688	4,36E+07	14474	57718
3	3,04829	4,36E+07	18460	75232
2,8	3,05882	4,39E+07	20951	86388
2,6	3,06651	4,40E+07	23626	97878
2,5	3,06637	4,41E+07	25294	104943
2,4	3,06427	4,43E+07	27259	113440
2,3	3,07357	4,53E+07	29425	122937
2,2	3,07059	4,54E+07	31769	133089
2,1	3,07262	4,47E+07	34689	145971
2	3,07331	4,50E+07	38564	163650

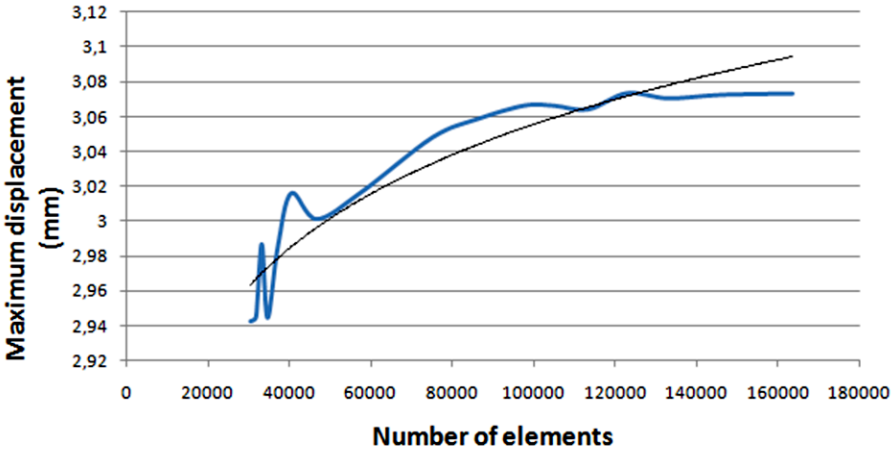

Figure 4.10: Convergence mesh results, Maximum displacement v.s. Number of elements

As mentioned before, a mesh is considered adequately refined when its displacement does not change significantly with the increase of the number of elements. The difference of the 2,5mm mesh size to the previous mesh size, 2,6mm is less than 1% when an increase of $1x10^7$ is observed.

According to this, based on displacement v.s. number of elements graphical results, to conclude that the mesh size of 2,5 mm is the one which satisfy the convergence criteria.

4.3.2 Load cases results

After the mesh is defined, the numerical models were processed in order to evaluate the principal strains on the surface of the tibia.

The real knee joint receives medial and lateral load (physiologic load), because of this and in order to assess what happens in this joint, two load cases will be described (just a medial load of 1600N and a medial-lateral load 1600N-870N).

The principal strains were analysed on the cortical surface periphery along the 2mm, 7mm and 17mm guide lines. As complement and according the objective of this study, the maximal and minimal principal strains were analysed on the cancellous bone on the different implants.

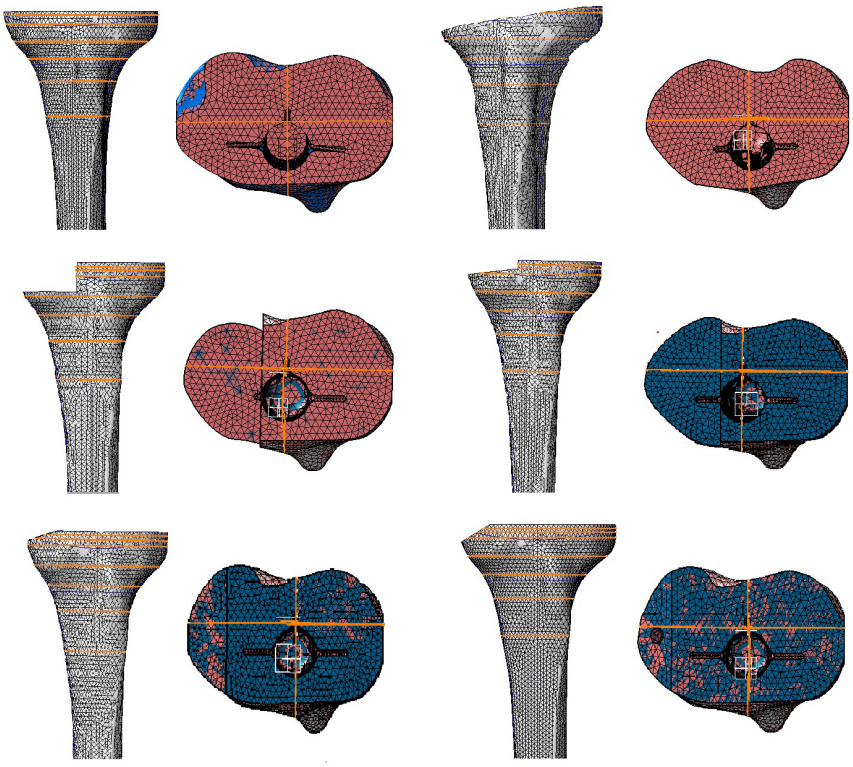

Figure 4.11: Principal strain guide lines

A graphical representation of the maximum and minimum principal strain at 2mm, 7mm, 17mm and frontal plane was made in order to simplify the analyses of the numerical models.

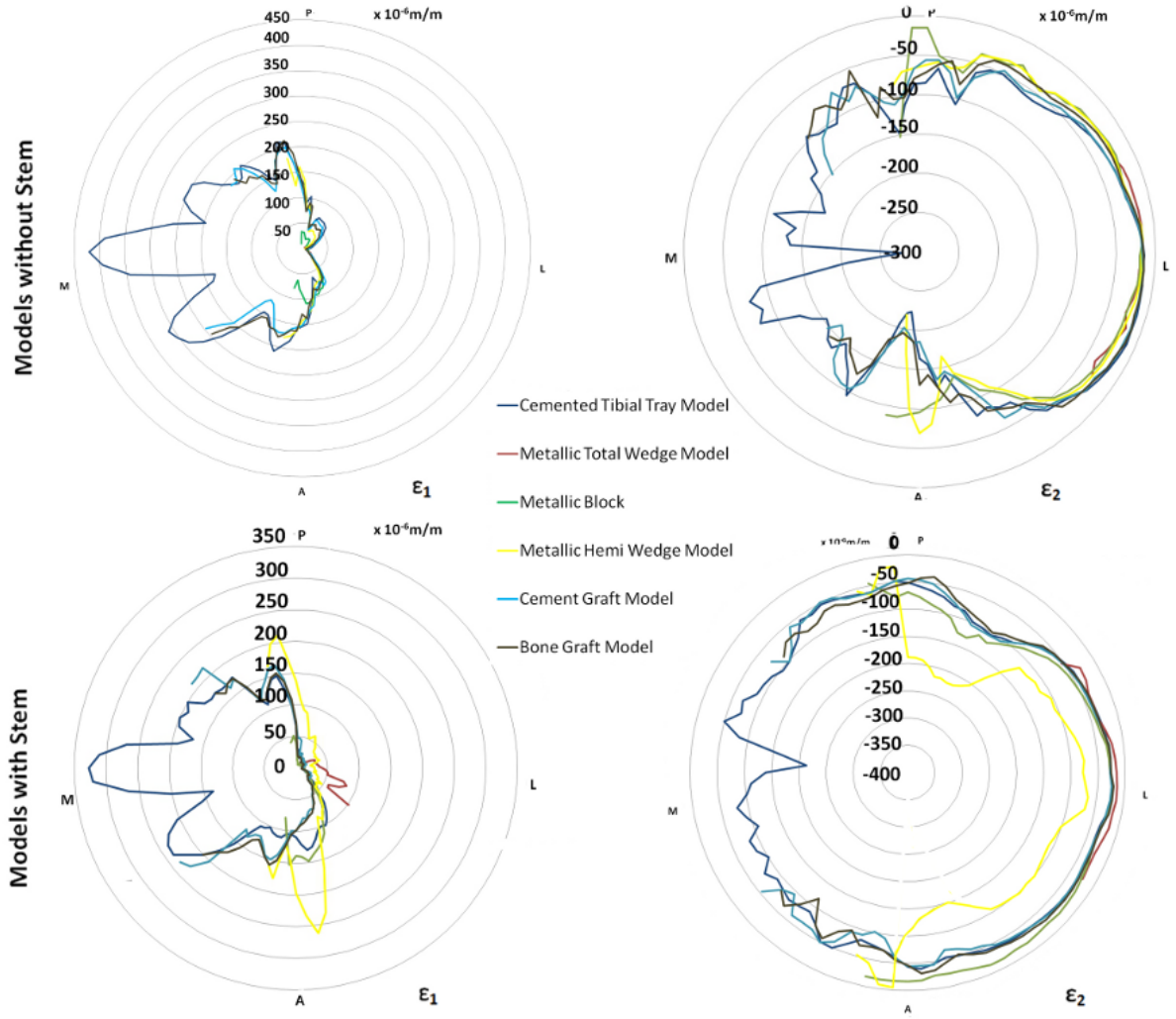

Figure 4.12: Medial load cases: Principal strains on the models with and without stem on the cortical bone: 2mm from the reference

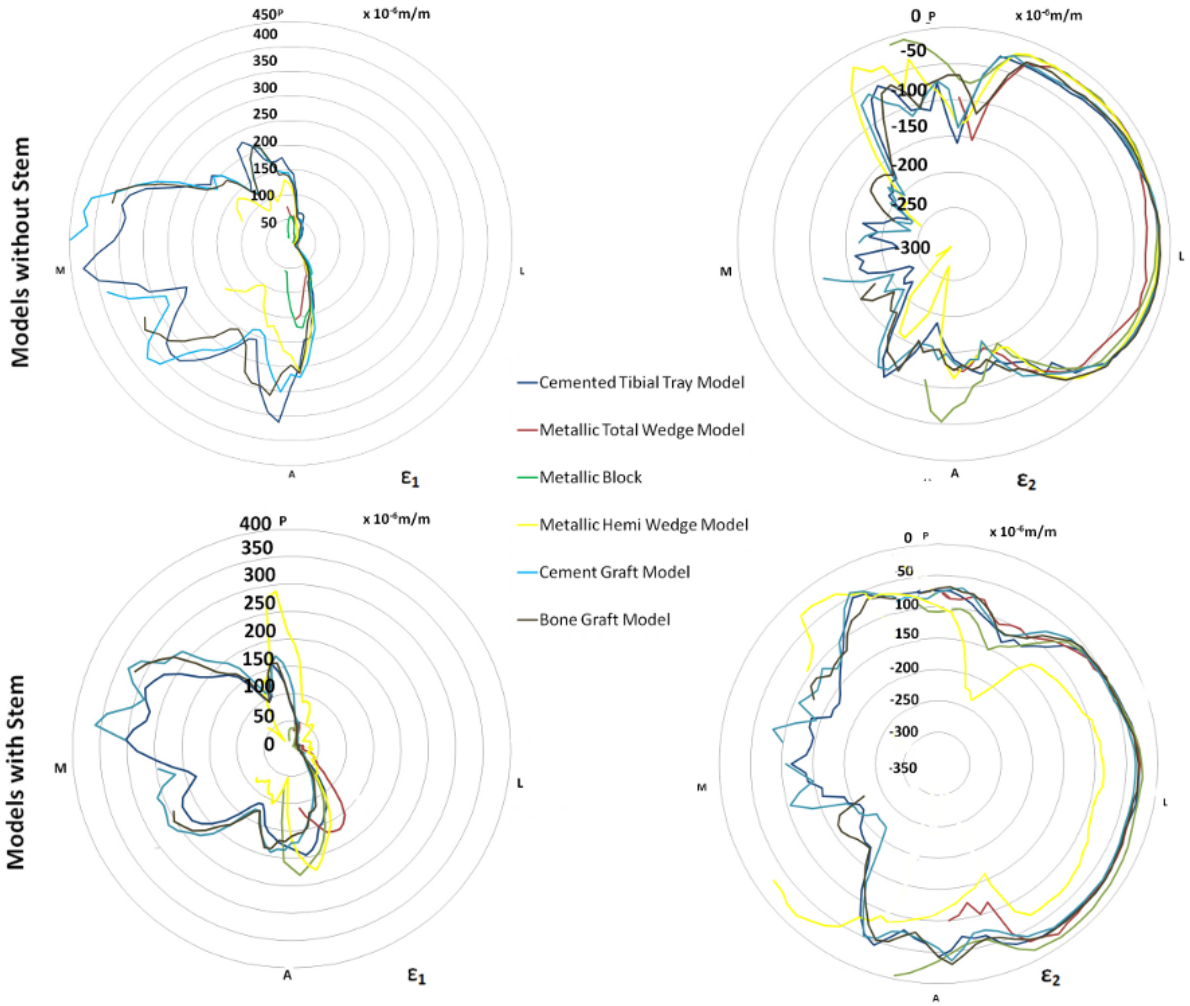

Figure 4.13: Medial load cases: Principal strains on the models with and without stem on the cortical bone: 7mm from the reference

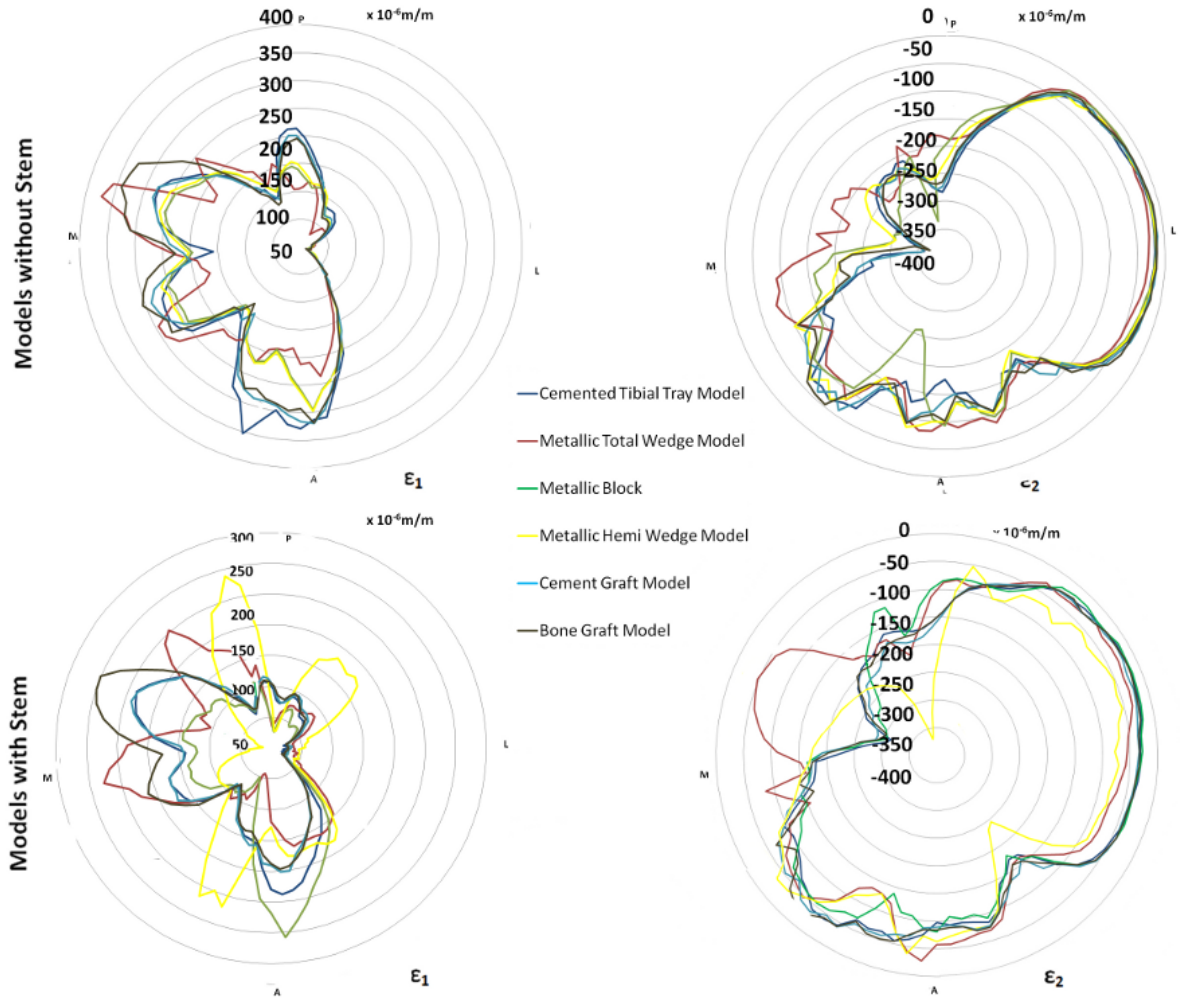

Figure 4.14: Medial load cases: Principal strains on the models with and without stem on the cortical bone: 17mm from the reference

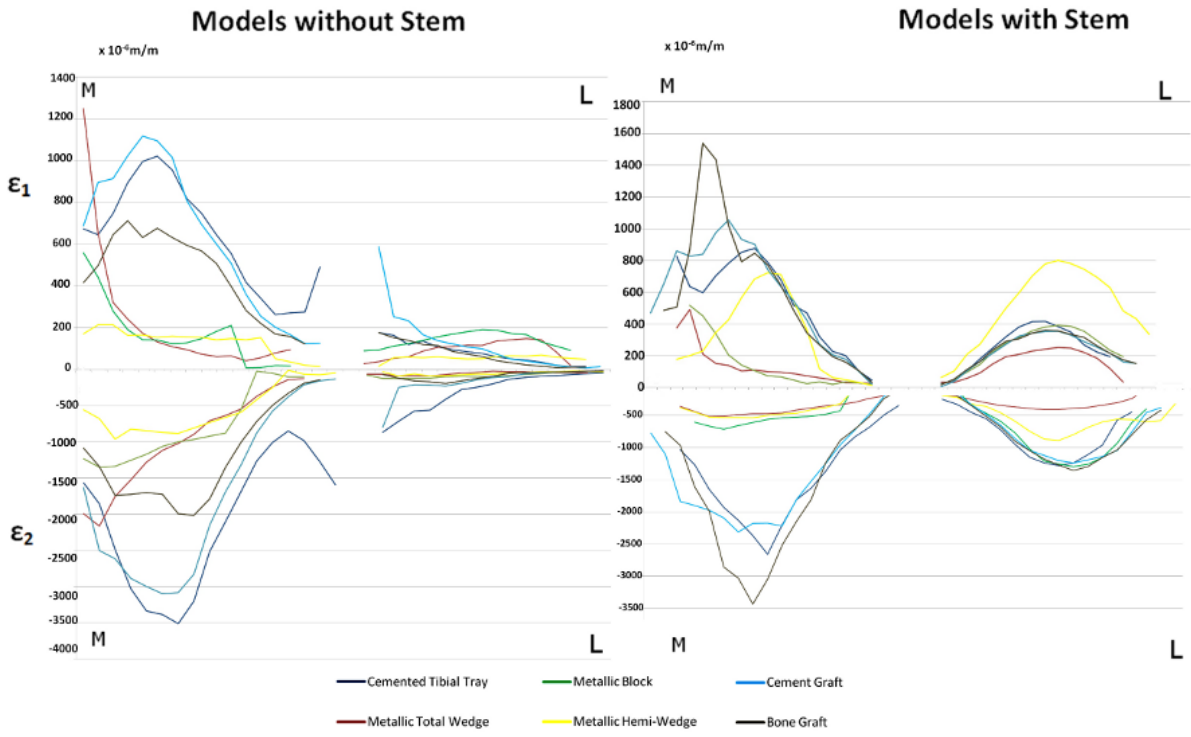

Figure 4.15: Medial load cases: Principal strains on the models with and without stem on the cortical bone: frontal plane on the cancellous bone

We can see from figure 4.12, that the maximum principal strains at 2mm from the reference are majority distributed on the medial side (M) of the model. On the lateral side (L) we observe that the values of ε_1 are significantly lower when compared with the medial side, showing a difference of approximately 350μ strain. On this side all the models have a similar behaviour, where there is no significant difference to point. In the anterior side (A) we observe that the ε_1 distribution on this position is similar to the posterior side (P). On this position there is no significant difference between anterior and posterior sides.

When compared to the model using a stem, we can see that occurs a significant decrease of the ε_1 in all positions of almost all models.

Regarding the minimum principal strain at 2mm from the reference we can observe that is in the medial side that the higher values of ε_2 are distributed. Despite a small area is covered, we can see that in this side the cement graft model is the one that shows higher values. On the other positions, anterior (A), posterior (P) and lateral (L), the models show that the distribution of ε_2 is similar to the model with a cemented tibial tray model.

When we compare the minimum principal strain of the models with and without stem we can see that a small decrease is observed on the medial (M) side. On the P side, an increase of the ε_2 is registered on the hemi-wedge, as well as on the A side. On the lateral side is where the biggest difference between stemmed and non stemmed models happens, specially on the models with hemi–wedge. This model shows an increase of 100 μ strain when compared with the model without stem.

The ε_1 of the models with a medial load at 7mm from the reference, are mainly distributed on the M side of the models. On the medial side the cement graft is the model that shows the highest values, showing a little difference to the cemented tibial tray model. On the A side, the models show a distribution of ε_1 inferior than on the M side (50μ strain). On this side, the cemented tibial tray is the model that shows higher values when compared with the other models. The model that is closer to this one is the bone graft model. On the P side no significant difference between models is observed as well as on the lateral side, where the ε_1 distribution is about 200 μ strain and 50μ strain, respectively.

When compared to the models with stem, we may observe that a general decrease of values occur in each position. The main difference registered happens on the medial side, where a decrease of 100μ strain occur, which means a reduction of 20% when a stem is used. The stemmed cement graft models are the ones that are closer to the cemented tibial tray model, when compared to all the other stemmed models.

Regarding the minimum principal strain, we may observe, on the medial side (M), that the highest values are distributed on this position, specially on the model with a metallic hemi–wedge, which is the most distant model to cemented tibial tray model. On the other hand, lateral side (L) is where the lower values of μ strain are distributed. On this side there is no significant difference between models. On the P position we can see that all models show a similar distribution, except the metallic-hemi wedge model which shows the lowest and the most distant values to cemented tibial tray model. On the A position we can observe that the metallic block shows the smallest and most distant values from the cemented tibial tray model, while the metallic hemi–wedge shows the higher ones.

When we compared these models with the models with stem, we observed that the μ strain suffered a decrease, specially on the M and A position about 30%. On the other hand, the metallic hemi–wedge shows an increase of 50% and is the model where the difference is higher.

At 17mm from the reference, after the implants, we may observe that the maximum principal strain distribution on the medial side (M) shows smaller values than the anterior one. On M

position we can see that the bone graft model and metallic total wedge are the two models that are more distant from the cemented tibial tray model, showing higher values. The other models show similar values to cemented tibial tray model on this position. As mention before, the A position is where the higher values are present. On this case, the cemented tibial tray is the model that shows the highest values whereas the metallic total wedge has the lowest ones. On the P position the difference to the cemented tibial tray is not that much, but also in this position, the metallic total wedge is the one that shows the smaller values of ε_1. On the L position, all the models have almost the same behaviour. On this position any significant difference can be shown.

When compared with the stemmed models we can see that ε_1 decreases in all, the tibia surface. With stem, the model with a metallic block is the one that shows the biggest difference to the cemented tibial tray model, showing smaller values than this one, specially on the M position.

About the minimum principal strain we can see that, is on the medial side that the higher values are present. On this side, we can see that the model with metallic total wedge is the model that shows smaller values and where the difference to the reference model is bigger (1000μ strain), representing a decrease of about 50%. On the anterior position (A), we can see that the generally values of ε_2 is 100μ strain and the difference between models is insignificant, excepts with the metallic block, that shows a 200μ strain, 30% higher values. On the posterior position P, we can see that that's where the higher values are concentrated, showing values of about 250μ strain. On this position, the model where the difference to the cemented tibial tray model is bigger is the one with total wedge, showing a difference of 50μ strain. Finally on the lateral side, (L) the difference between models is not significant, showing all of them similar values to cemented tibial tray. It's also on this position that the ε_2 has smaller values. When compared with the stemmed models we can see a significant decrease of the ε_2 on the P position.

On the anterior medial position we can see that increase the ε_2 occurs, except in the model with metallic total wedge. So, this is the model that shows more different values when compared with the cemented tibial tray model. The other positions, despite the normal decrease of 30% when compared with the models without stem, do not show any significant difference when compared with the cemented tibial tray model. On the medial position M we can see that that the metallic hemi-wedge shows smaller values when compared to the cemented tibial tray.

The distribution of the ε_1 on the surface of the tibial plateau (bone–cement interface) shows higher values on the medial side (medial condyle). The model that less differences show to the cemented tibial tray model is the cement graft model, showing a difference of about 72μ strain, about 7% higher values. The model that shows the biggest difference is the metallic total wedge, since on the medial side this model is the one that shows the lower values of ε_1. This difference is about 98x10μ strain, around 90% lower values. On the lateral side, the distribution of the maximum principal strain is very similar in all the models, although the model where a metallic block was used we can observe higher values and a bigger distance to the cemented tibial tray.

When compared with the models with stem we can see that there is a small decrease of the models maximum principal strain values, except on the bone graft model on the medial side and on the hemi–wedge model on the lateral. This changes on this two models represents the biggest differences to the non stemmed models.

About the minimum principal strain on the tibial plateau surface, we can see that on the medial side of the models without stem, the cemented tibial tray model is the one that higher values present, specially on the medial side of the surface. On this case, the metallic hemi–wedge is the one that lower values present and also the more distant ones. Where a cement graft was used, we can see that the ε_2 distribution is very similar to the cement tibial tray model. On the lateral side, there's nothing to declare, since the distribution of the ε_2 is very similar on all the

models.

When compared with the models with stem, we can see that the bone graft shows a peak on the condyler surface, being the model that shows the higher values of ε_2. Despite this, the differences between stemmed and non stemmed models show a significant decrease of the ε_2 distribution in the models with cement graft, cemented tibial tray, metallic block and total wedge (20%). Although, the metallic hemi-wedge model doesn't show a significant difference. On the lateral side, when compared with the models without stem, we may observe that exists an increase of the ε_2 values.

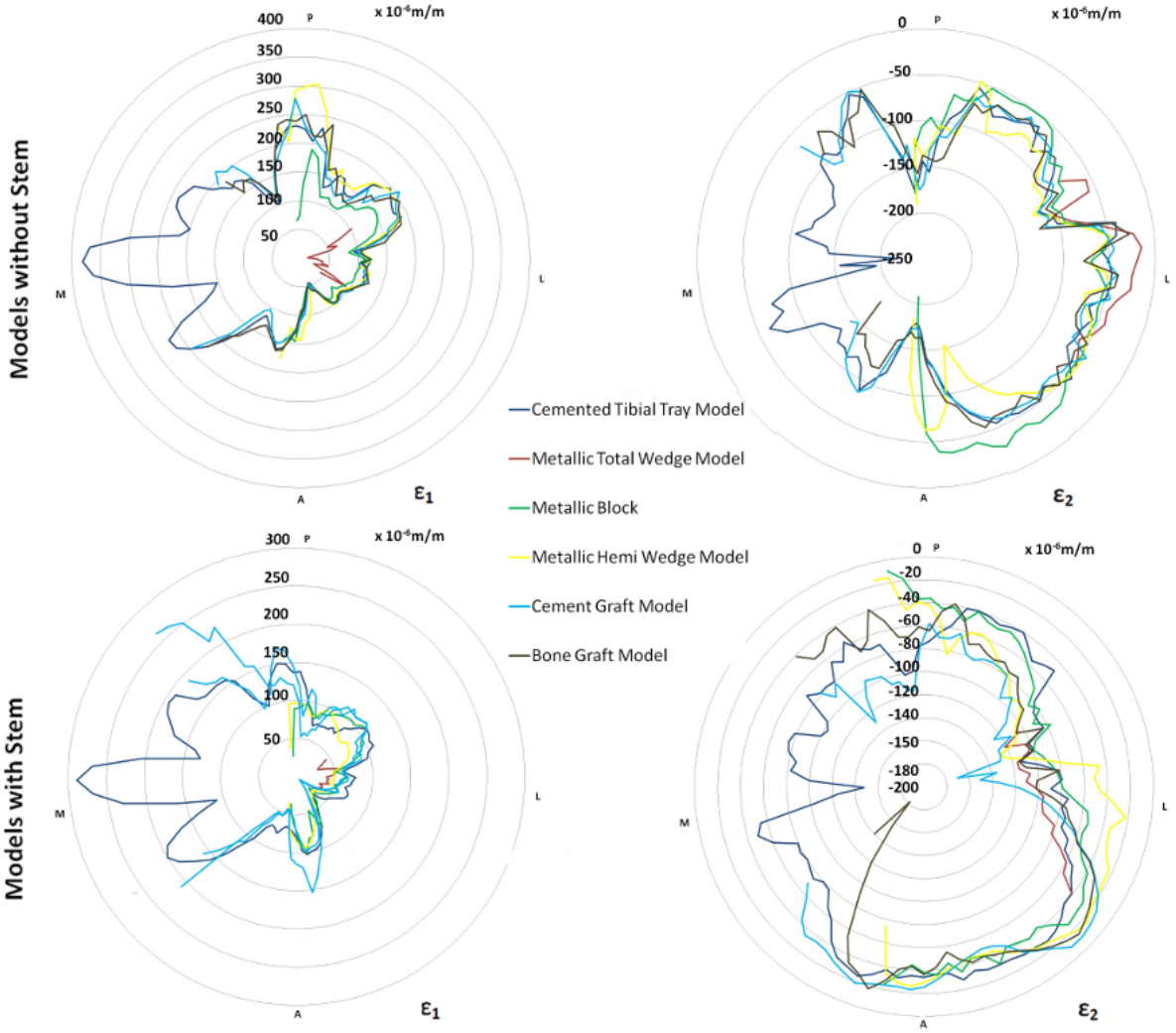

Figure 4.16: Medial/Lateral load cases: Principal strains on the models with and without stem on the cortical bone: 2mm from the reference

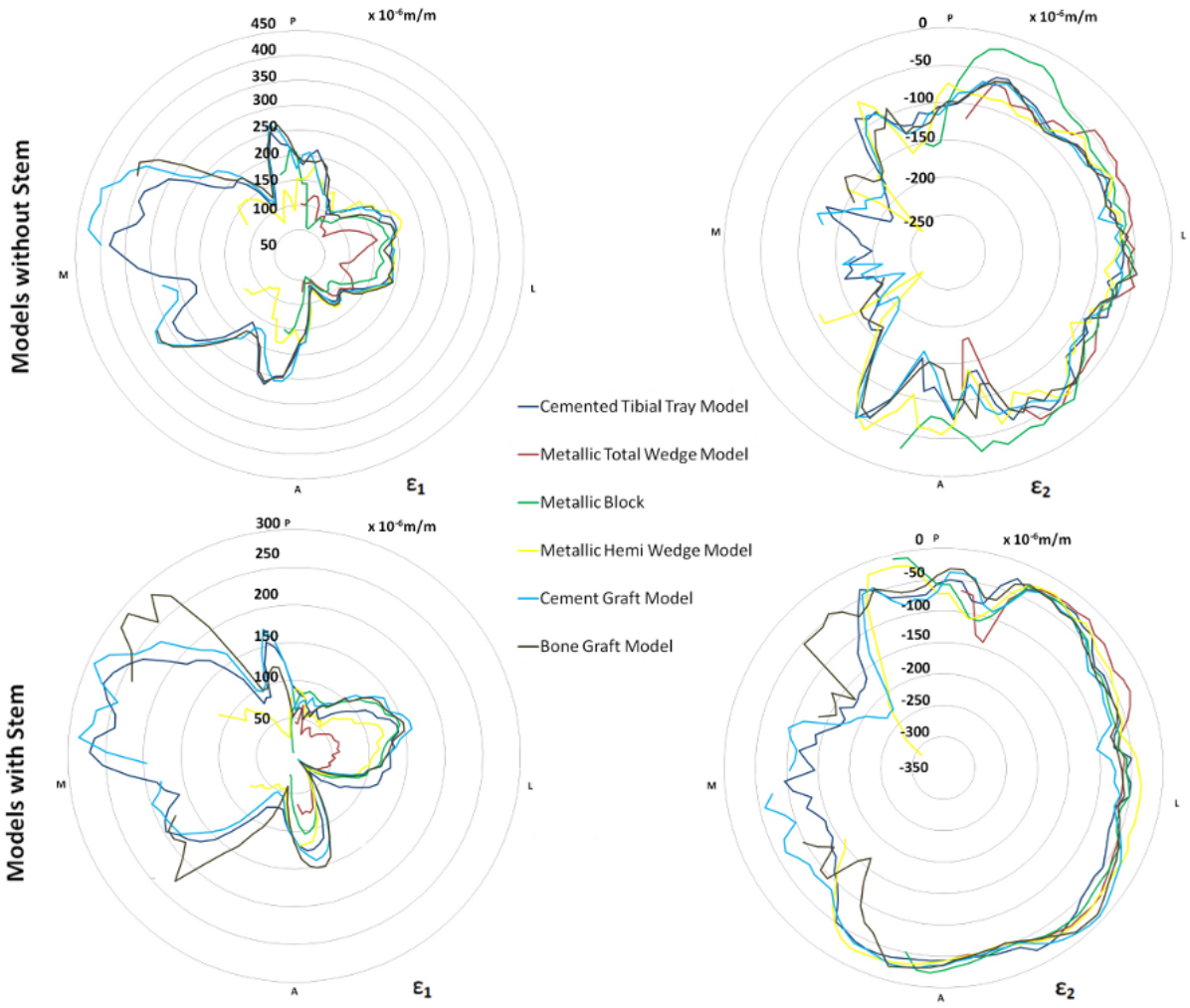

Figure 4.17: Medial/Lateral load cases: Principal strains on the models with and without stem on the cortical bone: 7mm from the reference

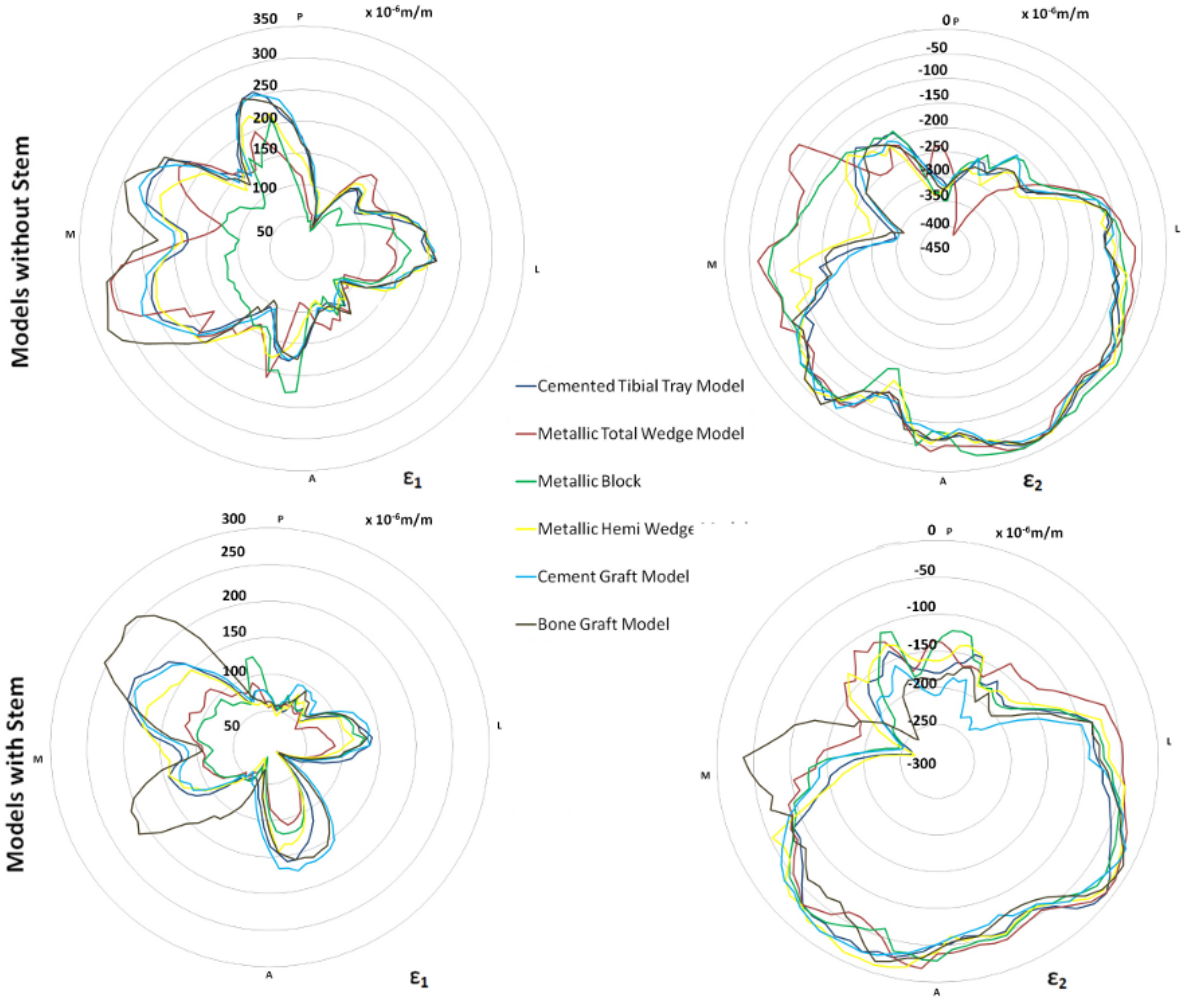

Figure 4.18: Medial/Lateral load cases: Principal strains on the models with and without stem on the cortical bone: 7mm from the reference

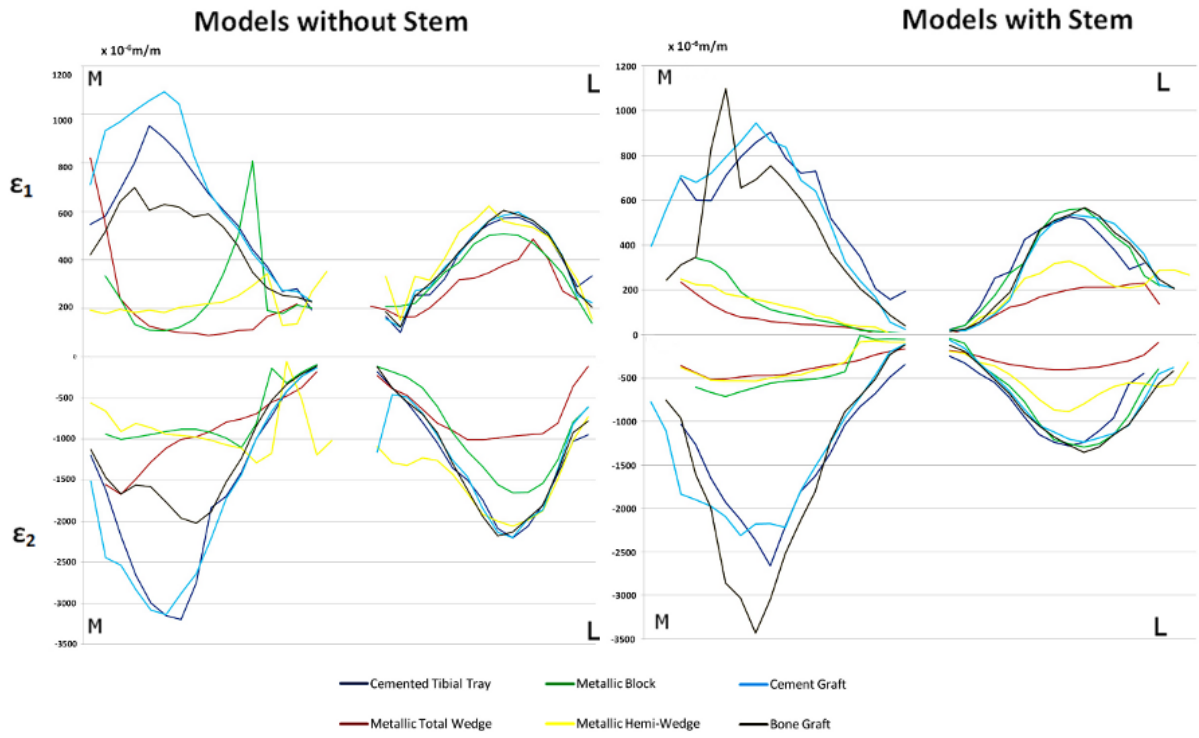

Figure 4.19: Medial/Lateral load cases: Principal strains on the models with and without stem: frontal plane on the cancellous bone

We can see at 2 mm from the reference that the maximum principal strains are distributed majorly on the medial side of each models. On the anterior position, A, we can see that the ε_1 are lower, when compared with the other positions. On the other hand, the P and L position show a very similar distribution. The models that show the biggest differences in the cemented tibial tray are where a metallic hemi–wedge was used, specially on the P side. The metallic block is the model that shows lower values of ε_1 on the P side.

Regarding the stemmed models, we can see that the distribution around the tibia surface is similar between models with and without stem, although the models without stem have higher values than the models with stem.

On the model where a metallic hemi–wedge (without stem) was used we can see that it is on the posterior position that the values of maximum principal strain are higher, registering a considerable difference to the metallic hemi wedge model with stem (about 200μ strain which represents a 66% lower values).

As well, we can see on the maximum principal strain figures that the model with metallic block was the one with lower values of ε_1 and the values of the bone graft are the closest ones to the cemented tibial tray model, specially on the lateral side. The values of cement graft show on the posterior medial side a considerable difference to the model with cemented tibial tray.

The minimum principal strain at 2 mm shows the highest distributions on the medial side of the models, although the difference between sides is not so big. On the other hand, the values shown on the lateral side, L, are the lowest on each model and any significant change is noted between models. So, we can see that the posterior medial side is where the highest values of ε_2 occurs but, on the other hand, the anterior lateral side is where the lowest values of ε_2 are distributed.

When we compare the models with and without stem, we can see that the ones without stem show higher values than the models with stem, about 18% on the medial side, 35% on the lateral, 40% on the anterior and 20% on the posterior side. The side where the biggest difference was registered using a stem was on the L side. With a stem, on the P and A position the models get closer to the cemented tibial tray model.

In general, all the models have similar behaviour around the tibia surface although the model with bone graft and metallic block are the ones closer to the cemented tibial tray models.

The maximum principal strain on the models without stem at 7mm from the reference shows higher values on the medial side On this position, we can see that the bone graft model and the cement graft are the ones that more similar values present on the entire surface of the tibia, despite the other models shows not so different values. On the P and A side, the results are similar, and on these positions we can see that the metallic hemi-wedge is the model which has the most different values when compared to the cemented tibial tray model. On the L position the situation changes, because, the metallic hemi–wedge shows very closer values to the cemented tibial tray model. On this position, the metallic total wedge is the one that shows the most distant values.

When compared with to models with stem, we can see that as well as the models with stem, the higher values of ε_1 are located on the medial side, although this values are smaller.

The metallic total wedge is the model with the smallest values of maximum principal strain, specially on the models with metal stem.

The bone graft models show, on both groups, that its medial side has the highest values which are and very similar values to the cemented tibial tray model.

Regarding the minimum principal strain, we can see that the highest values are concentrated on the medial side. On the L side we can see that the difference between models is not significant. Near the P side, we can see that the metallic block values show a smaller decrease when compared with the other models, but on the P position this decrease is not observed. On the A position we

may see that the bone graft model is the one that shows higher differences when compared to the cemented tibial tray model.

The difference between models on the medial side is not significant around the tibia. Despite this, the values between models with stem and without stem is about 32%, according to the maximum values of each model, on each position. The difference between medial side and lateral side is about 150 μ strain. That difference on models with stem is about 100 μ strain.

At 17mm from the reference, after the implants, we may observe that the maximum principal strain distribution on the medial side (M) shows the highest values, although there is a very small difference to the posterior side. On M position we can see that the bone graft model and metallic total wedge are more distant from the cemented tibial tray model, showing higher values. The other models show similar values to cemented tibial tray model on this position.

On the A position we can see that all the models have similar behaviour, specially the cement graft model, that shows a similar distribution than cement tibial tray model. On this position, the metallic block is the model which more distanced to the cemented tibial tray are.

On the P position, the difference to the cemented tibial tray is not that much. In this position, the metal block is the one that shows the smaller values of ε_1 and the metallic hemi–wedge, cement graft and metallic total wedge the closest values. On the L position, all the models have almost the same behaviour. On this position any significant difference can be shown. When compared with the stemmed models we can see that the ε_1 decrease in all the tibia surface is about 30% generally. With stem, the model with a bone graft is the one that shows the biggest difference to the cemented tibial tray model, showing higher values than this one, specially on the M position. The metall block and metallic total wedge are the ones that lower values shows.

Regarding the minimum principal strain we can see that is on the medial side, M, that the highest values occur, despite the values on the P side not being so distant. We can see on the M side that the metallic total wedge and metallic block are the ones which present lower and more distant values to the cemented tibial tray model. The remain models show similar behaviour to the cemented tibial tray model.

On the L and A positions, the registered values are almost the same and them difference to the cemented tibial tray is not significant.

When compared to the models with stem, although a reduction on the P side is noted of about 40%, any other change is noted.

The maximum and minimum principal strain were also analysed on the frontal plane of the tibial plateau, in order to evaluate de tibial tray stability. The maximum principal strain of the models without stem shows higher values on the medial side, specially the models with cement graft and cemented tibial tray, which are very closer.

The models with metallic block and metallic total wedge show the smaller values of maximum principal strain on both sides, and they are more distant to the cemented tibial tray. The cement graft is the model with closer results on the medial side present.

On the lateral side, we can see that all the models have a similar behaviour to the cemented tibial tray model.

When compared to models with stem we can see that the values are not so different on the lateral side, showing very close values to the non stemmed models.

About the minimum principal strain, on the medial side, we can see that the the cement model is the one that shows closer values to the cemented tibial tray model. The most distant models to the reference one are the models with a metallic hemi–wedge and metallic block. This difference is about 2000 μ strain, which is about 60% different. On the lateral side, we can see that only the metallic block and metallic total wedge shows a significant difference to the cememtned tibial tray

model. This difference is about 480 μ strain on the metal block and 1200 μ strain on the metallic total wedge.

The minimum principal strain shows higher values on the medial side of the models either on the stemmed or non stemmed models.

The difference on the medial side between models with and without stem is significant, about 20%, except in the bone graft model with stem, which shows similar values to the models without stem.

On the lateral side, although the values of the models with stem are lower than the models without stem, the difference is just about 500 μ strain.

4.3.3 Experimental Models v.s. Numerical Models Results

In this section the results of the validation made on our models will be presented, as well as the difference between numerical and experimental models.

The numerical models validation will be presented on the figure 5.12.

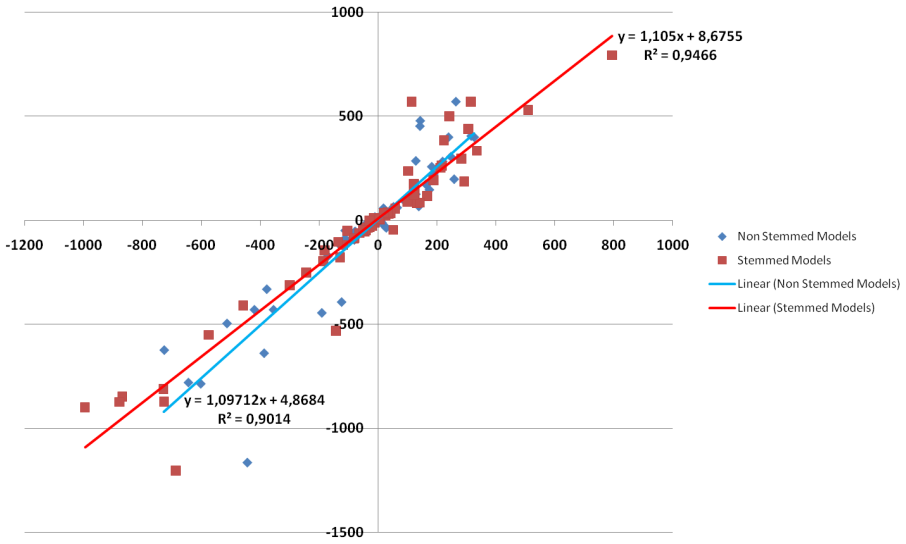

Figure 4.20: Numeric models validation

We can see that the values of the linear regressions show values of R^2 near 1 as well as values of the linear regression slopes.

On the next figure will be shown the graphical differences between numerical and experimental models of the maximum and minimum principal strain obtained.

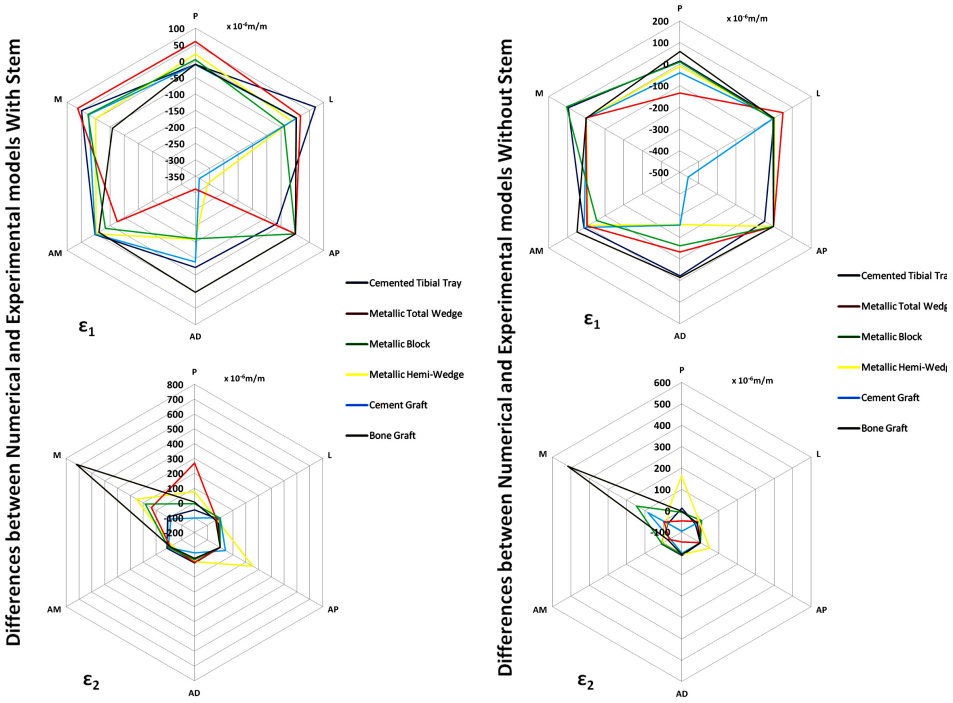

Figure 4.21: Comparison between numeric and experimental models

We see on the figure 4.18 that on the maximum principals strain of the models with stem the differences between numerical models and experimental models are bigger on the A_D position of the metallic total wedge and on the A_P position of the metallic hemi wedge and cement graft.

The minimum principal strain of the stemmed models shows the biggest differences on the M and A_P side.

According to the results of the non stemmed models we can see that the only the cement graft shows a considerable difference between numerical and experimental models on the $_P$ position.

At last, we also compared the differences between minimum principal strain on the models without stem. We see that the main differences happens on the M and P sides of the bone graft and hemi–wedge models.

4.4 Discussion

The first important point to discuss regards to the mesh dimension. The mesh used was 2,5 mm since this value was where the values of the maximum displacement v.s.number of elements started to converge, and there was no reason to choose smaller elements than 2,5 mm because the convergence was achieved, because that would just increase the computation time and wouldn't make any significant improvement on the results obtained.

We will focus our discussion on the medial/lateral load case because this is closer to a physiological situation. The medial load case was only important to assess the veracity and feasibility of the numerical models when compared to the experimental ones. It is important to refer that the results of this comparison are very positive, showing similar results to the experimental model, which guaranties a good replication of the numerical models.

So, in order to evaluate the validation of the numerical models, a comparison between numerical and experimental models was made. This comparison demonstrates that the experimental models in fact validate the numerical models, as mentioned by Jeremy et al [77].

The validation results are very satisfactory, since the R^2 is near 1 and the the regression line is also near 1. These values mean that the correlation between experimental and numerical models was achieved.

A general illustration of this correlation has been shown, and also an individual analysis was made in order to assess how each model contributes to this correlation. According to this we saw that, in general, all the models show satisfactory values of R^2 (near 1), except the last two models, bone graft and metallic block model. These models, metallic block and bone graft, show different results because the values of R^2 and regression line are distant than 1 (0,91 and 1,2 respectively). We think that this happened because of the problem on the white filament of the posterior strain gauge, which was accidentally damaged during the surgical procedure.

According to this, and despising this situation, we may say that the relationship between experimental and numerical models is good, which validates our numerical models.

By other words, we have observed that both the maximum and minimum principal strains obtained on the numerical models followed the behaviour of the maximum and minimum principal strain of the experimental models. Since a good replication of the numerical models was guaranteed, their use is allowed to investigate the principal strains in areas where it is impossible to evaluate through experimental test.

According to the results obtained with the comparison between numerical and experimental models we may say that the position which shows more differences in all the comparisons graphs is the A_P position. This probably happened because of the strain gauge position on the surface of the tibia, which was set in a prominent surface of the experimental model. When comparing to the numerical model, we should see the principal strain values on the same position. So, because this strain gauge was set is a prominent surface, the approximation made by finite element method, on that same position, could be a bit far from reality.

The minimum principal strain differences on the M position of the stemmed and non stemmed models can only be explained by the use of a screw on bone graft numerical models, in order to fixate the bone graft to the tibial bone. On the experimental models we didn't use any screw, and that may be the explanation for the difference occurred.

According now to the obtained values from the numerical models we may conclude that, in general, the models with medial load show the expected behaviour in all the different distances to the reference.

As expected, the highest values of the compression forces occur on the medial side of the models, since only a medial load was applied.

The implant that less influence causes to the bone is the cement graft, as well as the metallic hemi–wedge, because the principal strains registered on these models are very similar to the cemented tibial tray model. Both models show less differences to the cemented tibial tray model on the M position. Despite that, we can also see that the other models do not change significantly on the lateral side, because only a medial load was applied.

The model that more changes causes to the bone, when compared with the cemented tibial tray, is the bone graft model. On the M position of this model is where the differences to the cemented tibial tray are higher.

On the L position, the difference of each model to the cemented tibial tray is insignificant, which is normal since only the medial side has been loaded. According to this, the compression forces on this side are insignificant, leading to small changes on the models.

On this load case, although the results should be taken into account, the problematic situation may not occur on the physiologic load situation, where the loads are applied on the both medial and lateral sides.

On the models where we tried to simulate the physiological case, with medial and lateral load, the scenario was different, specially, and as expected, on the lateral side.

The cement graft model is the model that, either on the beginning, middle or after the implant, shows similar results to the cemented tibial tray model, although in some positions may occur occasional bigger differences. These differences never exceed 15%. According to this, the risk of hypertrophy or even bone resorption is not significant. The values are specially closer to the cemented tibial tray on the lateral, posterior and anterior positions, which was expected since the defect is on the medial side, which is reinforced by the strains distribution on the medial side that also shows closer results to the cemented tibial tray, as we can see on the figure 4.18.

We can see, specially after the implant, at 17mm to the reference, that the bone graft is the model that shows a bigger difference to the cemented tibial tray, specially on the M position(where the defect is). According to this, we may say that when this model is used the chance of fatigue failure on the medial side increases, since there is an increment of 25% of the maximum principal strain.

The models with metallic hemi–wedge show that in all the different distances to the reference, its values are closer to the cemented tibial tray values, specially on the lateral side (L). When this technique is used, the increases registered are never higher than 20%.

The metallic total wedge, specially on the side of the defect, may cause fatigue failure to the bone since there is an increase of 25% of the principal strains registered, when compared with the cemented tibial tray model.

The implant that guarantees better results on the tibial plateau of the cancellous bone was assessed with the measurement of the interface bone–cement. According to this, we may see that the cement graft is the model that shows better results, since there is only a small difference to the cement tibial tray, about 14%. This result could be improved with the use of a metallic stem, decreasing to a 10% difference.

On the other hand, the models with metallic wedges and bone graft enhance the risk of bone resorption on the cancellous bone, specially on the medial side of the models, because their principal

strain values show a reduction, when compared with the cemented tibial tray model. This reduction is about 40% on the bone graft model, and between 65 to 78% on the models with metallic wedges and block. On the lateral side these problems just occurs on the metallic total wedge, which shows a reduction about 50 % of minimum principal strain when compared to the cemented tibial tray. According to this, the model with metallic total wedge can cause bone resorption on the lateral side.

We can affirm, based on the numerical tests, that the metal stem provides a decrease of the principal strains on the cortical and cancellous tibia. This results are consistent with Jeremy et al [77] previous studies.

According to these results, we can conclude that the models with cement graft and metallic hemi–wedge are the ones where the use of a metal stem makes sense. However, when a decrease of the principal strain is needed the stem is useful.

When an intervention is required, in order to repair any type of the defects mentioned in our work, we should use a metallic hemi–wedge with a metal stem or a cement graft, because those are the models that less interferences cause to the subjacent bone.

Chapter 5

Conclusions and Future Works

5.1 Conclusions

The obtained results from the numerical models reflected the principal strains behaviour of the experimental models on the analysed positions. This shows the ability of the numerical models to replicate the behaviour of the experimental models.

The results obtained from the different analysed models allow us to conclude that the load cases, the technique to repair the defect and the use of stem influence the levels of strains in the bone, as well as the implant stability.

We also concluded that the metallic total wedge and metal block increases the principal strains near the implant, on the medial side of the cortical bone. However, when compared these models with the bone graft model, we can see that this one shows the biggest difference. According to this increase of principal strains, a tendency of hypertrophy or fatigue failure on this side of the cortical bone when the most invasive techniques are used, may occur.

On the cancellous bone, the cement graft is the model that closer are to the cemented tibial tray model, according to this, we may say that is the less invasive to the bone. On the other hand, the metallic wedges/block models are the ones that a bigger changes cause in the cancellous bone, specially on the medial side(defect side). These models increase the potential of bone resorption, since the principal strains of these models show a relatively decrease when compared with the cemented tibial tray model. The bone graft also shows a significant difference to the cemented tibial tray model on the medial side of the cancellous bone which also cause the bone resorption.

According to our study we also concluded that the use of a metal stem guarantees an extra stabilization effect on the models and should be used, specially on the simplest implants, where cement graft and metallic hemi–wedge was used.

The metallic stem is not important on the metallic total wedge model and metallic block model because their principal strain values don't show a significant variation with the use of a stem, as shown in our tests. This behaviour can be justified by geometry and big dimensions of these kind of implants.

On our study, with the displacement comparison between tibia and tibial tray, we concluded that the metal block is the more stable model, since the displacement registered on this case was very small when compared with the other models

5.2 Future works

In order to provide more knowledge about revision of total knee arthroplasty will be presented some suggestions for future studies in this area attempting to give more answers about the mechanical behaviour of the knee joint and especially about osteolysis and stress-shielding.

In order to increment the feasibility of this study, we propose the use of cadaveric bone in similar tests in order to evaluate the differences between this resource and the composite material.

Since on this study just a static load case was applied, we think that would be suitable to verify how the used techniques on this study behave when exposed to a severe fatigue tests.

We also propose experimental tests with different types of stem since, that on this study, just one type of stem was tested. We suggest the use of modular stem, press fit, and combined tibial tray with decentered fixation stem, with different lengths, in order to assess which ones have better results. It should be also tested the use of cement in the stem fixation.

Bibliography

[1] M. Nordin and V. H. Frankel. *Basic Biomechanics of the Musculoskeletal System*. Williams & Wilkins, 2001.

[2] http://www.nlm.nih.gov, 2008.

[3] Susana Meireles. Strain shieldingindistalfemurafterpatellofemoralarthroplastyunder different activityconditions. Master's thesis, Universidade de Aveiro, 2009.

[4] http://www.upmc.com, 2008.

[5] A. Completo. Estudo numérico e experimental da biomecânica da prótese do joel. Master's thesis, Universidade de Aveiro, 2006.

[6] Ammeen D. J Engh, G. A. Bone loss with revision total knee arthroplasty defect classification and alternatives for reconstruction. *Instr Course Lect*, 48:167–175, 1999.

[7] P.F.C: Sigma Knee System. *P.F.C: Sigma Knee System*. Depuy a Johnson and Johnson Company.

[8] Bournet R.B. McLeant J Finlay, J. B. A technique for in vitro measurement of principal strains in the human tibia. *J. Biomechanics*, 15:723–739, 1982.

[9] Prendergast PJ. Murphy BP. Measurement of non-linear microcrack accumulation rates in polymethylmethacrylate bone cement under cyclic loading. *J Mater Sci*, 10:779–81, 1999.

[10] Whiteside LA. Selective ligament release in total knee arthroplasty of knee in valgus. *Clin Orthop*, 17:23–27, 2002.

[11] http://en.wikipedia.org.

[12] Ana Rego. Estudo experimental do efeito das hastes femorais na tibia na ratj. Master's thesis, Universidade de Aveiro, 2008.

[13] www.daviddarling.info.

[14] Henry Gray. Anatomy of the human body.

[15] http://www.bartleby.com/.

[16] J. Goldblatt and J. Richmond. Anatomy and biomechanics of the knee. *Operative Techniques in Sports Medicine*, 11:172–186, 2003.

[17] Lubinus H. H. Patella glides bearing total replacement. orthopedics. *Journal Bone Joint Surgery AM*, 2:119–127, 1979.

[18] Kummer F. Jazrawi L., Bai B. The effect of stem modularity and mode of fixation on tibial component stability in revision total knee arthroplasty. *The Journal of Arthroplasty*, 16: 759–767, 2001.

[19] Leila Castro Michelle Ferrandis Priscila Lopes Sandra Santoro Paulo Roberto, Flavio Oliveira. Estudos apresentados no seminário velox de atualização científica. In *Análise biomecânica do agachamento e as principais lesões relacionadas ao joelho*, 2007.

[20] Cheryl Perry. *Anatomica, the complete home medical reference*. Global Book Publishing, 2005.

[21] http://pt.wikipedia.org/wiki/Menisco.

[22] Rik Huiskes Van C. Mow. *Basic orthopaedic biomechanics*. Lippincott -Raven, New York, 1997.

[23] J. Fritz. Articular cartilage defects in the knee basics, therapies and results. *Injury Int. J. Care Injured*, 39S1:50–57, 2008.

[24] www.answers.com.

[25] Carol Eustice. What is varus or valgus knee deformity? About.com Guide, 2008.

[26] Windsor RE. Correction of deformity: When the implant itself is not enough. In *Current Concepts in Joint Replacement*, 2010.

[27] Adam Sertaoggi, 5 2008.

[28] Gregory M Martin. Total knee replacement.

[29] Simon H Palmer. Total knee arthroplasty. *Medscape Reference*, .:., May,2011 2011.

[30] P Dieppe. Osteoarthritis: time to shift the paradigm. *British Medical Journal*, 7192-7200: 318, 1999.

[31] Ines Marques Martins Silva. Estudo experimental das tensões no osso na revisão da artroplastia total do joelho com haste press-fit. Master's thesis, Universidade de Aveiro, 2008.

[32] Filho J. Mestriner, L. Artroplastia total do joelho em osteoartrose. *Revista Brasil Ortop.*, .:., 1993.

[33] Pécora J. Infecção nas artroplastias do joelho. *Revist@ do Joelho*, .:., 2006.

[34] Ivan Oransky. The effects of osteolysis and aseptic loosening. *Medscape Orthopaedics*, .:., 2001.

[35] Oxford Dictionary of Sports Science & Medicine.

[36] Dorr L. Bone grafts for bone loss with total knee replacement. *Orthop Clin North Am*, .:., 1989.

[37] Rand J. Bone deficiency in total knee arthroplasty. use of metal wedge augmentation. *Clin Orthop*, 271:63–71, 1991.

[38] Rorabeck C Engh G. A classification of bone defects in revision knee arthroplasty. *Baltimore: Williams & Wilkins*, 6:63–120, 1997.

[39] Lotke PA. Elia EA. Results of revision total knee arthroplasty associated with significant bone loss. *Clin Orthop*, 392:213–220, 1991.

[40] Rand JA Pagnano MW, Trousdale RT. Tibial wedge augmentation for bone deficiency in total knee arthroplasty. a follow-up study. *Clin Orthop Relat Res*, 321:151–155, 1995.

[41] Healthbase Online Inc, 2011.

[42] Shalby Hospitals. Total knee replacement (tkr).

[43] Santavicca EA Insall JN Bartel DL, Burstein AH. Performance of the tibial component in total knee replacement. *J Bone Joint Surgery Am*, 76:769–777, 1982.

[44] Toms AD. Whittaker JP, Dharmarajan R. The management of bone loss in revision total knee replacement. *J Bone Joint Surg [Br]*, -:–, 2008.

[45] D. McClelland L. Chua R. Spencer-Jones J.-H. Kuiper A. D. Toms, R. L. Barker. Repair of defects and containment in revision total knee replacement. *The Robert Jones & Agnes Hunt Orthopaedic Hospital, Oswestry, England*, -:–, 2008.

[46] Puri N. Lotke PA, Carolan GF. Impaction grafting for bone defects in revision total knee arthroplasty. *Clin Orthop*, 406:145–151, 2006.

[47] Richard David Scott James V.Bono. *Revision Total Knee Arthroplasty*. Springer, 2005.

[48] Humble RS et al. Fehring TK, PeindlRD. Modular tibial augmentations in total knee arthroplasty. *Clin. Orthop.*, 17:207–327, 1996.

[49] Ewald FC Brand MG, Daley RJ. Tibial tray augmentation with modular metal wedges for tibial bone stock deficiency. *Clin Orthop Relat Res*, 248:71–79, 1989.

[50] Guerin J Bourne RB Rorabeck CH. Patel JV, Masonis JL. The fate of augments to treat type-2 bone defects in revision knee arthroplasty. *J Bone Joint Surg Br.*, 9:86–195, 2004.

[51] Burt M. Sawhney J Barrack R., Rorabeck C. Pain at the end of the stem after revision total knee arthroplasty. *Clin. Orthop.*, 19:119–124, 1999.

[52] Kloepper R. Mohr R. Peters C., Erickson J. Revision total knee arthroplasty with modular components inserted with metaphyseal cement and stems without cement. *The Journal of Arthroplasty*, 9:320, 2005.

[53] Freeman M. Albrektsson B., Carlsson L. The effect of a stem on the tibial component of knee arthroplasty: roentgen stereophotogrammetric study of uncemented tibial components in the freeman-samuelson knee arthroplasty. *J Bone Joint Surg Br*, 35:33, 1990.

[54] Burt M. Hopkins S. Barrack R., Stanley T. The effect of stem design on end-of-stem pain in revision total knee arthroplasty. *The Journal of Arthroplasty*, 19:119–124, 2004.

[55] Buma P. Sloof TJ, Schimmel J. Cemented fixation with bone grafts. *Orthop Clin North Am*, .:., 1993.

[56] Ling RSM Gie GA, Linder L. Impacted cancellous allograft and cement for revision total hip arthroplasty. *J Bone Joint Surg Br*, 39:133–296, 1993.

[57] Gregory F. Carolan MD Paul A. Lotke, MD and BS Neil Puri. Technique for impaction bone grafting of large bone defects in rtka. *The journal of arthroplasty*, 21:., 2006.

[58] Haas SB Becker-Fluegel MW Windsor RE. Scuderi GR, Insall JN. autogeneic bone grafting of tibial defects in primary total knee arthroplasty. *Clin Orthop Relat Res*, 24:60–65, 1994.

[59] Crawford H. Bourne R. Principles of revision total knee arthroplasty. *Orthop Clin North Am*, 29:331–337, 2003.

[60] Wikipedia.

[61] S. J. Kreuzer S. Condit MA, Ilario. From 50th annual meeting of the orthopedic research society; march 7-10, san francisco, ca. In *Mechanical validation of a foam tibial model for evaluating fixation of revision tibial components.*, 2004.

[62] Gautier E. Cordey, J. Strain gauges used in the mechanical testing of bones, part ii: in vitro and in vivo technique, injury. *Int. J. care Injured*, 30:14–20, 1999.

[63] MESSPHYSIK. *MESSPHYSIK - Materials Testing Version 5.25.0*. MESSPHYSIK - Materials Testing, 5.25.0 edition.

[64] http://www.instron.com.br.

[65] J. B Morrison. The mechanics of the knee joint in relation to normal walking. *JBiomech*, 3: 51–61, 1970.

[66] I. J. Harrington. A bioengineering analysis of force actions at the knee in normal and pathological gait. *Biomed Eng*, 11:167–172, 1976.

[67] Viceconti M. Cristofolini, L. Mechanical validation of whole bone composite tibia models. *Journal of Biomechanics*, 33:279–288, 2000.

[68] Brown T. D Heiner, A. D. Structural properties of a new design of composite replicate femurs and tíbias. *Journal Biomechanics*, 34:773–781, 2001.

[69] Walker P.S. Scott R. D Brooks, P. J. Tibial component fixation in deficient tibial bone stock. *Clin Orthop*, 184:302–308, 1984.

[70] www.sawbones.com.

[71] Professor online, 2010.

[72] Mediped.

[73] Joana Miguel da Silva Leal Pereira. Caracterização numérica e experimental do cotovelo nativo e protésico. Master's thesis, Universidade de Aveiro, 2010.

[74] E. Pena. A three-dimensional finite element analysis of the combined behavior of ligaments and menisci in the healthy human knee joint. *Journal of Biomechanics*, 39:1686–1701, 2006.

[75] J. W.] Fernandez and P. J. Hunter. An anatomically based patient-specific finite element model of patella articulation: towards a diagnostic tool. *Biomech Model*, 4:20–38, 2005.

[76] J.A. Simões A. Ramos. Tetrahedral versus hexahedral finite elements in numerical modelling of the proximal femur. *Medical Engineering and Physics*, 28:916–924, 2006.

[77] Nicole Davis Timothy M. Wright PhD Russell Windsor MD Jeremy J. Rawlinson PhD, Robert F. Closkey Jr MD. *Stemmed Implants Improve Stability in Augmented Constrained Condylar Knees*. The Association of Bone and Joint Surgeons, 2008.